Energy Consumption and GHG Emissions Evaluation of Conventional and Battery-Electric Refuse Collection Trucks

by

Rojin Derakhshan
BA., Urmia University, 2007
M.Sc., South Azad Tehran University, 2012

A Thesis Submitted in Partial Fulfillment
of the Requirements for the Degree of

Master of Science

in the Department of Mechanical Engineering

Supervisory Committee

Energy consumption and GHG Emissions Evaluation of Conventional and Battery-Electric Refuse Collection Trucks

by

Rojin Derakhshan
BA., Urmia University, 2007
M.Sc., South Azad Tehran University, 2012

Supervisory Committee

Dr. Curran Crawford, Department of Mechanical Engineering
Supervisor

Dr. Zuomin Dong, Department of Mechanical Engineering
Departmental Member

Abstract

The notorious fuel consumption and environmental impact of conventional diesel refuse collection trucks (D-RCTs) encourage collection fleets to adopt alternative technologies with higher efficiency and lower emissions/noise impacts into their fleets. Due to the nature of refuse trucks' duty cycles with low driving speeds, frequent braking and high idling time, a battery-electric refuse collection truck (BE-RCT) seems a promising alternative, taking advantage of energy-saving potentials along with zero tailpipe emissions. However, whether or not this newly-introduced technology can be commercially feasible for a collection fleet and/or additionally mitigate GHG emissions should be examined over its lifetime explicitly for the specific fleet. This study evaluates the performance of a D-RCT and BE-RCT in a collection fleet to assess the potential of BE-RCT in reducing diesel fuel consumption and the total GHG emissions.

A refuse truck duty cycle (RTDC) was generated representing the driving nature and vocational operation of the refuse truck, including the speed, mass, and hydraulic cycles along with the extracted route grade profile. As a case study, the in-use data of a collection fleet, operating in the municipality of Saanich, BC, Canada, are applied to develop the representative duty cycle. Using the ADVISOR simulator, the D-RCT and BE-RCT are modeled and energy consumption of the trucks are estimated over the representative duty cycle. Fuel-based Well-to-Wheel (WTW) GHG emissions of the trucks are estimated considering the fuel (diesel/electricity) upstream and downstream GHG emissions over the 100-year horizon impact factor for greenhouse gases. The results showed that the BE-RCT reduces energy use by 77.7% and WTW GHG emissions by 98% compared to the D-RCT, taking advantage of the clean grid power in British Columbia. Also, it was indicated that minimum battery capacity of 220 kWh is required for the BE-RCT to meet the duty cycle requirements for the examined fleet. A sensitivity analysis has been done to investigate the impact of key parameters on energy use and corresponding GHG emissions of the trucks. Further, the lifetime total cost of ownership (TCO) for both trucks was estimated to assess the financial competitiveness of the BE-RCT over the D-RCT.

The TCO indicated that the BE-RCT deployment is not financially viable for the examined fleet unless there are considerable incentives towards the purchase cost of the BE-RCT and/or sufficient increase in carbon tax/diesel fuel price. From the energy use

evaluation, this study estimates the required battery capacity of the BE-RCT for the studied fleet, and the TCO outputs can assist them in future planning for the adoption of battery-electric refuse trucks into their collection fleet where the cost parameters evolve.

Keywords: Refuse collection truck, Representative duty cycle, WTW GHG emissions, Total cost of ownership (TCO)

Table of Contents

List of Tables

List of Figures

List of Abbreviations

A	Ampere
AC	Alternative current
ADVISOR	Advanced Vehicle SimulatOR
Ah	Amp-hour
Aux	Auxiliary
Bat	Battery
BC	British Columbia
BE-RCT	Battery-electric refuse collection truck
BE-truck	Battery-electric truck
BEV	Battery-electric vehicle
BSFC	brake specific fuel consumption
$CAD	Canadian dollar
CBD	Central Business District
Charac accel	Characteristic acceleration
Charac decc	Characteristic deceleration
CNG	Compressed natural gas
CO2,eq	Carbon dioxide equivalent
CSHVC	City-Suburban Heavy Vehicle Cycle
D-RCT	Diesel refuse collection truck
DC	Direct current
DOE	Department of Energy
Drv. spd.	Driving speed
EM	Electric motor
ESS	Energy storage system
GHG	Greenhouse gases
GPS	Global Positioning System
GWP	Global warming potential over a 100 year period
GWR	Gross Weight Ratio
HDDV	Heavy-duty diesel vehicle
HEV	Hybrid electric vehicle
hp	Horsepower
IESVIC	Integrated Energy Systems at the University of Victoria
IPCC	Intergovernmental Panel on Climate Change report
kWh	Kilowatt-hour
L	Litre

LCA	Life-cycle assessment
LD	Light-duty
L_D	Liter of diesel fuel
$L_{D,eq}$	Liter of diesel fuel equivalent
LDV	Light-duty vehicle
LNG	Liquefied natural gas
MDV	Medium-duty vehicle
MOVES	Motor Vehicle Emissions Simulator
mpg	Mile per gallon
MSW	Municipal solid waste
Mt	Mega tonne (10^9 kg)
NREL	National Renewable Energy Laboratory
NRTC	Neighborhood Refuse Truck Cycle
NYCC	New York City Cycle
OCTA	Orange County Transit Authority
OCV	Open-circuit voltage
PHEV	Plug-in hybrid electric vehicle
PM	Particulate matter
PTO	Power take-off
PTW	Pump-to-Wheel
RCT	Refuse collection truck
Rint	Internal resistance
RO-RCT	Roll-off refuse collection truck
RTDC	Refuse truck duty cycle
SL-RCT	Side-loader refuse collection truck
SOC	State of charge
Std	Standard deviation
STP	Specific tractive power
t	Metric tonne (1000 kg)
TCO	Total cost of ownership
Tot. spd.	Total speed
VKT	Vehicle kilometres traveled
WECC	Western Electricity Coordinating Council
WTP	Well-to-Pump
WTW	Well-to-Wheel
y	Year

Acknowledgments

I should start to thank my supervisor, Dr Curran Crawford for his the precious guidance, friendly helpfulness, patience and, most importantly compassionate support when I needed it the most through my years of study.

I would also like to sincerely thank Dr. Ned Djilali for his insightful point of views during the meetings and giving me clues through the complexities that I encountered along the way.

I am grateful to Julian Fernandez-Orjuela, the postdoc fellow member of PICS transportation group, for all his technical and timesaving help during the model development and most importantly his generous knowledge sharing and encouragements.

Despite being away from home, I had the wholehearted support from Sue and Pauline that helped me to stand against ups and downs through this journey. Sue, I always had your motherhood care and comforting thoughts. Thank you for your endlessly kindness and warmth, and being an inspiration to me, and also your beautiful cards! And Pauline, thank you so much for your forever positive attitude and good will towards the life which aspired me to make my best efforts.

My thanks also to Orhan Otabay another postdoc fellow member of PICS group for his useful guidance on the modeling and providing me with the essential technical details.

In addition, my sincere thanks go to other members of PICS transportation group, Sahand, Mojtaba, Anaissia, Alyona, Daniel, Pouya, Autumn for the interesting discussions on up-to-date topics of renewable technologies and keeping the refreshing environment to the group.

I would like to say thanks to all my friends here for their evermore support and smile bringing enjoyable time spending with them. Thank you all for your constant companion.

On top of all, I would like to thank and dedicate this thesis to my family, the treasure of my life.

My big brothers, thank you so much for always being there for me regardless of distance bringing me comfort, joy and ease of mind. Thanks for being such full of love and support!

And the first and foremost, Mom and Dad, I am deeply grateful to have you two angels by my side. You have always held my back through all the ups and downs and supported me throughout my life. I cannot thank you enough for your true love and devotedness. Love you!

Chapter 1: Introduction

1.1 Background

Rising environmental concerns have led to the impetus for decreasing the consumption of fossil fuels to reduce greenhouse gases (GHG) emissions in energy sectors. Due to the heavy reliance on fossil fuels, the transportation sector is a significant contributor to GHG emissions and air pollutants, represents the first largest GHG emitter in the US and the second in EU accounting for 28% and 25.8% of the total GHG emissions in 2016, respectively [1], [2]. In Canada, in 2016 the transportation sector was the second largest contributor to GHG emissions (closely following the oil and gas sector with 26% of total emissions), accounting for 180.3 $MtCO2_{eq}$ and 25% of total emissions with a 7% increase since 2015 [3]. Within the sector, the majority of emissions are related to Road Transportation including personal transportation (light-duty vehicles and trucks), and heavy-duty trucks. The growth in road transport emissions are mainly due to an increase of 38% since 2005 and most notably for trucks, to the total vehicle fleet and consequently more kilometers driven overall [3]. Medium- and heavy-duty trucks are made up the second largest contributor to on-road GHG emissions (36%) while heavy-duty trucks emitted solely 30.6 $MtCO2_{eq}$ standing for 22% of on-road and 6% of the total GHG emissions, respectively [4].

At the same time, an enormous amount of municipal solid waste is generated each year which should be dumped in landfills or recycled/composted/incinerated. Waste is non-hazardous materials discarded from any source including but not limited to garbage, recyclable materials, organics, and bulky items [5]. In Canada, about 31 million tonnes of solid waste is produced each year, and about 70% of it is disposed of accounting for about 25 and 2.6 million tonnes of disposal in 2016 across Canada and BC, respectively [6]. Either the waste is being dumped or recycled; first, it should be collected and moved to landfills or other places to be treated appropriately (either recycled, incinerated, or composted) [7]. This is accomplished employing the heavy-duty refuse collection trucks (RCTs) while their energy-intensive operation is a significant contributor to not only the total waste disposal costs (reported as 40%), but also the destructive environmental impacts

[8], [9]. This has continuously challenged collection fleets to adopt alternative technologies with higher efficiency and lower emissions/noise impacts within reasonable marginal costs.

The results from an in-depth analysis of the vehicle's energy consumption along with a life-cycle assessment can be key decisive factors in the deployment of the alternative technologies. Within the mentioned work frame, in this study, we evaluate the potential for the deployment of a battery-electric refuse truck into an examined collection fleet through an energy-use and life-cycle emissions analysis.

1.2 Refuse Collection Trucks (RCTs)

The refuse trucks are typically classified as heavy-duty vehicles with the Gross Weight Ratio (GWR) of more than 15 tonnes, being considered as vocational vehicles with appropriate on-board mechanical devices (lift, compactor) to load the waste [10]. They are mostly operating on diesel trucks and depending on the application different configurations for the vehicle can be found including front-loader, rear-loader, side-loader, and roll-off refuse collection trucks (RCTs) by either public or private sectors [10]. Fuel consumption and GHG emissions may vary considerably within the configuration of refuse trucks with a noticeable difference in activity pattern, duty cycle and auxiliary power requirements, as well as the fuel type [8]. Sandhu et al. evaluated in-use fuel consumption and emissions for different types of refuse trucks [10]–[12]. Roll-off refuse collection trucks (RO-RCTs), Figure 1, are large trucks primarily employed for commercial purposes to haul construction/demolition and yard waste in significantly large weights [10]. They use a mechanism to pull the container, typically between 10 to 30 m^3, to the truck and transport and drop the trash off at the dumping site. Within their activity pattern with the least amount of stops compared to other types of RCTs and no need for compaction load, the fuel economy of the RO-RCTs is higher than front-loader/rear-loader/side-loader with an average about 55 L/100km [10].

Figure 1) 2002 Mack MR690S roll-off refuse truck [13]

Front-loader trucks, Figure 2, can be used for both commercial and residential purposes. They have a mechanical lifting fork to lift about 100 to 200 containers a day, with an intermediate size of about 2 to 6 m3 each. Their daily activity cycles have less stop-and-go driving than rear- or side-loaders and more than roll-offs resulted in average fuel consumption of 70 to 100 L/100km [11].

Figure 2) 2002 Mack MR690S front-loader refuse truck [13]

Rear-loader refuse trucks, Figure 3, are used commonly for residential purpose and similar in weight, body and activity pattern to side-loader RCTs [14]. Rear-loader RCTs may either have a lifting mechanism to empty the bin with about 130 to 360 liters trash capacity or need an operator to empty the carts manually. The waste is compacted by a moving wall operated through a hydraulic mechanical system.

Figure 3) 2018 ISUZU NRR rear-loader refuse truck [13]

Side-loader refuse collection trucks (SL-RCTs), Figure 4, the focus of this study, are mainly operating in urban areas to collect residential waste. Their activity is mostly comprised of traveling phase including urban/highway driving (from depo to the collection site, from the collection site to the landfill, and from the landfill to depo) and refuse collection, and the duty cycle is a complete cycle of collecting, transporting and dumping the waste. They equipped with a side-arm, packer, and telescoping cylinders to pick-up, pack and dump the trash. The arm and packer are operated by hydraulic components, including a hydraulic pump, which in case of a conventional diesel truck it runs mostly on a direct drive shaft from the engine [15]. In a day SL-RCTs typically collect 500 to 1200 mobile bins of 180 to 360 liters each, transport and dump the waste with a trip or two to

the dumping site [10]. In this application, the engine is designed for running the vehicle at higher speeds during the trips from and to the depo/dumping sites which leads to inefficient use of the engine during the collection phase. Driving with low speed and frequent stop-and-go, high idling time combined with body hydraulic loads through the collection phase as well as the large payload transportation to the dumping site, the SL-RCTs have a considerably energy-intensive duty cycle, and rank for the high level of fuel consumption (80-120 L/100km) compared to other types of heavy-duty trucks (30-35 L/100km) [16]. Hence, their operation contributes to a significant rate of greenhouse gases emissions (mainly CO_2, N_2O, CH_4) as well as the air pollutants [8]. To control the tailpipe emissions, the conventional RCTs are fueled with low-sulfur diesel and equipped with exhaust catalysts devices, however, the device considerably increases the weight and correspondingly fuel use and operational costs. In addition to their energy/emissions-intensive operation, the conventional refuse collection trucks generate high noise levels brought about noise pollutions and hearing problems for the operator [8].

Figure 4) Heil automated side-loader refuse truck[13]

1.3 Alternative Technology Refuse Collection Trucks

Currently, about 90% of refuse collection trucks are diesel-powered [10], but the low efficiency operation and their consequence environmental impacts have emerged the alternative technologies (e.g., CNG/ LNG, biodiesel, hydraulic hybrid, all-electric, fuel-cell trucks) into this sector. Some technologies are already adopted into refuse collection fleets such as CNG, biodiesel and hydraulic hybrid trucks with about 10% and 5% penetration in the US, respectively [16]) and some are newly-introduced technologies to the market such as all-electric and fuel cell refuse collection trucks [17], [18].

CNG refuse trucks are currently being used in refuse collection fleet with about 10% of the total trucks and is considered to remain one of the primary alternatives for petroleum displacement, estimated for about 50% of new refuse truck sales [19]. In a report published by the US Department of Energy (DOE), it is estimated that operation of CNG trucks can reduce the fuel costs and tailpipe GHG emissions by about 50% and 20%, respectively [16]. However, the shorter range with a full-tank CNG truck than that of the diesel truck as well as the CNG station availability and infrastructure costs are key concerns in switching to this alternative technology while the latter may extend the payback 3 to 4 years longer [19].

The hydraulic hybrid technology is developed specifically for refuse collection trucks and demonstrated an efficient alternative by recapturing the braking energy which is generally wasted in a conventional refuse truck [20]. The regenerated energy provides required hydraulic loads with the advantage of the engine being off during the idling time improving the fuel economy by about 25% to 30% compared to a conventional counterpart [21]. Currently, 69 hydraulic hybrids refuse trucks are being operated in Miami-Dade Waste Management fleet in Florida, and three in Ohio in a demonstration project to evaluate the potential in fuel saving through the improved technology [22].

With respect to the goal of zero tailpipe emissions, drivetrain electrification is the alternative technology introduced the battery-electric, fuel-cell and hybrid-fuel cell/battery vehicles, which the two latter are likely the long-term options being deployed in refuse collection fleets [23]. Recently, Scania has introduced the first fuel cell refuse truck powered by hydrogen fuel cell modules to run the electric motors providing both propulsion and compactor power [18]. It is expected that the first fuel-cell refuse truck will

be delivered to Renova, a Swedish waste management company, by the end of 2019/beginning of 2020. Previously, a 500-km fuel-cell electric heavy-duty freight truck was developed by Scania in cooperation with a Norwegian food wholesaler [18]. However; within the fuel cell technology, in addition to the challenges for fuel supply and hydrogen filling station, the ability and reliability of the refuse truck in providing operational patterns with repetitive stops-and-goes along with aggressive accelerations and heavy payload are key factors which should be well-developed for adoption into collection fleets [24].

1.4 Battery-Electric Refuse Collection Trucks (BE-RCTs)

Within the refuse trucks application, drivetrain electrification can be a promising alternative technology to depress the adverse environmental impacts of the counterparts with significant emissions rates. Due to the nature of the duty cycle in a refuse collection with low-speed driving, frequent braking and high idling time, battery-electric refuse trucks can take advantages of significant energy savings, along with benefits of zero tailpipe emissions and a considerable reduction in operational noise levels. Using the high-efficiency electric motors and regenerative braking system, they are featured with lower energy consumption and consequently operational fuel costs, as well as maintenance costs due to fewer moving parts and fluids to change, and less brake wear compared to the diesel-powered refuse trucks. The battery-electric refuse trucks (BE-RCTs) are newly-introduced to the market and not still adopted commonly in collection fleets, except through few demonstrations in the pilot projects.

Motiv Power System delivered the first all-electric refuse truck in the US to the city of Chicago in 2014 [25], and the second demonstration to the City of Sacramento, CA, in 2017 [26]. They offer a scalable and modular design for BE-RCTs, which can be matched to meet the duty cycle's demand for battery-electric refuse trucks being retrofitted from medium-duty to heavy-duty diesel trucks [26]. The Motiv BE-RCT operating in Chicago, Figure 5, has ten battery packs with a 200 kWh energy capacity which can be charged in 8 hours using the Motiv fast charger system. It has a rear-loader body designed to meet the Chicago collection fleet's demand specified as a 100-km daily range and a payload capacity of about nine tonnes in a day [25].

Figure 5) Motiv rear-loader battery-electric refuse collection truck [27]

Peterbilt also unveiled an all-electric class 8 side-loader refuse truck at WasteExpo 2017, as the first battery-electric refuse truck offered by a US truck manufacturer [28]. The all-electric Model 520, Figure 6, has the same chassis used in the diesel and CNG -powered counterparts and equipped with a 300 kW TransPower powertrain and 315 kWh battery capacity to provide it with a range of about 130 km [29].

Figure 6) Peterbilt, Model 520 all-electric side-loader refuse collection truck [29]

In 2017, the electric-vehicle manufacturer BYD introduced its first all-electric refuse truck, a class 6 side loader truck, which is equipped with a 220 kWh battery powering both propulsion and hydraulic systems and providing a 120-km range [30]. Followed by the class 6, BYD also unveiled a class 8 fully automated side loader refuse truck, Figure 7,

with a 295 kWh battery capacity ensure a 90-km range in addition to 600 pickups through the collection phase [31]. The battery can use AC charging or DC fast charging systems being charged in about nine or two to three hours, respectively [31]. It's announced that BYD will deliver two class-8 battery-electric refuse trucks to operate in Seattle in the first half of 2019 [32], followed by a pilot project in 2017 to test the class 8 all-electric refuse truck customized for operation in Palo Alto, CA, with a10-tonne payload and a 188-kWh battery capacity ensures a 100 to 120 km ranges for the truck [33].

Figure 7) BYD 8R all-electric fully automated side-loader refuse collection truck [33]

Moreover, Volvo Trucks presents two classes of battery-electric trucks to the market for deployment in refuse collection fleets, as well as the distribution operations in urban area.

Volvo FL all-electric refuse truck is featured with a refuse collection body by Faun manufacturer with gross weights of up to 16 tonnes, and equipped with an electric driveline with a 130 kW electric motor (185 kW max power) and an onboard battery which can be fit to 100 to 300 kWh energy capacity for a range of up to 300 km. In early 2019, an FL truck, Figure 8, has been delivered to a waste and recycling company Renova, in Hamburg, Germany [34], [35]. With a larger capacity, Volvo FE is rated as a heavy-duty 27-tonne all-electric refuse truck equipped with an electric motor rated for 260 kW continuous power and 370 kW peak power, a Lithium-Ion battery pack of 200 to 300 kWh capacity for a

maximum range of 200 km. The 300 kWh empty battery can be fully charged with 22 kW AC power in 10 hours or 150 kW DC power in 1.5 hours. It is announced that the FE truck will be ready for deployment in European markets in the second half of 2019 [36].

Figure 8) Volvo FL all-electric refuse collection truck [17]

As presented, it can be seen that the trucking industry is ready to bring the developed battery-electric refuse trucks to this sector, which not only they eliminate the tailpipe emissions, but offer also a considerable improvement in operational features, e.g., fuel economy, maintenance costs, and noise level. However due to their high purchasing cost (usually two to three times as expensive as conventional diesel trucks [16] along with the limited available in-use data, the waste private and public haulers may still be concerned about the improvement potential and the feasibility of electrification for their collection fleets. An energy and emissions life-cycle assessment can enlighten the implication of battery-electric refuse trucks in a collection fleet, being set the primary purpose of this study.

1.5 Literature Review

The notorious fuel consumption and environmental impact of conventional refuse collection trucks lead to emerging the alternative fuel-powered vehicles (CNG trucks, biodiesel trucks, hydraulic/electric hybrid trucks, electric trucks, etc.) to this sector. With low or zero tailpipe emissions and higher efficiency, alternative technologies can reduce the environmental impacts and/or the operational costs of diesel-powered refuse trucks.

Some studies have been conducted to analyze the financial and environmental impacts of adopting alternative technologies into collection fleets.

The studies mostly concentrate on fuel type of the truck to evaluate if the replacement of diesel fuel with alternative technologies can both environmentally and economically improve the operation. The majority of studies focused on the performance of the diesel-powered refuse trucks and CNG trucks a more common alternative adopted into collection fleets in recent years (about 10% [16]). Rose et al. (2013) assessed the life-cycle impact of CNG refuse collection trucks compared to the diesel counterparts considering their in-use operational data of a collection fleet operating in Surrey, BC, Canada. They used the GHGenius modeling tool with a Canadian database to conduct the life-cycle analysis, including both the fuel cycle and the vehicle cycle based on a 5-year lifetime. The assessment was done to determine the cost-effectiveness of the CNG-powered over the diesel-powered truck in terms of life-cycle cost per unit reduced GHG emissions ($/t$CO2_{eq}$). It was estimated that the operational energy use of the CNG truck is about 16% higher compared to the diesel-powered, while the total life-cycle energy use was approximately 3% lower due to higher energy required for diesel fuel production process. The total life-cycle GHG emissions of the CNG truck was estimated 6.08 kg$CO2_{eq}$/km, estimated about 24% less than the diesel refuse truck. A total lifetime cost savings of 330 and 650 $\$_{CAD}$ per reduced tonnes of $CO2_{eq}$ was estimated with no and 0.30 $\$_{CAD}$ per liter diesel fuel tax, respectively. As a result, presented in the paper, with switching to CNG truck although a net energy gain was not expected, the main advantages were the reduction of the overall GHG emissions (about 24%), and a total lifetime cost savings of 330 $\$_{CAD}$ per reduced tonne of $CO2_{eq}$ excluding fuel tax. In parallel, some studies focused more on emissions data captured from the tested engines. Walkowicz et al. (2003) conducted a chassis-based testing analysis to assess the emissions performance of a fleet of refuse trucks. In the study, it was determined that the tested Caterpillar C-10 CNG engine emits less CO_2 and NO_x emissions, but more CO compared to the similar Caterpillar C-10 diesel engine and considered the PM emissions were similar in both case. Some studies discussed the fuel economy along with fuel types. López et al. (2009) conducted a well-to-tank (WTT) GHG emissions analysis of three types of diesel, bio-diesel 30% (B30) and CNG refuse trucks from the collected operation data of a fleet in the city of Madrid, Spain. It was

founded that the diesel truck has the lowest tank-to-wheel energy consumption with (27.39 MJ/km) followed by the CNG truck (28.56 MJ/km), and the B30-powered truck was rated for the highest energy use with 31 MJ/km. However, the well-to-wheel GHG emissions were estimated about 1.8 $kgCO2_{eq}$/km, 2 $kgCO2_{eq}$/km and 2.3 $kgCO2_{eq}$/km for the CNG truck, diesel truck, and B30-powered truck, respectively. Hence, it is found that the diesel truck operates more efficient compared to the B30-powered truck with the same trend compared to the CNG truck, while the latter can result in a total GHG emissions reduction of about 13% compared to a diesel truck. The basis for the comparisons, the trucks' type, and the results vary significantly. However, results of these studies with a similar trend shows that the CNG option has lower life-cycle GHG emissions, but may not necessarily reduce the fuel cost. Furthermore, it is concluded that the low-carbon fuel alternatives emit significant GHG emissions in some capacity, and exploring for a better alternative is required to reduce the environmental impacts more effectively [37]. Zhao and Tatari (2017) have conducted a hybrid life-cycle energy use and GHG emissions assessment of different types of refuse collection trucks including the diesel, CNG, hydraulic hybrid, and battery-electric trucks based on the literature referenced or manufacturer's available data. The hybrid LCA method has covered the common process-based LCA, also used in [38], and the input-output analysis, by which the environmental impact of a product/process is defined by the relevant multipliers corresponding to related industrial sectors. Based on the results, and the CNG truck demonstrates the highest energy use, about 1.6 times greater than the diesel truck due to the considerably lower fuel economy, resulted in a 20% increase of the life-cycle GHG emissions in contrast to the results presented in [38]. For both trucks, estimated tailpipe GHG emissions account for approximately 80% of the total GHG impact of trucks, estimated about 800 tonnes of $CO2_{eq}$ and 900 tonnes of $CO2_{eq}$ for the diesel and CNG trucks, respectively over a 10-year expected lifetime. The hydraulic hybrid refuse truck was demonstrated the lowest life-cycle emissions impact due to its regenerative braking system which reduce operation phase's energy use and consequently tailpipe emissions compared to diesel or CNG trucks, but the tailpipe phase is still contributed the most to total life-cycle GHG emissions estimated about 600 tonnes of $CO2_{eq}$ over the lifetime [38].

Muncrief and Sharpe (2015) have categorized the HDVs assessed their fuel consumption and market in the European Union (EU) and compared the EU and the US fuel use trends and markets for the HDVs. In the paper, the inventory data of the HDVs are categorized in four vehicle's types as tractor-trailer trucks, rigid trucks (including refuse hauling trucks), buses and pickup trucks. Rigid/straight trucks follow tractor trucks have the second largest market sales of the HDVs in the EU, which for both categories the market is dominated by five European manufacturers, Daimler, Volvo, PACCAR, Volkswagen, and Iveco, while the last three are also dominant in the US market. As discussed in the paper, the HDVs in total emit 75% of the EU's CO2 emissions and it is also growing in the EU. They have suggested higher CO2 standards to change the trend while has been started in the US market with efficiency improvements. Within the presented inventories, the trailer-tractors accounts for 15% and 45% of the market sales while their fuel consumption are estimated as 60% and 59% of the total HDVs' fuel use in the US and EU, respectively. High fuel use of the trailers in the US is due to the high average annual traveled km of trailers in the US (191,000 km) which is 1.8 times higher compared to the EU (65,000 km). In case of rigid trucks, they are estimated to for 13% and 31% of the market sales and 16% and 20% of the total HDVs' fuel use in the US and EU, respectively. The testing data has provided shown average fuel use of 35 L/100km per truck in the EU, which represents a relatively constant fuel efficiency over 2000 to 2014. However, as the paper has discussed, in the US fuel consumption of the trailers has and expected to continue a downtrend between 45 to 30 L/100km through 2010 to 2030 due to the fuel efficiency improvements motivated by the US regulations which is implemented in two phases.

Maimoun et al. (2013) have conducted a parametric analysis of factors that will impact the deployments of advanced fuel technologies for Class 7 – 8 trucks through 2050, in the US. It is concluded that the greatest impact in reducing diesel consumption and GHG emissions of heavy-duty trucks is possible through the efficiency improvement for all powertrains, especially the conventional diesels which has been considered to still be the majority of the stock. As presented, the CNG trucks deployment is more dominant in urban fleets e.g., while can be viable in private sectors. However, in a technology assessment report released by the US National Research Council [39], it is analyzed that the fuel efficiency improvement corresponding to the rolling and/or drag resistances have less

impact on a refuse truck fuel use, while within high idling time and stop and go driving cycle the hybridization would have a considerable utility for refuse truck application.

Ercan et al. (2015) have studied the impact of natural gas composition on the exhaust emissions of a refuse collection truck on a chassis dynamometer over the William H. Martin Refuse Truck Cycle. Their results reveal a higher fuel economy, CO_2 and NOx emissions for higher hydrocarbons and consequently higher energy content gases, while, the emission levels have shown increases over the higher speed and collection phase of the refuse cycle.

Larsen et al. (2009) have analyzed the diesel consumption per tonne of waste using measured data of fuel use of collection trucks in two municipalities in Denmark. They have categorized the collection trips into 14 collection schemes, based on the type of housing and the waste mass at each stop. Based on their result the diesel consumption per tonne of waste changes between 1.4 to 10.1 L_D/t with n the collection schemes which is affected by the distance between the stops and the amount of collected waste per stop affects average fuel use between the schemes. The paper has presented that there is a significant reduction by 60% in the environmental impact of waste collection trucks by the transition from the Euro II standard to the Euro V standard between 1998 to 2008.

Talebian et al. (2018) have analyzed the CO_2 reduction potential through the road freight electrification (by battery-electric and fuel cell electric vehicles) in British Columbia (BC), Canada. In order BC can achieve its target to reduce the transportation GHG emissions by 64% by 2040, they concluded that 65% of conventional freight trucks should be replaced by the all-electric counterparts corresponding to the 100% of the market sales as early as 2025.

To consider the vehicle's operation conditions, some studies have discussed the effects of the driving cycle metrics on life-cycle GHG emissions and fuel consumption, as well [37], [40], [41]. Ercan et al. (2015) also conducted a hybrid life-cycle GHG emission analysis of a battery-electric and diesel bus over three transit drive cycles Manhattan, CBD (Central Business District), and OCTA (Orange County Transit Authority). It is estimated that within the US electricity generation's average GHG emissions (670 $gCO2_{eq}$/kWh) and depending on the transit drive cycle; the battery-electric bus may reduce the life-cycle GHG emissions by 51–68% compared to the diesel counterpart. About the duty cycle

development, few studies can find which have considered route and the operating characteristics of refuse trucks, including both the kinematic and hydraulic operations [41], [42]. The developed duty cycles can be a basis for analyzing the advantages of the alternative technologies being deployed in refuse collection service and used by fleet's owners or manufacturers to develop energy improvement strategies. Ivanič (2007) has developed a representative duty cycle of refuse trucks within a residential refuse collection activity in New York City. The recorded speed, route, engine operation and fuel use data has been analyzed to develop the micro trips representing several categories of the truck's activity. The representative duty cycle was developed to better understand the truck's operation and assess the potential of a hybrid hydraulic technology deployed in New York City refuse truck service. In research conducted by Soliman et al. (2010), a methodology to generate a representative duty cycle for refuse trucks including the speed trace, grade, mass, and hydraulic loads has been developed. In the study, the data has been collected from testing collection fleets operating in five cities in the US, and the statistical characteristics and distributions of field data have been matched to the generated duty cycles. The fuel economy over the developed duty cycles has been compared to in-use fuel consumption, using the vehicle simulator, ADVISOR [43]. The results found that the fuel economy estimates the average measured fuel economy for each testing city within 5% errors, except two cities due to loss of data during the collection time. In our research, the adopted duty cycle in Soliman et al. (2010) has used as a basis in the development of the representative hydraulic cycle, to better simulate the performance of refuse collection truck more closely to its operational activities.

The GHG emissions impact of vehicle electrification significantly depends on the driving conditions of the vehicle as well as the electricity grid mixture [16], [44], [45]. Tong et al. (2015) have studied the life-cycle GHG emissions of medium-duty and heavy-duty within natural gas pathways including the battery-electric vehicles (BEVs), and found that the electric vehicles are the alternative that can achieve significant emission reductions for medium-duty and heavy-duty trucks, and within the other alternative fuels (CNG and propane) the GHG reduction cannot attain the BEV advantage. It was estimated that using natural gas-produced electricity to power BEVs, a GHG emissions reduction of 31–40% for medium-duty BEVs and 31% for heavy-duty BEVs can be predicted compared with

gasoline or diesel counterparts. Lee et al. (2013) estimated the life-cycle energy use and GHG emissions of the diesel-powered and all-electric urban delivery vehicles, and concluded that over the New York City Cycle (NYCC) the reduction in energy use and emissions are 31% and 42%, respectively which are higher compared to the City-Suburban Heavy Vehicle Cycle (CSHVC) accounting for 5% and 19%, since the NYCC has a lower average speed and more frequent stops relative to CSHVC. It is estimated that energy use and GHG emissions ratios of BEV to diesel vehicle within ranges of 157 $gCO2_{eq}$/MJ to 279 $gCO2_{eq}$/MJ electricity generation mixture vary between 48 to 82% and 25 to 89%, respectively.

Zhao and Tatari (2017) have also predicted the impact of the electric power mixes on the upstream emissions of electricity, and consequently, the effectiveness of battery-electric refuse trucks in GHG mitigation. Based on the assumed fuel economy reported as the manufacturer's data, the life-cycle energy consumption of the diesel truck (within 3.90 mpg, diesel fuel economy) is estimated about 15,000 GJ over the expected 10-year lifetime; for the battery-electric refuse truck (within 3.33 kWh/mile fuel economy) it is accounted about 20,000 GJ over the lifetime with respect to the Western Electricity Coordinating Council (WECC) electricity power mix (composed of 25% hydropower). It was concluded that the most contributor to the life-cycle GHG emissions of the battery-electric refuse truck, likewise the life-cycle energy use, is the electricity generation phase. The total GHG emissions of the battery-electric truck were calculated over 1200 tonnes, $CO2_{eq}$ over the projected lifetime, which is even higher than the rate for the diesel truck estimated as 1000 tonnes, $CO2_{eq}$ over ten years. Although the all-electric truck has no tailpipe emissions, the life-cycle analysis has demonstrated that it can bring environmental advantages where the regional power generation source is primarily based on renewable resources with low GHG emissions intensity. It is reported that, within the reference study LCA assumptions and the US current average electricity source, the all-electric refuse collection truck does not have a lower GHG emissions compared to the diesel truck, unless in the regional grid mix a minimum share of 35% renewable energy and/or 50% natural gas power sources can be allocated.

As described, Zhao and Tatari (2017) study involves a life-cycle energy/emissions assessment of the newly-emerged all-electric refuse trucks, while the analysis has been

done based on the manufacturer's specification data. The literature is missing a comparative study that evaluates life-cycle emissions of conventional diesel and battery-electric refuse trucks based on the duty cycle's energy requirements, which can cover the operational activity of this type of vocational trucks. Since newly-introduced battery-electric refuse trucks have still been deployed in a few pilot projects (described in 1.4), and there was a lack for the availability of in-use data for the battery-electric refuse truck, in this study we estimate energy use of the electric truck as well as the diesel truck through a vehicle simulator tool, ADVISOR [43], to better assess the potential for energy improvement and emissions reduction through the adoption of the battery-electric truck in collection fleets.

1.6 Purpose of assessment and motivation

The impacts of climate change are noticed continuously which bring a strong need for effective actions toward emission reduction and global warming control. The environmental policies and pollution regulations along with rising fuel prices, urge the emission/energy-intensive waste collection fleets to improve the fleet's efficiency and consequently reduce the emissions and operational costs.

This research involves a municipal refuse collection fleet operating in Victoria, BC, as a case study. In 2010, the Saanich municipality committed to taking actions to move them towards their 2020 GHG reduction targets addressing the climate change at the regional level [45]. The 2020 targets have been set to a 33% GHG reduction in the community, and a 50% reduction for municipal operations compared to 2007 as a baseline. With updated targets in 2018, the actions have been continuously undertaken with the main focus in the transportation sector and buildings to reduce GHG emissions by 80% by 2050 and shift to a 100% renewable energy community [45].

The emissions data for the municipality reveals that the transportation sector is the largest GHG emitter responsible for 52% of the district's total emissions. It is increased by 7% between 2007 and 2016, due to an increase in vehicle size and gaseous/diesel fuel use within low fuel prices [45]. Effective actions to decrease transportation emissions are required if the municipality tends to meet its climate target. To this goal, a set of plans both in corporate and community-wide is undergoing through a Climate Action Plan [46]. Among them, some plans in the transportation sector are increasing the transportation

system efficiency, reduction in municipal fleet fuel use, promoting multimodal transportation, supporting the use of alternative fuel vehicles, e.g., PHEVs and BEVs by provincial rebates and incentive programs, planning to design and install more charging stations including DC fast charges. Within the municipality, the main contributor to the transportation carbon footprint is related to the fleet's diesel use in heavy-duty vehicles and trucks. Early reductions incorporate GHG emissions are made by replacing the light-duty fleet to more efficient vehicles and alternative technologies, e.g., deployment of EVs as well as car-sharing programs, resulting in a 53-tonne of CO2eqemissions reduction in 2017 compared to 2016 [46].

Within the heavy-duty vehicles it has been limited to switching to low carbon fuel options (e.g., biodiesel) and still, there is a significant potential to reduce their fuel consumption, which is account for 42% of Saanich fleet's total fuel consumption [45]. That encourage the municipality to monitors the market options for a further fleet replacement that would enable them to reduce heavy-duty fleet fuel use and emissions, which remains a constraint to achieve the 2050 corporate GHG reduction. Within the total HDVs, the refuse collection fleet contributes to a 55% share of heavy-duty fleet's fuel use and consequently a significant carbon footprint. Deployment of a battery-electric truck with zero tailpipe emissions can save annually about 20,000 L of diesel fuel per truck along with a considerable reduction in GHG emissions, taking advantage of the 98% renewable-based electricity in BC.

However, to perform an integrated assessment, detailed modeling is required to estimate the potential impact and commercial viability of the battery-electric refuse truck deployment from a life-cycle perspective. This, in turn, needs to develop a comprehensive energy consumption modeling in parallel with an adopted duty cycle representative of the fleet's operational activities. Within the Saanich refuse truck fleet, the main focus of this research is first to develop a duty cycle representative of refuse collection activity, second to get a detailed assessment of energy consumption of the battery-electric refuse truck compared to the diesel counterpart over a representative duty cycle, and finally estimate the potential for total fuel savings and emissions mitigation of the battery-electric refuse truck through an energy life-cycle analysis. Energy consumption of conventional and battery-electric trucks is estimated with a vehicle simulator, ADVISOR [42]. A key point

of the vehicle simulation is to model the vehicle's systems/sub-systems accurately, for which the application of a refuse truck the hydraulic load (pickup/pack/dump loads) is a considerable energy use component and should be applied through the representative duty cycle. Thus, the comprehensive modeling of the trucks in the simulator parallel with the developed duty cycle gives a better understanding of energy use of refuse trucks within their vocational application. Moreover, estimating energy use over the duty cycle can provide the necessary data for selecting the all-electric refuse truck with the battery matched to the duty cycle energy demand.

By conducting an fuel-based GHG emissions analysis, the potential for fuel cost savings as well as GHG emissions reduction of the battery-electric refuse truck is estimated over the perspective lifetime. The fuel-cycle emissions analysis considers both upstream and downstream GHG emissions of the diesel fuel/electricity, with which the impact of the grid's GHG intensity on upstream emissions of electricity can be examined. By conducting the Total cost of ownership (TCO) assessment, it evaluates the competitiveness of the BE-RCT compared to the diesel counterpart as well as its potential for operational cost savings over the trucks' lifetime. Moreover, the financial analysis can assist the Saanich municipality in taking proper deployment plans for future replacement of diesel trucks in their fleets.

1.7 Thesis contributions

This research presents an analysis of fuel consumption and GHG emissions of refuse trucks, the conventional diesel and newly-introduced all-electric alternative. It examines the benefit of the battery-electric technology adoption for a refuse fleet operating in Saanich municipality in Victoria, BC; however, the assessment methodology can be used extensively for other fleets in this application. The thesis's specific research contributions are summarized as follows:

- The study implements fuel consumption model for the refuse truck application using the ADVISOR simulator. Vehicle simulation is carried out for two different technologies; the conventional diesel and battery-electric refuse trucks. In developing the simulation model, the vehicular parameters are being updated based on the refuse trucks' specification.

- The research considers a case-study refuse truck fleet operating in Saanich municipality in Victoria, BC, Canada. The fuel consumption model evaluates the energy use of the D-RCT and BE-RCT based on the Saanich fleet's operational characteristics and annual utilization and determines the potential of the BE-RCT in diesel fuel saving for the proposed fleet.
- This study proposes a refuse truck duty cycle, considering the stop-and-go nature of performance along with their vocational application for waste collection. The parasitic hydraulic load for trash collection/dump is considered and applied in the auxiliary load (which is not specifically discussed in previous studies). Correspondingly, the incrementally-added payload mass is implemented through the time variable mass cycle. The trip route and road gradient data, which are not available in the employed dynamometer driving cycle, are synthetized for a selected collection area in the municipality as a case study. The total duty cycle is obtained through the composition of the speed profile, grade data, mass cycle, and vocational auxiliary load.
- A fuel-cycle GHG emissions analysis is conducted considering in-use GHG emissions associated with the fuel production and distribution, as well as GHG impacts associated with the consumption of fuel for D-RCT and BE-RCT. It evaluates the WTW GHG emissions of both technologies and helps with estimating the potential of the BE-RCT in GHG mitigation compared to the conventional counterpart.
- This research gives the financial analysis of the D-RCT and BE-RCT to estimate the annual operational costs as well as the lifetime ownership cost for both trucks. These evaluate the competitiveness of the BE-RCT compared to the diesel counterpart for the proposed fleet and help them with an informed choice for the deployment of the BE-RCT in their fleet. The decision criteria for policymakers are recommended in order to highlight the feasible deployment scenarios of the BE-RCT into waste collection fleets.

1.8 Thesis overview

This chapter has provided an introduction to refuse trucks along with a literature review on refuse collection trucks, as well as the motivation of doing this research. Chapter 2

presents the methodology for developing the refuse truck duty cycle considering all auxiliary load and configurations modeled in ADVISOR for diesel and battery-electric refuse trucks to estimate the power flow and energy consumption in this application. Chapter 3 assesses the energy use and fuel-cycle emissions analysis of both technologies over the duty cycle, along with a sensitivity analysis investigating the impact of critical parameters (the BE-RCT battery capacity, route grade, mass, and auxiliary load) on energy use and GHG emissions. It also recommends an appropriate battery capacity for the battery-electric refuse truck based on the adopted duty cycle. It ends with a TCO analysis to estimate the feasibility of battery-electric refuse truck over the conventional counterpart based on energy use and operational and maintenance costs. Chapter 4 summarizes the thesis findings and proposes outlines for future research work.

Chapter 2: Input data and duty cycle modeling

The primary objective of this study is to quantify energy consumption and GHG emissions rates for conventional diesel refuse collection trucks (D-RCTs) and battery-electric refuse collection trucks (BE-RCTs). To examine the performance and energy consumption, models of both trucks are developed in the Advanced Vehicle Simulator (ADVISOR) [43], and the simulation is conducted over a generated representative duty cycle for refuse trucks. The simulation results provide a thorough overview of the performance of electric trucks over the duty cycle in comparison to diesel trucks generally used in this application. In this study, the modeling is done based on the data for a fleet of 13 refuse collection trucks operating in Victoria, BC. The data shared through a collaboration between the Saanich municipality and the University of Victoria. The simulation result of the diesel truck is validated to the in-use fuel consumption of the municipality fleet. Moreover, based on the captured fleet duty, the required battery capacity for an electric refuse truck is estimated to assist the municipality in future planning for the adoption of battery-electric refuse trucks. In following sections, we provide the fleet statistics data and describe how the fleet representative duty cycle is being adapted and applied to the simulation model in ADVISOR.

2.1 Adapted data: Saanich municipality fleet

The Saanich municipality owns 309 vehicles (LDVs, MDVs, HDVs, and equipment) in total, with the overall fuel consumption and equivalent CO_2 emissions of 883,000 L and 2201.65 tonnes in 2017, respectively. A break-down of the fleet's vehicle and operational fuel use and emission rates, reported by the municipality are presented in Table 1 and Figure 9. From late January 2018, the data for vehicle operation of the entire fleet was stored on the server "Fleet Complete" [47], through which the activity data of operation, such as average speed, max speed, traveled distance, moving/idling duration, and GPS data is accessible. Out of the total fleet, there are 13 heavy duty refuse trucks, accounting for 27% of the total heavy-duty vehicles in operation. The fuel consumption of the refuse collection fleet in 2017 is reported as 203,808 L of B5 diesel, which is about 23% of the total fleet and 55% of the heavy-duty vehicles fuel consumption. The accumulated kilometers traveled of 161,557 km is recorded in 2017 for ten trucks in operation. The

assumed life-cycle of refuse trucks is about seven years. Having resupplied in 2014, the next replacement time is expected to be in 2021.

Table 1) Saanich fleet statistics

Fleet	No. of vehicle	% of total	Fuel use (1000L/y)	% of total	Tailpipe $CO2_{eq}$ emissions (t/y)	% of total
LDV	164	53%	339	38%	774	35%
MDV	41	13%	112	13%	293	13%
HDV	42	14%	369	42%	969	44%
Equipment	62	20%	63	7%	165	8%
Sum	309	100%	883	100%	2201	100%

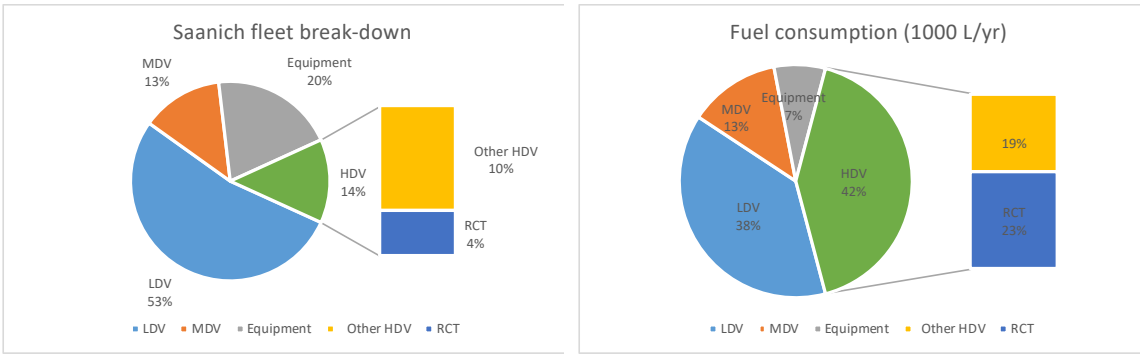

a) Fleet break-down b) Vehicle fuel consumption

Figure 9) Saanich vehicle statistics: a) Fleet break-down, b) Fuel consumption

Table 2 and Table 3 [48] give the fleet characteristics and refuse truck's specification, used as a basis for the simulation of the refuse truck presented later in 3.2.1.

Table 2) Saanich refuse fleet specification in 2017

No. of truck	13
Type of truck	Peterbilt 320
Fleet annual fuel consumption (L_D/y)	203,808
Fleet annual traveled kilometers (km/y)	161557
No. of trucks in operation per day	10 out of 13
Annual duty days per vehicle	234
Annual fuel consumption per vehicle (L_D/y)	20,380
Annual traveled kilometers per vehicle (km/y)	16,155

Table 3) Refuse truck fleet specification

Equipment	
Make	Peterbilt (Labrie Automizer)
Model	320, Automated Side-loader
Year	2014
Licensed GVWR (kg)	28,123
Tare (kg)	15,070
Payload (kg)	9152
Transmission	
Make	Allison
Model	3000 Rds-P Trans Gen5
Type	Auto 6 Speed
Diff. Ratio	6.14
Engine	
Make	Paccar
Model	Px-9 370 hp
Size	8.9L
Horsepower	320@2000rpm
Fuel	Diesel
Aux. Equipment	
PTO Adapter- Front Engine Mount	
Pump	Parker Pump Model P350 Dual Output Body (packing): 94.1 mL displacement, 2” Gear width Arm (pickup): 83.6 mL displacement, 2.25” Gear width

2.2 Refuse truck duty cycle

Energy consumption of any vehicle depends on its driving and operational condition, titled the vehicle duty cycle. Side-loader refuse trucks, the purpose of this study, are generally used for waste collection purpose in residential areas and their operation includes urban driving, highway driving, waste collection and dumping [8]. Their operation includes low driving speeds with frequent stop-and-go and high idling time, vocational loads applied for use of mechanical devices (lift, compactor), and large payloads, which brings about

high fuel consumption and emission rates. Through the collection route, they travel between pickup locations (residential houses), loads and compacted the trashes in the truck's body. The trash bins are picked from the side, lifted either manually (semi-automated side-loaders) or automatically (automated side-loaders) by a mechanical arm and flipped down to get the trash emptied into the truck's hopper,

Figure 10 [14]. Through the dumping sequence, using the hydraulic power the tailgate is opened and the truck's body is lifted to unload collected trash by the gravity force, next the body is lowered followed by the tailgate closure. The trash loading and unloading sequences form the mass cycle of the refuse collection truck, which considers the waste mass added incrementally to the truck during the collection phase and unloaded in dumping sequence.

(a)

(b)

(c)

Figure 10) Peterbilt 320 refuse truck hydraulic arm operation: a) Reach a trash bin, b) Grab a trash bin, c) Lift/unload a trash bin

In addition, the waste loading/unloading applies corresponding cycles of hydraulic power required through the pickup/packing and dumping functions. The duty cycle of a refuse truck, which should consider both the driving condition and the vocational operation of the vehicle, is defined as a combination of road load variables (including the driving speed and road grade) and the mass cycle along with corresponding hydraulic loads. Following, the development of the driving cycle, as well as the mass cycle and hydraulic load, will be described.

2.2.1 Driving cycle

The daily activity of a refuse truck consists of traveling phase, including trips from the depo station to the residential collection area, from the collection area to the dumping site and from the dumping site to the main depo, and the collection phase consists of the trips through the collection routes, where the waste mass is loaded to the truck by means of the hydraulic system.

Since one-hertz speed data of fleet's trucks were not available, NREL Neighborhood Refuse Truck Cycle (NRTC, Figure 11) [49] is used to develop the total speed profile data. It is a chassis test cycle presented the operation of an automated side-loader refuse truck and developed by the US DOE National Renewable Energy Laboratory (NREL) for the Environmental Protection Agency's (EPA) SmartWay program [49]. Selected cycle metrics of the test is provided in Table 4:

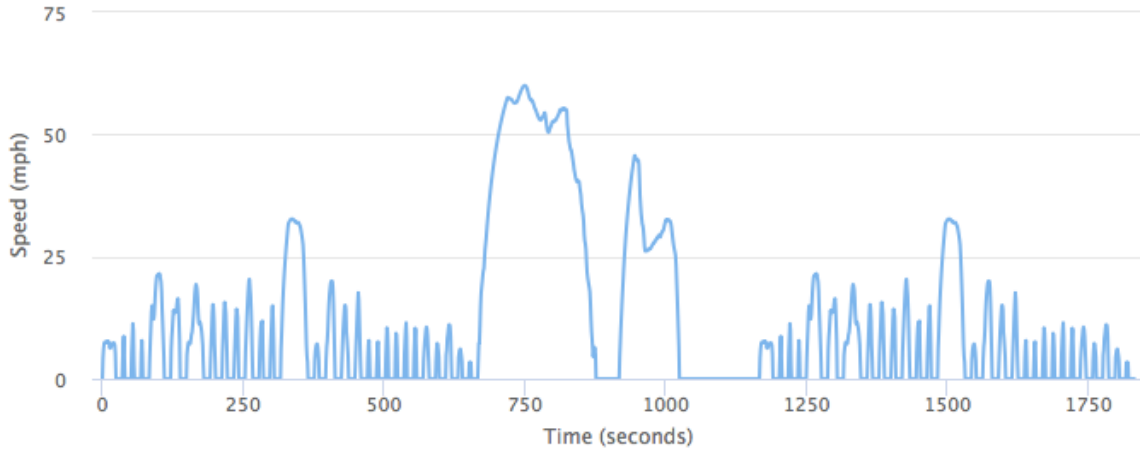

Figure 11) NREL Neighborhood Refuse Truck Cycle [49]

Table 4) NRTC driving cycle metrics [49]

Driving cycle	Time (min)	Distance (km)	Ave spd. (km/h)	Ave driving spd. (km/h)	Max spd. (km/h)	Stop (#)	Stop/km
NRTC	30.55	9.16	18	34.6	96.5	60	6.55

The cycle consists of two collection phases, each taking about 665 s with 29 stops and the traveling trips to and from the dump yard. We use these trips data as the sub-trips to generate the total drive cycle of the refuse truck (Figure 14-a) including the collection phase plus the trips from and to the main depo, the dump area, and the collection area.

For the purpose of this study, one of the typical operation routes of the truck id#18572 is used (Figure 12) to develop the total road cycle. The average data recorded for one month (20 working days) operation of the truck, obtained from the 'Fleet Complete' server, is presented in Table 5:

Table 5) Saanich refuse truck average activity data over a twenty-day working period

Truck no.	Time (hr/day)	Distance (km/day)	Ave spd. (km/h)	Ave driving spd. (km/h)	Ave max spd. (km/h)	Idle time (%)
'18_572'	6.66	63.4	10.1	26.5	36.2	61.8

The average daily trip distance is 63.4 km, including the traveling phase and collection phase, through which about 670 household's bins are picked up. The distance from the depo to collection area is 4.1 km, from the collection area to dump 12.7 km and from the dump yard to the depo is 8.5 km. Using the NREL collection cycle with 29 stops for each collection segment, the total collection phase is assembled from 23 collection segments. The road elevation data is extracted from the Google earth (Figure 13) and TCX converter tool [50] and smoothed by applying a Savitzky-Golay filter [51] to capture the changes in elevation and eliminate the errors. By applying the filtered elevation data through the traveled distance, the grade profile is obtained and is combined with the speed trace to define the driving cycle, presented in Figure 14-b.

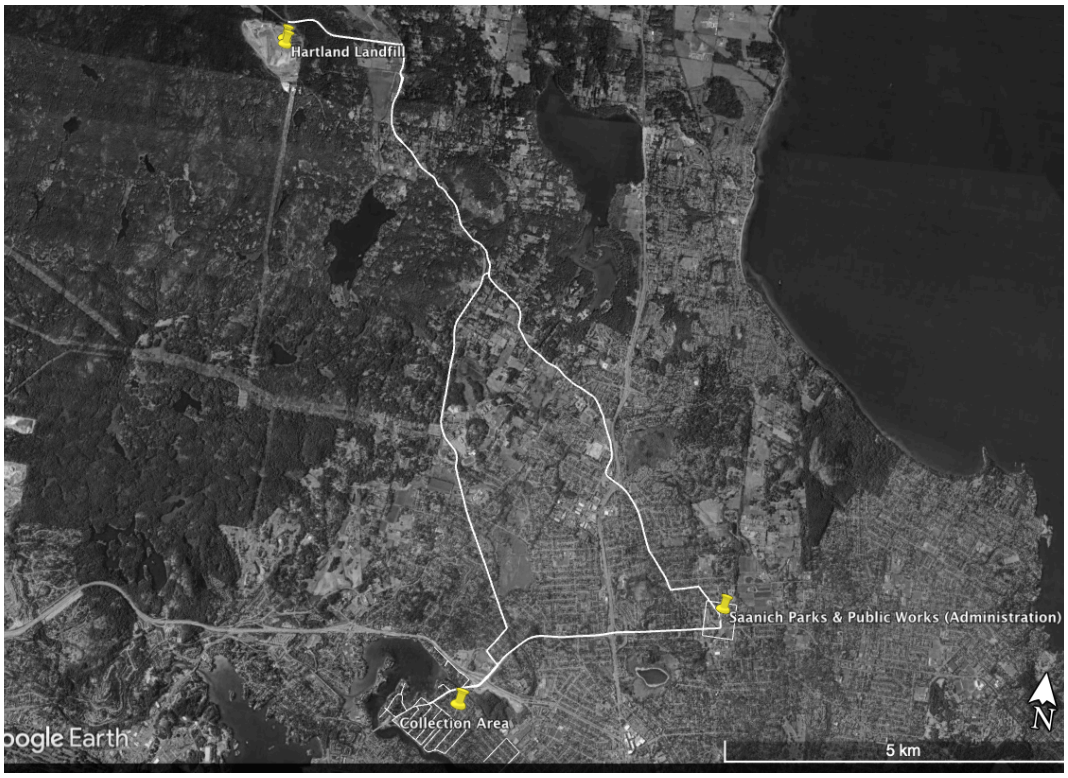

Figure 12) Refuse truck traveling routes

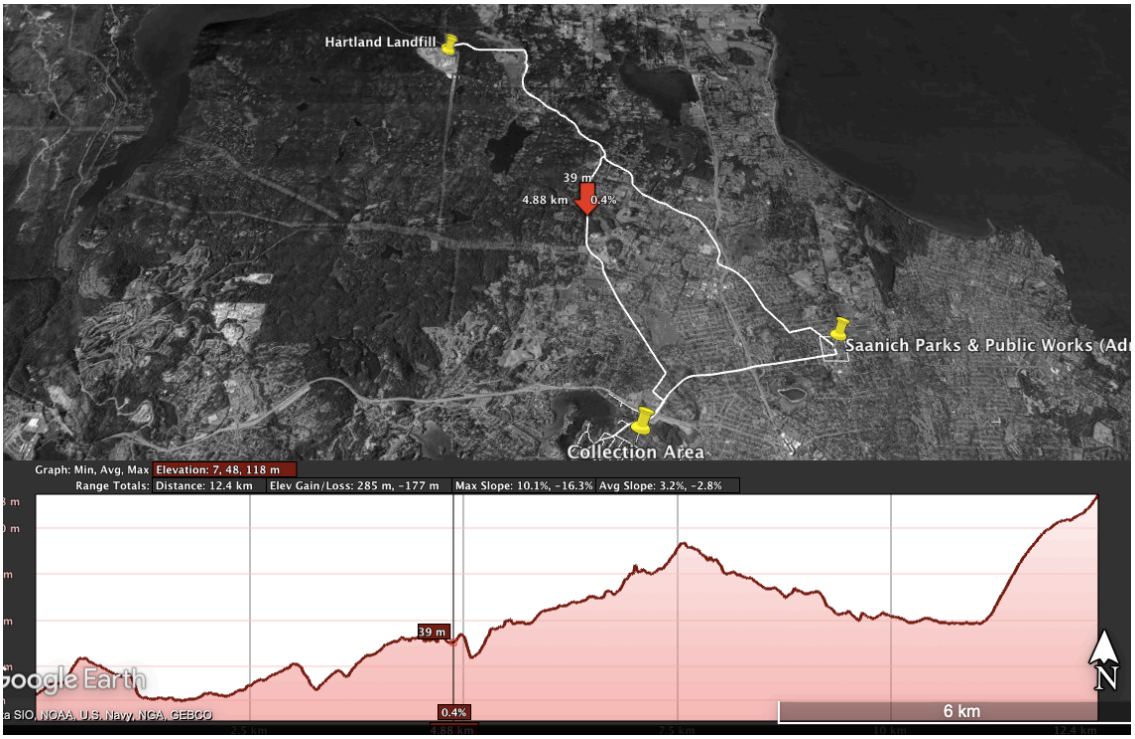

Figure 13) Elevation profile of the refuse truck travelling route (collection area to landfill)

Table 6) Refuse truck duty cycle (RTDC) metrics

Duty Cycle	Time (min)	Distance (km)	Max speed (km/h)	Ave speed (km/h)	Ave driving speed (km/h)	Idle time (%)	Stops (#)	Stop/km	Ave / max upgrade (%)	Ave / max downgrade(%)
RTDC	290	65.5	96.6	13.6	26.6	48.4	669	10.2	3.2/8.8	-3 /-7.5

2.2.2 Mass cycle

Given the municipality report, refuse trucks are operating on a nine-day cycle every two weeks. Out of 13 trucks, on each operation day ten trucks are in operation, five trucks for the garbage collection, five for the organics collection, and the remaining three will be spare. The only exception is for months of April to June when there will be an additional truck in operation due to the extra organics loads. The average daily tonnage for operating trucks is presented for each month in 2018, in Table 7.

Table 7) Average collected refuse mass (t/day) in 2018

2018 Average daily tonnage	Total collected garbage mass	Garbage mass per truck	Total collected organic mass	Organic mass per truck
January	38.76	7.75	32.19	6.44
February	34.62	6.92	28.48	5.70
March	35.06	7.01	32.24	6.45
April	38.92	7.78	43.19	7.20
May	38.88	7.78	50.39	8.40
June	36.81	7.36	41.93	6.99
July	36.68	7.34	36.05	7.21
August	39.02	7.8	35.2	7.04
September	40.52	8.1	36.52	7.30
October	36.45	7.29	38.26	7.65
November	39.09	7.82	39.25	7.85
Average		7.54		7.11
Mean of the mean (per truck)	7.83			

With one extra truck operating during spring months, the average daily tonnage of the collected refuse is 7.83 t/day for each truck, adjusted for the simulation. To derive the mass

cycle, it is assumed that the empty truck travels to the Collection Area, and through the collection phase, one bin with an average of 11.7 kg is collected at each stop (household). Next, the total waste mass is transferred and dumped to the dump yard, and the truck travels back to the main depo.

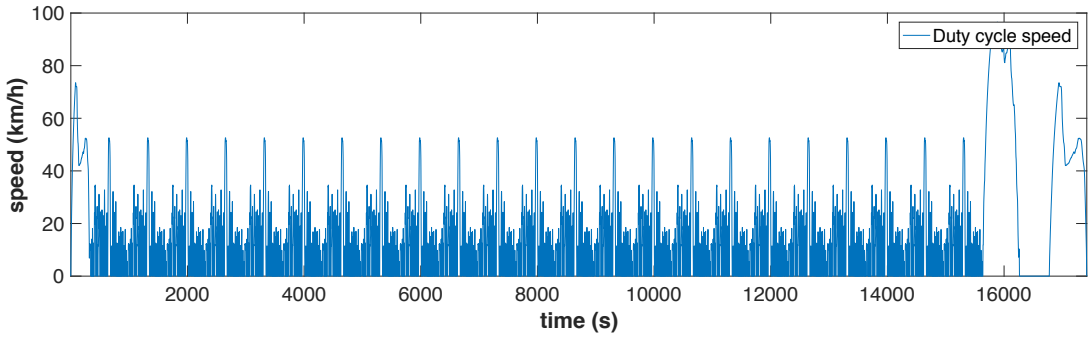

(a)

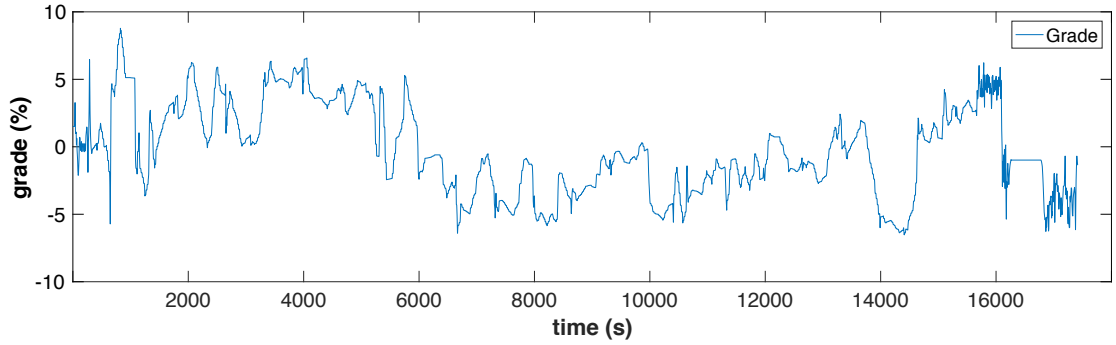

(b)

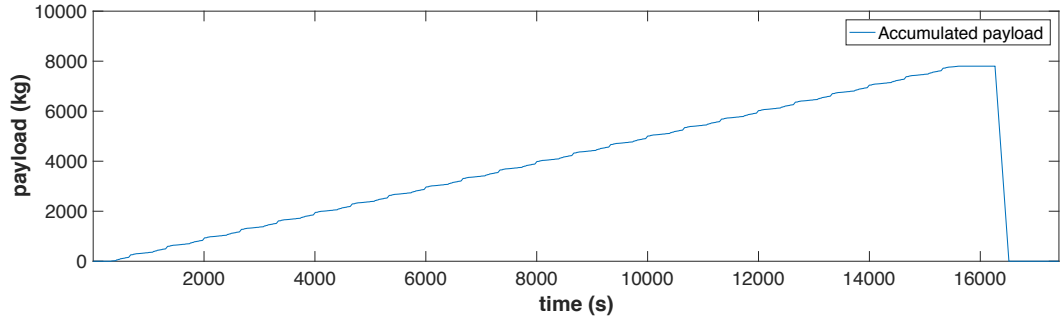

(c)

Figure 14) Refuse truck representative duty cycle a) Speed trace, b) Route grade, c) Mass cycle

A total average of 7830 kg has been considered in the simulation, and sensitivity analysis will be presented in Chapter 4 to explain the effect of the loaded mass on energy

consumption of the refuse truck. Figure 14-a, Figure 14-b, Figure 14-c present the adapted speed profile, route grade and mass cycle of the refuse truck, respectively through a daily operation as a representative RTDC.

2.2.3 Hydraulic load cycle

The hydraulic load consists of the overall required power for pickup, packing, and dumping of the waste along a given route. For the purpose of this study, the pump model, the required hydraulic pressure for refuse lift/pack/dump and the method for applying the hydraulic cycle are adopted from [42], using the collected measured data of refuse trucks operating in five different cities in the US. To develop the hydraulic cycle, a pickup/packing micro hydraulic load is considered through each stop from one household to the next one on the collection route. The micro hydraulic load is defined at each stop as the power required for the pump to provide the hydraulic pressure, which either runs on a direct drive shaft from the engine of a diesel RCT, power take-off (PTO) system or is driven by an electric-motor in a battery-electric refuse truck. As reported in [42], depending on the number of bins at each stop and operator function, different numbers of pressure spike were found in each pick-up/packing cycle. The hydraulic dump cycle is considered once when the truck stops to unload the waste at the dump yard. Based on the recorded dump pressure sequences presented in [42] the total time for the cycle is about 260 sec with 200 bar maximum hydraulic pressure. The pickup/packing and dumping hydraulic pressure sequences are presented in Figure 15 adopted based on the recorded sample cycles in [42]. The pick-up/packing/dumping power cycle is developed based on the mechanical power corresponding to the pump outlet pressure. Figure 16 presents the manufacturer's data for the mechanical power required at the inlet shaft within the pump speed and specific gear widths. The data provided in Table 8 is based on the pump output flow at the maximum rated pressure, 190 bar and 210 bar for the arm and body hydraulic system, respectively [52].

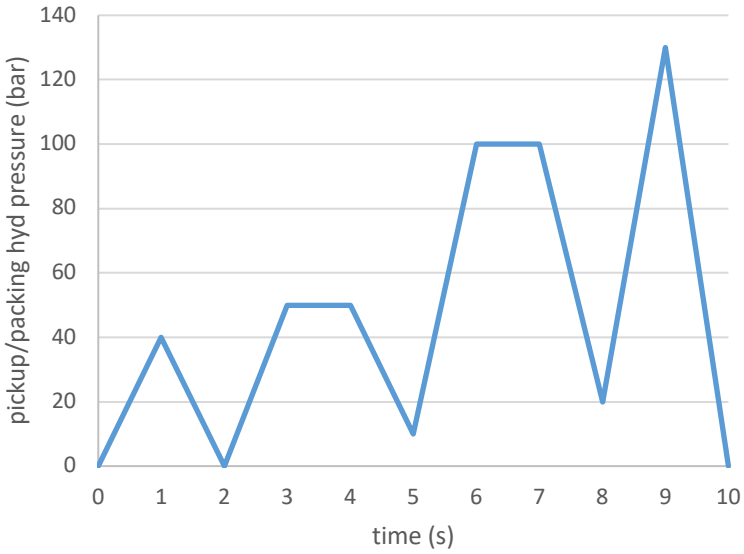

(a)

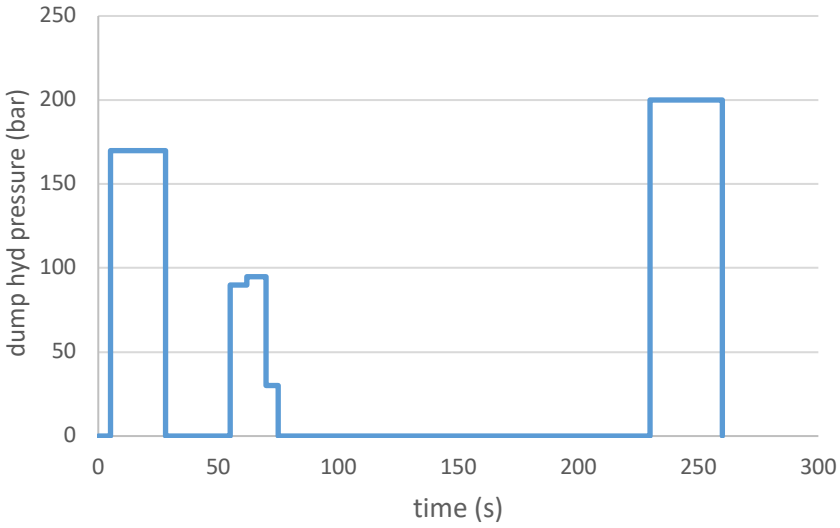

(b)

Figure 15) Hydraulic pressure cycles a) Pickup/packing pressure, b) Dumping pressure

In case of the diesel RCT, the pump speed considered the same as the engine's and the hydraulic power developed at the correspondent idle speed at each stop (650 rpm, based on the engine specification data described in 3.2.1). Given the pump speed and the full-load power at the inlet shaft, the proportional mechanical power is determined at each pressure level representing the hydraulic cycles as shown in Figure 17.

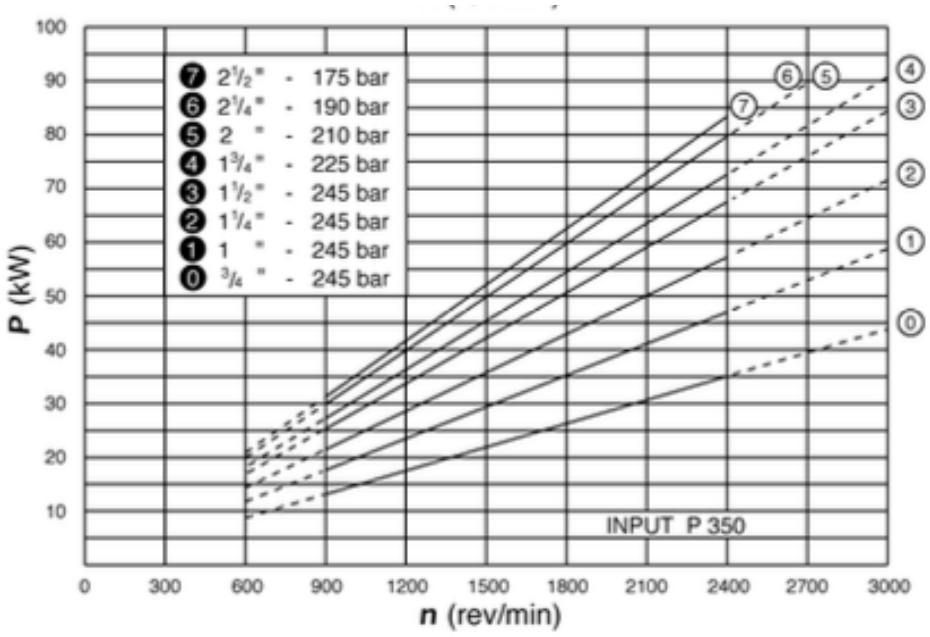

Figure 16) Pump input power at the maximum rated pressure [52]

Table 8) P-350 Parker pump, performance manufacturer data [52]

P-350 Parker pump	Arm	Body
Gear width (inch)	2 1/4	2
Rated pressure (bar)	190	210
Speed (rpm)	Power @ inlet shaft (kW)	Power @ inlet shaft (kW)
600	28	29
900	38	39
1200	47	49
1500	57	58
1800	66	68
2100	76	78
2400	85	87

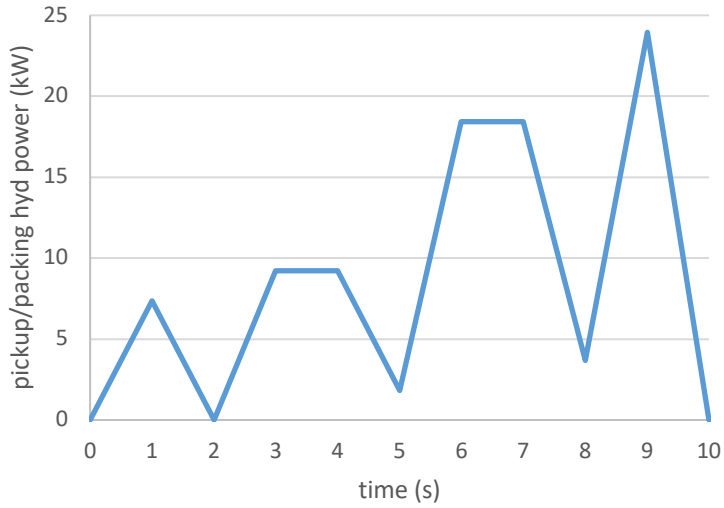

(a)

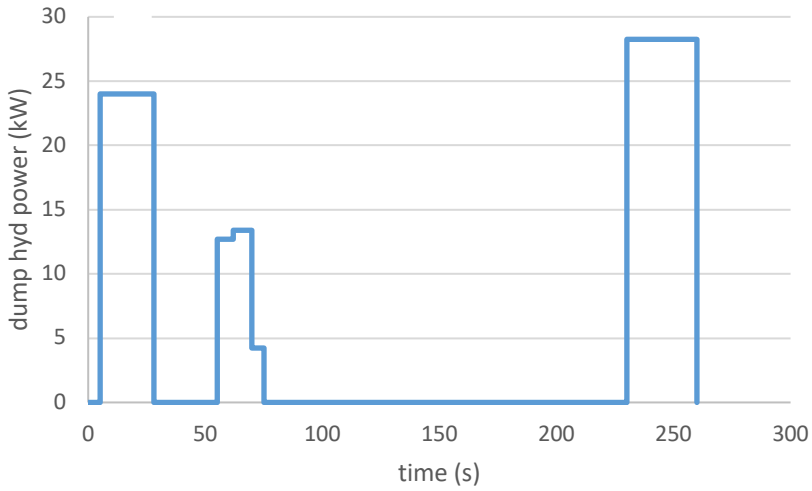

(b)

Figure 17) Hydraulic load cycles: a) Pickup/packing power, b) Dumping power

On a diesel refuse truck, the hydraulic pump can be disengaged, but typically it is operating continuously, and the flow is adjusted through a relief valve. During the traveling phase, with no pick-up/packing/dumping vocational load, the valve will be activated and sends the unused oil flow back to the oil tank. The pump is turning at the engine's rpm during the transportation at pressures below 20 bar [52], which includes a low-pressure hydraulic load added to the vocational load. Considering that the traveling phase takes about 40% of the total trip, this parasitic power taken from the engine is still considerable. Hence in the simulation of the D-RCT, continuous operation of the hydraulic pump over

the driving phase is considered in hydraulic load modeling to evaluate its effect on fuel use. Ultimately, the total hydraulic load of the D-RCT is defined by applying the adopted pickup/packing cycle through each collection stop, the dump load and the low-pressure idle hydraulic load through the traveling phase, which is presented in Figure 18.

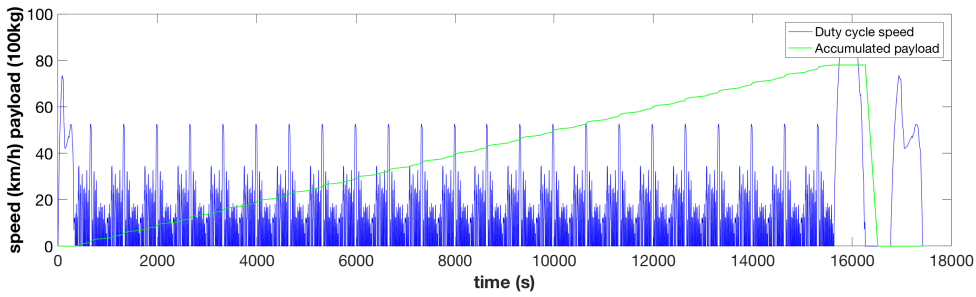

(a)

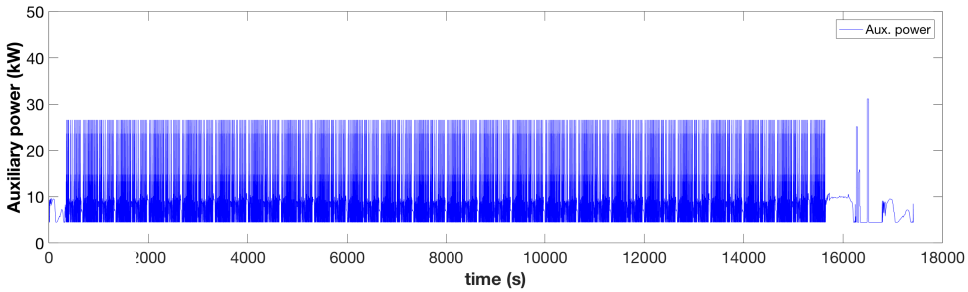

(b)

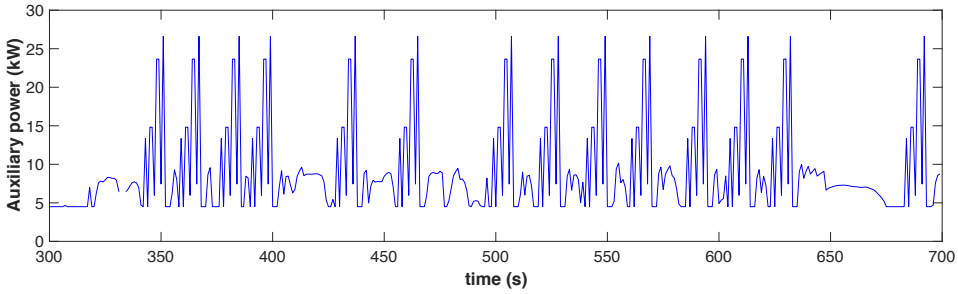

(c)

Figure 18) Accessory hydraulic load of the D-RCT: a) Speed profile, b) Total auxiliary power, c) Higher resolution of example auxiliary power including the hydraulic load

For a BE-RCT, it is assumed that the mechanical power required for pickup/packing/dumping functions is the same as that of the diesel RCT, and the corresponding hydraulic cycle is developed based on the required mechanical load and efficiency of the auxiliary electric-motor. However, for the BE-RCT, the no-load operation

of the hydraulic pump and the corresponding energy losses are eliminated as it is assumed that the auxiliary motor will be turned on when the vocational hydraulic load is required. The total vocational load developed for the BE-RCT is presented in Figure 19.

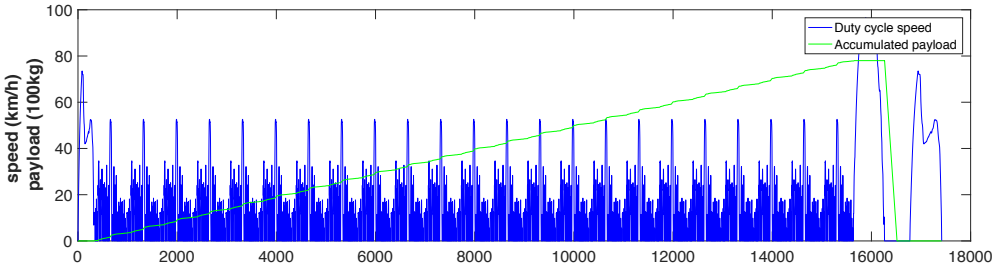

(a)

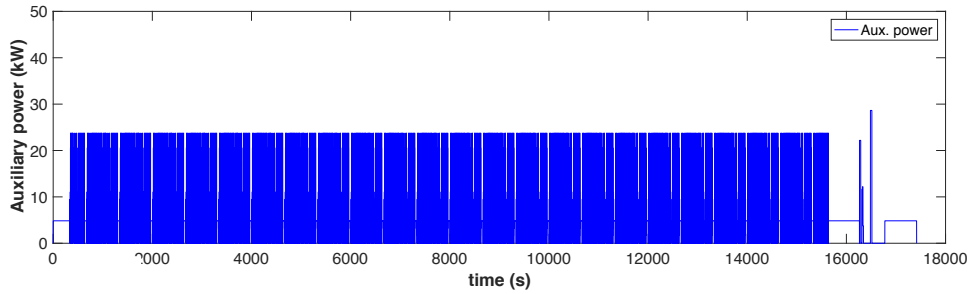

(b)

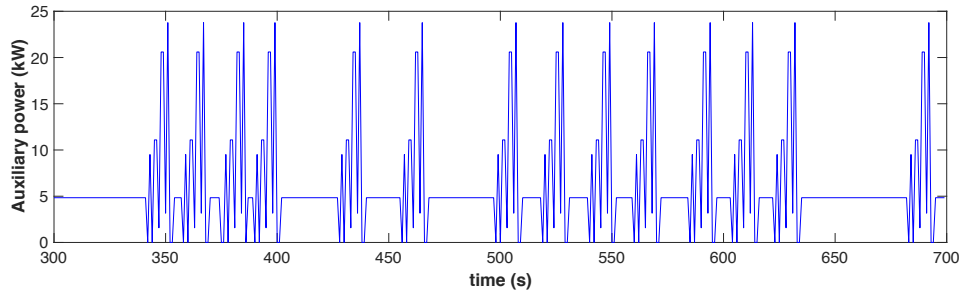

(c)

Figure 19) Accessory hydraulic load of the BE-RCT: a) Speed profile, b) Total auxiliary power, c) Higher resolution of example auxiliary power including the hydraulic load

Next section, the modeling approach input parameters for the simulation of RCTs will be described in details.

Chapter 3: Modeling and simulation

3.1 Modeling

As motioned earlier, in this study ADVISOR (Advanced Vehicle Simulator) [43] is used to simulate energy consumption of conventional and battery-electric refuse trucks driven on the representative duty cycle. ADVISOR is a set of models to simulate drivetrain components of a vehicle to analyze the performance and energy consumption running in MATLAB and Simulink environment. It can be applied to simulate different technologies including conventional diesel/gaseous vehicles or the advanced-technology vehicles (i.e., HEV/PHEV/BEV, and fuel cell technology) over a variety of standard or developed drive cycles. In addition to the standard models and drive cycles provided by the software developer (NREL), flexible modeling can also be conducted by applying user-defined drivetrain component blocks, control logic, and drive/duty cycles to simulate a vehicle. The vehicle model composed of the component blocks is connected to the defined duty cycle to understand how the power is provided with operations of the powertrain components and estimate energy consumption over the duty cycle.

The total energy consumption is the summation of energy required to provide the tractive effort, and the accessory loads should be estimated. In case of a vocational vehicle, e.g., a refuse truck, in addition to the standard accessory loads, the vocational loads (e.g., refuse pickup/packing, boom operation,...) can account for a considerable level of energy consumption over the duty cycle. Thus for refuse trucks application the hydraulic load cannot be neglected, and in the simulation, it is considered through the generated hydraulic cycle described in 2.2.3. For the conventional diesel heavy-duty vehicles, another noticeable term is fuel use when the vehicle is idling. In this study, the idling mode refers to the period when the refuse truck is stopped and not supplying the vocational load (the hydraulic pickup/packing/dumping loads) , but the engine is still on. In case of the battery-electric truck, likewise the typical electric vehicles, this term is eliminated as the traction motor is automatically turning off when the vehicle comes to a stop and restarting it instantly when it is started to move. Summing up, the total energy consumption for the refuse truck consists of energy required for the truck to meet the duty cycle includes the road load, the hydraulic load, and the electrical/mechanical accessories.

In the following section, we describe first the data flow path in ADVISOR and its approach for estimating the required power from energy source, and next the configuration and assumption for developing the diesel and battery-electric refuse trucks models is presented.

3.1.1 ADVISOR approach

ADVISOR is a combination of backward and forward simulation, more closely to the backward approach [43]. The backward simulation estimates the required torque and speed of each component based on the requested wheel speed. It can provide the power demand at each time step required to follow the specified duty cycle but is deficient in predicting the maximum performance of the vehicle. The forward modeling is based on a driver model that simulates driver commands to meet the duty cycle [53]. The engine torque is passed down through the driveline and translated to a force to compute the vehicle speed at the wheel. This model type can provide maximum effort calculations but are slow in computing vehicle behavior [54]. Figure 20 and Figure 21 show the Simulink model of a typical conventional and battery-electric vehicle, respectively presenting the data flow between the components/blocks. The backward approach transfers the required torque/speed/power to the upstream component. While the forward-facing model passes the available torque/speed/power data down through the drivetrain.

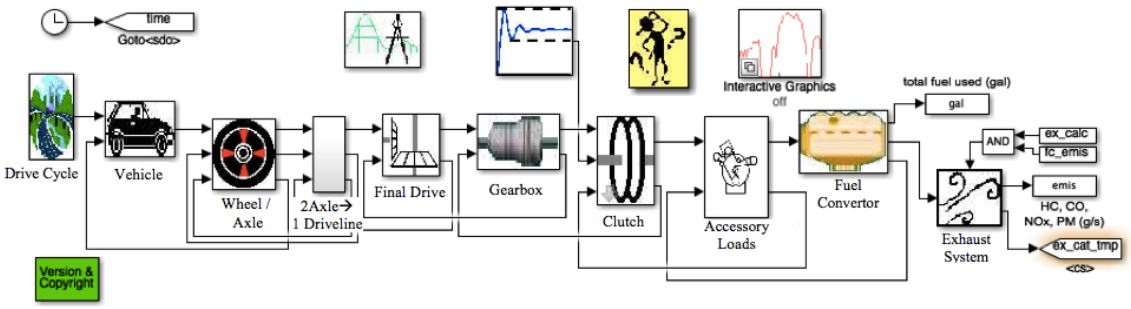

Figure 20) ADVISOR top-level block diagram of a conventional vehicle [55]

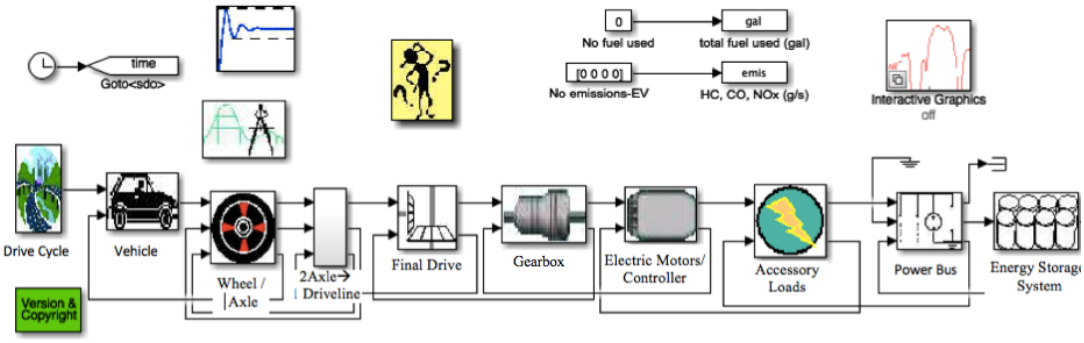

Figure 21) ADVISOR top-level block diagram of a battery-electric vehicle [55]

In the following section, the ADVISOR approach to compute energy consumption is described in detail.

3.1.2 Power flow description

Given the duty cycle, the force required to move the vehicle is defined at each time step from the requested speed profile. The tractive force is required to overcome the road resistance forces including aerodynamic drag, tire rolling resistance, gravitational force, and inertia, which is presented below by the classic longitudinal road load equation [56]:

$$F_{tr} = F_{drag} + F_{rolling} + F_{climbing} + F_{ineria} = \frac{1}{2}.\rho_{air} C_D A_f v^2 + (C_{r0} + C_{r2}.v^2).\cos\theta\,.m_{veh}.\mathrm{z} + m_{veh}.g.\sin\theta + f_m.m_{veh}.a_{pos} \quad \text{Equation 1}$$

where ρ_{air} is the air density (kg/m3), A_f is the frontal area of the vehicle (m2), v is the vehicle speed (m/s), C_{r0} and C_{r2} is the zero and second order tire rolling friction coefficients, θ is the road grade angle (rad), m_{veh} is the vehicle mass (kg), f_m is the mass factor to convert the rotational inertia of the powertrain to translated mass and a_{pos} is the vehicle acceleration (m/s^2). The traction power is expressed as [56]:

$$P_{tr} = F_{tr}.v = \frac{1}{2}.\rho_{air}.C_D.A_f.v^3 + (C_{r0} + C_{r2}.v^2).\cos\theta\,.m_{veh}.g.v + m_{veh}.g.\sin\theta\,.v + f_m.m_{veh}.a_{pos}.v \quad \text{Equation 2}$$

where P_{tr} is the instantaneous tractive power to drive the vehicle at speed v. Depending on the traction force, the vehicle operation mode during a period can be: traction mode (if $F_{tr} > 0$), or coasting mode (if $F_{tr} = 0$), or braking mode (if $F_{tr} < 0$). During the traction mode, the vehicle moves with speed higher than the coasting speed, and the tractive force overcomes the inertia and resistance forces. In coasting mode, the vehicle propulsion

system is not working, and its kinetic energy is decreased to overcome the resistance losses, while the vehicle speed remains constant at the coasting speed. Through the braking mode, the vehicle decelerates with speed lower than the coasting speed and the kinetic energy of the vehicle is being dissipated by the brakes or can be restored partly with a regenerative braking system. The braking power (P_b) is defined as:

$$P_b = F_b.v = f_m.m_{veh}.a_{neg}.v - \frac{1}{2}.\rho_{air}.C_D.A_f.v^3 - m_{veh}.g.\sin\theta\,.v \\ -(C_{r0} + C_{r2}.v^2).\cos\theta\,.m_{veh}.g.v \quad \text{Equation 3}$$

where F_b is the braking force, and a_{neg} is the vehicle deceleration. In ADVISOR, the regenerative braking system can be considered in the simulation. Through the modeling, the traction motor operates as a generator and provides the braking torque to the wheels being restored in the battery. The model is considered by a set of input parameters in the wheel block: the driveline brake fraction and friction brake fraction. Of the total braking force, a fraction is performed by the frictional braking and the rest by the driveline system, which the latter is the braking energy that can be potentially regenerated. The captured energy by the storage system is given by the driveline braking energy minus energy losses of upstream components, transmission, motor/controller and battery). The parameters are functions of the vehicle speed, provided in the data source in ADVISOR, which by default the regenerative potential is considered higher at high speeds.

In the wheel/axle block, the linear speed and traction force are translated to rotational speed and torque including the effects of wheel/axle rotational inertia, wheel/axle bearing and braking drag for the torque losses and tire slip. The tire slip is a function of the vehicle weight on the tire, speed, traction force, and slip coefficient of the tire. The wheel rotational speed is calculated considering the tire slip fraction [31], as follows:

$$\omega_{wh,req} = (1 + slip_{tire})\frac{v_{req}}{r_{wh}} \quad \text{Equation 4}$$

where $slip_{tire}$ is the tire slip coefficient, and its corresponding parameter is used as an input to the wheel/axle block in a set of data provided in ADVISOR. The maximum tire slip limits the maximum transmissible tractive force. Thus within the maximum possible acceleration corresponding to the limited traction force, the achievable required speed will

also be limited. To estimate the max speed limited to the max slip, ADVISOR uses the following equations at the maximum slip condition [31]:

$$F_{inertia,lim} = F_{tr,max-lim} - F_{drag} - F_{rolling} - F_{climbing} \quad \text{Equation 5}$$

$$\frac{dv_{req,lim}}{dt} = F_{inertia,lim}/m_{veh} \quad \text{Equation 6}$$

Once it is checked that the tractive force and linear speed at the tire are in the limit ranges, the required torque input to the axle is calculated as [31]:

$$\tau_{wh,req} = F_{tr,req}.r_{wh} + \tau_{wh,loss} + J_{wh}.\dot{\omega}_{wh,req} \quad \text{Equation 7}$$

where $F_{tr,req}$ is the required tractive force, $\tau_{wh,loss}$ is the bearing and brake drag torque losses, and $J_{wh}$is the rotational inertia of the wheels/axles.

Given the required torque and speed at the wheel, the transmission block delivers its torque and speed demand to energy conversion block considering the gear ratios and torque losses of the gearbox and final drive, which is provided by the block data source. It gives the required torque and speed of the drivetrain, which is provided by the conventional engine or the electric motor.

The engine block determines the operating point of the engine required to meet the transmission speed and torque requirements, the engine's inertial losses, as well as the mechanical accessory loads. The engine controller assures that the achievable speed and torque are within the operating speed and torque limits, then they are used to estimate fuel consumption and exhaust emissions by interpolating in fuel map, and emissions tables, provided in ADVISOR from the manufacturers test data.

Within the motor/controller block, the required speed is limited to the motor's maximum speed (Equation 8), and the max torque is limited between the minimum of the motor's maximum torque at the limited speed and the rotor inertia torque (Equation 9). By considering the required torque and speed, the required power of the motor/controller is estimated by interpolating in the power map (Equation 10) subject to the controller maximum current limit (Equation 11), The power map and allowable performance ranges are provided in the lookup tables and block's data source. The following equations describe the computation steps [31]:

$$\omega_{mot,req,lim} = min(\omega_{mot,req}, \omega_{mot,max}) \quad \text{Equation 8}$$

$$\tau_{mot,req,lim} = \min\left(\tau_{mot,max}, \tau_{mot,req} + J_{wh}.\dot{\omega_{mot,req,lim}}\right) \quad \text{Equation 9}$$

$$P_{mot,map} = f(\tau_{mot,req,lim}, \omega_{mot,req,lim}) \quad \text{Equation 10}$$

$$P_{mot,req} = min(P_{mot,map}, I_{cont,lim}.V_{bus}) \quad \text{Equation 11}$$

The required motor/controller input power should be provided by the batteries through the power bus. The battery is the electric vehicle energy source providing the power demand of the vehicle including the motors input power and the electrical auxiliaries. The capacity of the battery is the total amount of charge in Ampere-hours (Ah), that can be drawn from a fully charged battery, given that the current is reduced to maintain the operating voltage in the range limits [31], which is affected by the battery temperature and usage history. Various battery modeling approaches are provided in ADVISOR through the energy Storage System (ESS) block, including an internal resistance model (Rint) used to predict the performance of lithium-ion (Li-Ion) batteries. Rint model estimates the battery's temperature, voltage, current, and state-of-charge (SOC) at each time step. The battery is considered as an open-circuit voltage (OCV) source series with a resistor I, changing with SOC, temperature, and if the battery is being charged or discharged.

Given the current SOC and temperature, the open-circuit voltage (V_{OC}) and resistance (R) are interpolated in lookup tables and determined subject to a max power limit to assure that the operating voltage (V_{bus}) does not drop below either the battery's or motor's minimum voltage. The maximum power limit at the power-bus is determined by the following equation [31]:

$$P_{bus,req,lim} = V_{bus}.\frac{V_{OC} - V_{bus}}{R} \quad \text{Equation 12}$$

V_{bus} is either the battery's or motor/controller's minimum voltage limit. The current (I) is calculated by solving Equation 14 which is derived from the power equation (Equation 13) considering the requested power at the power-bus and power losses, within the terminal voltage limits.

$$P_{bus,req} = (V_{OC}.I) - R.I^2 \quad \text{Equation 13}$$

$$R.I^2 - V_{OC}.I + P_{bus,req} = 0 \quad \text{Equation 14}$$

Between the two results, the smaller solution should be considered to maintain the minimum terminal voltage limit. Also, the power-bus voltage is defined by Kirchoff's law presented in Equation 15, as follows:

$$V_{bus,req} = V_{OC}. - R.I \quad \text{Equation 15}$$

The state of charge (SOC) algorithm determines by the total Ah change in the battery (Ah_{used}). Ah_{used} is calculated by the summation of all discharging and charging current considering the battery's Coulombic efficiency (Equation 16). The SOC is determined by estimating the charged/discharged amp-hour (Ah) energy considering Coulombic efficiency losses by the following equations [57]:

$$Ah_{used} = \int_0^t \eta_{coulomb} A.dt \quad \text{Equation 16}$$

$$SOC = \frac{Ah_{max} - Ah_{used}}{Ah_{max}} \quad \text{Equation 17}$$

The flow is negative if the battery is charging and positive if the battery is being discharged.

The maximum capacity that a battery can deliver is a function of the discharged temperature and usage history of the battery. The model used in this study includes the thermal effects but does not consider the usage history of the battery. The lumped thermal model considers the battery pack as a single module to predict the average internal battery temperature and exit air temperature. Considering the internal resistance losses and the heat dissipated from the battery surface, the average battery temperature is calculated by the heat transfer equation:

$$T_{batt} = \int_0^t \frac{Q_{gen\_batt} - Q_{diss\_batt}}{m_{batt}.c_{p,batt}} dt \quad \text{Equation 18}$$

where Q_{gen_batt} is the heat generated from the internal resistance losses (RI^2), Q_{diss_batt} is the heat dissipation, m_{batt} is the battery mass and $c_{p,batt}$ is the thermal capacity of the battery module. Q_{diss_batt} is defined as:

$$Q_{diss\_batt} = \frac{T_{batt} - T_{air}}{R_{eff}} (Q_{diss\_batt} - Q_{diss\_batt}) \quad \text{Equation 19}$$

R_{eff} is the module effective thermal resistance which is calculated by Equation 20, considering both the conduction and convection heat transfers:

$$R_{eff} = \frac{1}{hA} + \frac{t}{kA}$$ Equation 20

where k is the module thermal conductivity, h is the cooling air heat transfer coefficient, A is the module surface area, and t is the module thickness.

When the battery temperature starts to exceed a set point temperature (35°C as the default in ADVISOR), forced air cooling is considered, in which the heat transfer coefficient is defined as $h_{forced} = 17.23\,(\frac{m}{\rho A})^{0.8}$, otherwise estimated as $h_{nat} = 4\,W/m^2K$. The temperature is considered for interpolation of the open-circuit voltage and resistance from the lookup data followed by estimation of current, and state-of-charge (SOC) of the battery.

Through the model described, the energy storage block estimates the battery SOC at each time step and correspondingly the energy of the battery-electric vehicle.

3.2 Powertrain configuration

Refuse trucks are categorized as vocational trucks since they have an intense duty cycle of the hydraulic system to lift, pack and dump heavy trash bins. Figure 22 and Figure 23 present diesel and battery-electric refuse trucks' configurations which are used through the simulation.

In conventional drivetrain, the internal combustion diesel engine provides the required traction power, the hydraulic load and rest of the mechanical auxiliaries (A/C, air compressor, engine cooling fan, steering pump). The speed/torque conversion is done by the mechanical transmission (includes clutches, gearbox, differential, and final drive) to provide the required speed at the rear wheels. Typically, on a conventional refuse truck, the mechanical accessories are belt driven directly off the engine, and the hydraulic pump is run on a direct drive shaft from the engine with the same speed as the engine and takes the corresponding power of it.

The battery-electric refuse truck model includes the battery (energy storage system/ESS), traction motor, auxiliary motor, and mechanical transmission. The battery provides the power demands of the vehicle including the traction power and auxiliary loads.

For the battery-electric truck configuration, the regenerative braking is considered by which a fraction of the kinetic energy can be stored in the battery during the braking mode. In its configuration, two electric motors (EMs), the main EM and the auxiliary EM, is

considered in parallel. The main electric motor is on when the vehicle is moving and either supplies the propulsion power or recharge the battery as a generator, and the auxiliary electric motor delivers power to feed the hydraulic load when the vehicle is stopped. The parallel design of the two Ems allows both the main and auxiliary motors to be appropriately sized and operate close to their nominal rate at high efficiency since the hydraulic load is required just through the trash collection phase. In both configurations, the electrical auxiliary-load (e.g., lighting, wipers, starter) are supplied by the battery.

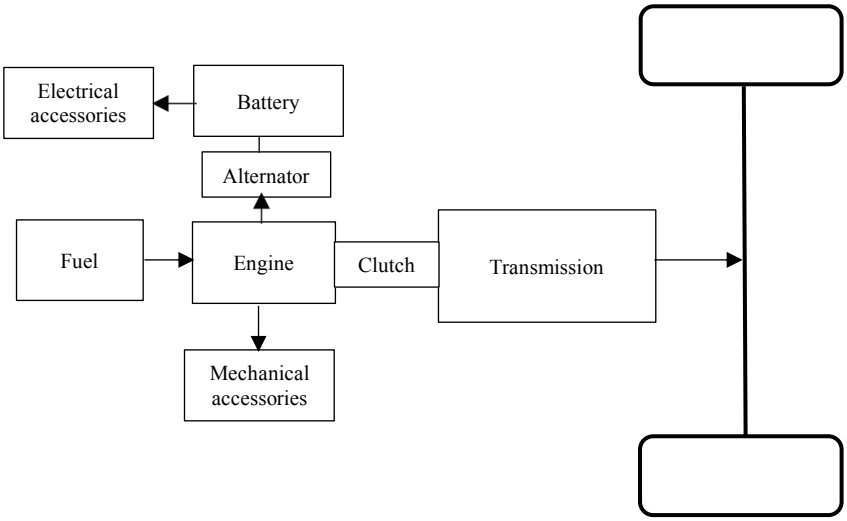

Figure 22) Configuration of the conventional diesel refuse truck

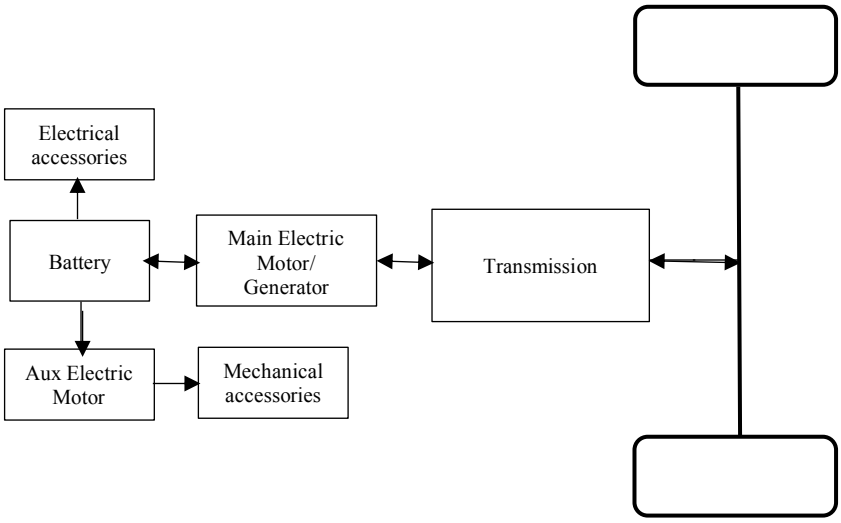

Figure 23) Configuration of the battery-electric refuse truck

3.2.1 Refuse truck models parameters

By using the model configurations described in 3.2, modeling of the component blocks and corresponding inputs for diesel and battery-electric refuse trucks are developed in ADVISOR. Figure 24 and Figure 25 show the component blocks containing input parameters and data sources of the diesel refuse truck the battery-electric refuse truck models. The diesel refuse truck is modeled compared to a Peterbilt 320 refuse truck specification (Table 2, [48]) and for the battery-electric refuse truck, a class 6 all-electric BYD refuse truck [31] is considered as a design reference for the component sizing. Table 9 presents the specification data of both trucks.

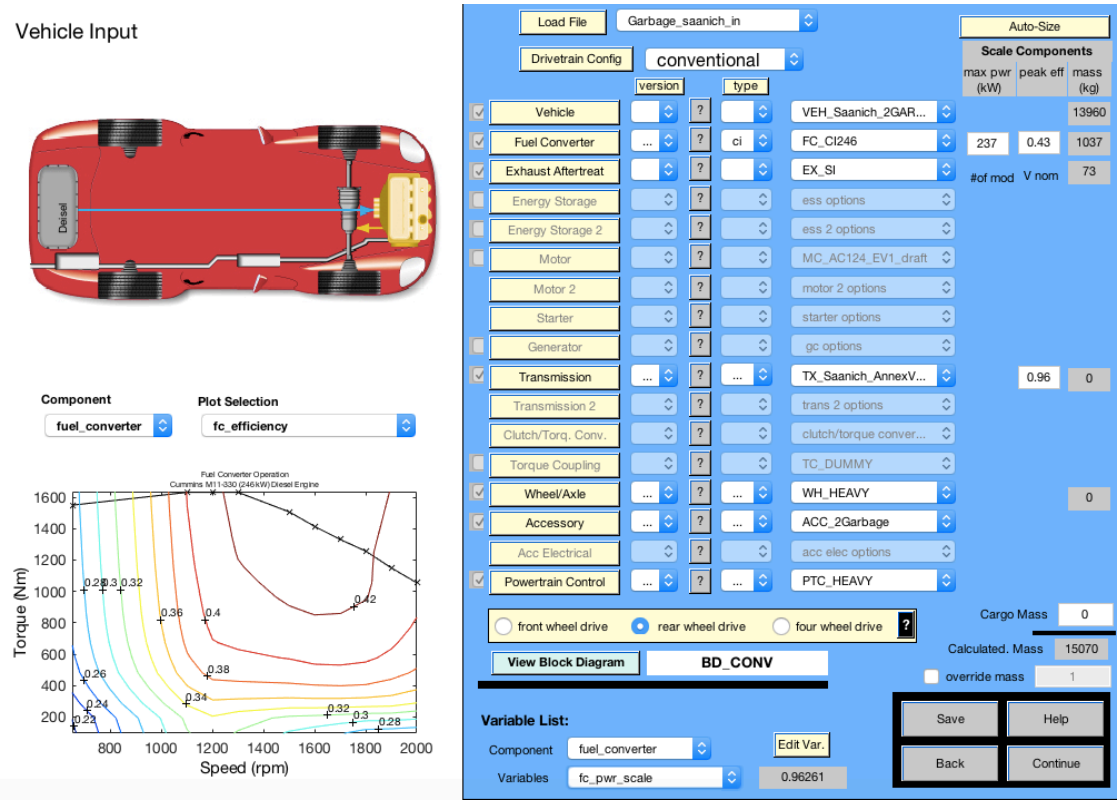

Figure 24) Component blocks of the diesel refuse truck model

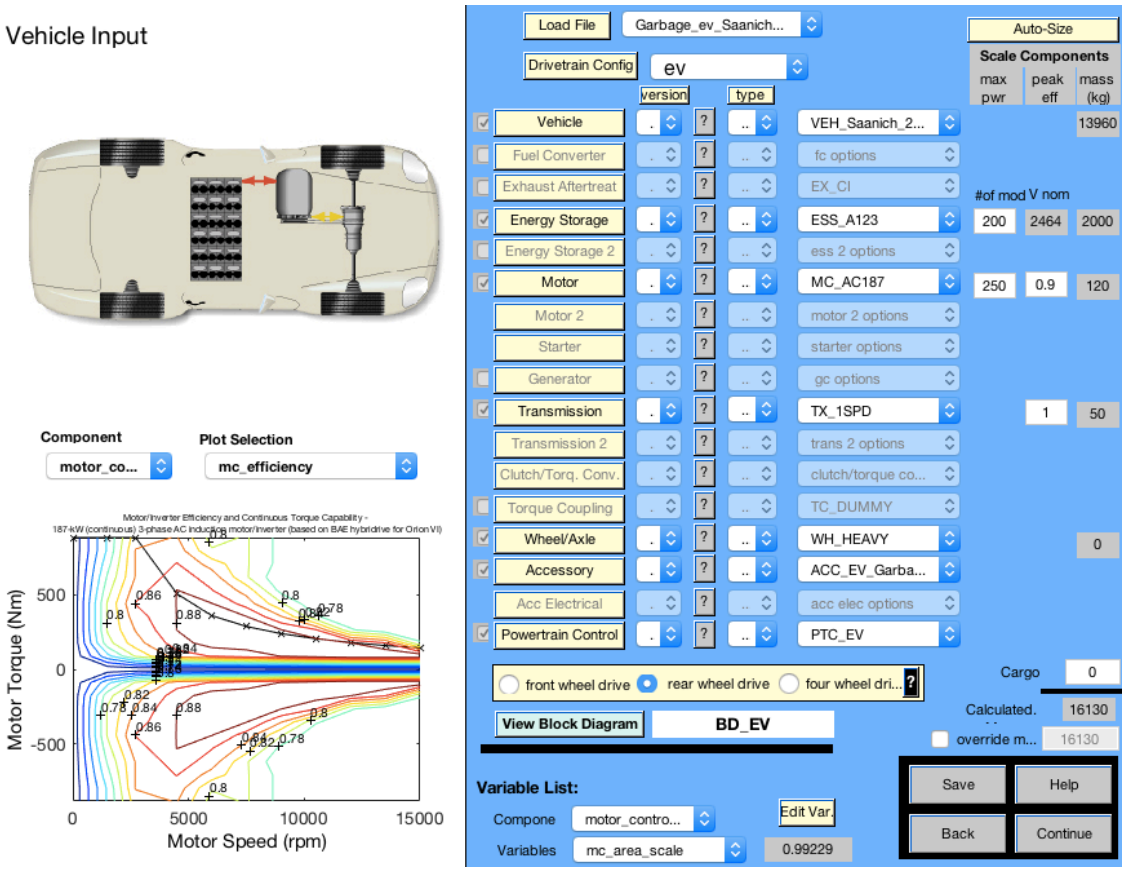

Figure 25) Component blocks of the battery-electric refuse truck model

With the reference models' specifications, the appropriate sizing of components is accomplished, and the input parameters for each component are selected from either the manufacturer catalogs and data sources or the ADVISOR directory data. Following describes the input parameters in detail. Trucks are configured based on a chassis weight capacity for the U.S. class 7 gross vehicle weight ranges (11,794 –14,969 kg) [58]. The chassis data is obtained from the data of a Kenworth T800 truck which is provided in ADVISOR and used as a default chassis block for heavy duty class vehicles. The aerodynamic drag coefficient is assumed 0.7 considering a typical heavy duty truck, the frontal area, the zero (Cr_0) and second (Cr_2) order of rolling coefficients are considered 8.5 m^2, 0.008 and 0.00938 (West Virginia University test data [54]), respectively. The chassis glider mass is 13960 kg, and a dynamic mass cycle is defined to be loaded to the truck's curb weight through the collection phase, presented in Section 2.2.2.

Table 9) Specification of the simulated diesel and battery-electric refuse truck

Fuel type	Diesel	Battery-electric
Model	Peterbilt 320 [48]	Class 6, all-electric BYD refuse truck [31]
Curb weight (kg)	15070 kg	16132 kg
Payload (kg)	0 to7830 kg	0 to7830 kg
Engine/Motor-controller: Max power(kW)/peak eff.	237 kW/ 0.43%	Main. EM: 250 kW, AC-Induction, 92% Aux. EM: 59 kW, AC-Induction, 91%
Transmission	Allison-Auto6Speed 3000 RDS (3.8: 0.65) Diff ratio:6.14	1-speed
Battery Capacity (kWh)/Weight (kg)	-	200 Li-ion modules, 220 kWh/2000 kg
Hydraulic Pump Max cont. pressure (bar) No-load system pressure	Parker Pump Model P350 210bar [31] below 20 bar [52]	Parker Pump Model P350 210bar [31] below 20 bar [52]

Trucks are rear-wheel drive, and the wheel/axle torque loss and slip coefficients are presented in Table 10 provided in ADVISOR reference data [54].

Table 10) Wheel/axle torque loss and slip coefficients

Vehicle mass (kg)	0	5000	10,000	15,000	20,000	25,000
Slip coefficient	0	0.025	0.05	0.075	0.1	0.125
Torque loss (N.m)	0	15	30	45	60	75

The truck tire radius is 0.5 m with the rotational inertia of 0.51 kg.m^2 for the axles, wheels, and tires [54]. The driveline and frictional braking fractions are presented in Table 11 to account for the regenerative braking energy through the simulation [54].

Table 11) Driveline and frictional braking fractions

Vehicle speed (km/h)	0	15	100	1600
Friction braking	0.6	0.4	0.1	0.1
Driveline braking	0.3	0.5	0.8	0.8

The engine data is available in ADVISOR for a Caterpillar C-10 L diesel engine, with 246 kW maximum power and 0.43% peak efficiency, however, in order to follow the fleet's truck engine specification, the power is scaled down to 237 kW. The engine's idle speed is 650 rpm. The max torque curve and fuel consumption (g/s) indexed by the torque (Nm) and engine speed (rad/s) are provided and used to generate the brake specific fuel consumption (BSFC) map (g/kWh) of the engine. The engine's mass is 1034 kg (including the fuel tank). The density and lower heating value of fuel is considered 0.85 (g/l) and 42.78 (kJ/g), respectively. For the diesel refuse truck, the transmission is considered a 6-speed automated Allison-3000RDS gearbox (Table 9) with a final drive ratio of 6.14 and gear ratios of 3.78, 2.21, 1.53, 1, 0.76, 0.65 [59] with corresponding up/down shifts and torque losses provided by the block's data source in ADVISOR.

In case of the battery-electric truck, we keep the chassis specification the same as the diesel refuse truck. The main motor/controller is chosen as a 187-kW (continuous) 3-phase AC induction motor/inverter. For the EM, the efficiency map indexed by the electric motor torque-speed and the max torque-speed curve is provided in the EM block, captured from a hybrid drive Orion VI presented in ADVISOR) [54]. The selected electric motor has the highest power level compared to the other EMs provided in the simulator, thus the max power is scaled to 250 kW to maintain with the manufacturer specification of the battery-electric truck [31]. The minimum voltage and maximum current allowed by the controller are 120 v, and 480 A with a maximum over torque factor of 1.2. The motor weight and rotor inertia are 142 kg and 0.0335 $kg.m^2$, respectively. The auxiliary electric-motor is selected to be able to provide the total accessory loads including the hydraulic load as well as the other accessories (electrical loads). The auxiliary electric-motor is considered an AC induction motor, with continuous power of 59 kW, and peak efficiency of 93%. The motor weight and rotor inertia are 70 kg and 0.0165 $kg.m^2$, respectively. The auxiliary load includes both the vocational parasitic hydraulic loads (2.2.3) and the other electrical/mechanical accessories applicable for a heavy-duty truck. A total of a 4.5 kW load is considered for the other accessory loads (1 kW electrical and an average of 3.5 kW for the mechanical driven loads [60]). In case of the battery-electric refuse truck, the adapted hydraulic load is applied to the simulator with respect to efficiency of the auxiliary

motor, and for the diesel truck, the continuous operation of the hydraulic pump is counted in estimating fuel consumption.

The battery block models a Lithium-ion A123 battery pack composed of 200 modules with corresponding voltage and resistance data indexed to the state of charge and temperature, provided in the ESS block in ADVISOR. The nominated voltage and max capacity of each module are 12.4 v and 91 Ah at C/5 rate, with the total energy capacity and mass of 220 kWh and 2000 kg, respectively [61].

Developing the truck models with the specified characteristics and input parameters, we import the models to the simulator to analyze the performance and energy use of each truck over the representative duty cycle. In the next chapter, the simulation results are presented, and through a sensitivity analysis the impact of grade, mass, and auxiliary load on energy consumption and emissions are examined.

3.3 Fuel-cycle GHG emissions

The life-cycle GHG emissions analysis is a methodology to evaluate the environmental impacts of different vehicle technologies by quantifying the emissions associated with the vehicle materials/manufacturing/assembly/recycling (vehicle-cycle) and fuel production/distribution/consumption over the expected lifetime [16], [62], [63]. The environmental LCA of conventional vehicles and alternative technologies is composed of vehicle-cycle and fuel-cycle GHG emissions using different LCA models and databases such as GHGenius [64], GREET (Greenhouse gases, Regulated Emissions, and Energy use in Transportation [65]), AFLEET (Alternative Fuel Life-Cycle Environmental and Economic Transportation [66]), and MOVES (Motor Vehicle Emissions Simulator [67]). Several studies, (Tagliaferri et al. (2016), Hawkins et al. (2013), Zhao and Tatari (2017), Zhou et al. (2017)) have assessed the life-cycle GHG emissions of light-duty conventional and alternative technology vehicles with different details of analysis, including the BEVs. The studies mainly focused on the analysis of energy requirements and GHG emissions impacts of manufacturing and use phases of the vehicle over its lifetime. Correia et al. (2014) have concluded that for BEVs, the contribution of embodied material emissions to total life cycle GHG emissions can be between 6 - 17%, depending on vehicle/battery's materials and respective weight. Egede et al. (2015) have demonstrated that the difference between the GHG emissions of conventional and battery-electric vehicles is expected to be

mainly due to differences between fuel-cycle GHG emissions. Based on GREET's LCA model, Ma et al. (2012) have determined that for LD ICVs and BEVs, the vehicle embodied material emissions (w/o the fuel tank/battery energy storage) of the conventional vehicle are about 9 - 14% higher than that of the battery-electric counterpart, with respect to BEV's lower curb weight (with no fuel storage). The main difference between embodied vehicle-cycle emissions of LD conventional and BE vehicles is found to correspond to the battery material/manufacturing/recycling process, while a wide range from 6 to 22 $gCO2eq/kg_{bat}$ is suggested for the GHG emissions factor depending on the battery's manufacturing process, specification and lifetime [68], [69], [70]. Unlike the light-duty classes, inventory data for heavy-duty BE-trucks is not included in LCA models, such as GREET and GHGenius [71]. There are limited studies in the literature for full environmental analysis of this class of BEV, Sen et al. (2017), Zhou et al. (2017), Papathomas et al. (2016), investigated the use-phase emissions as the main contributor to the total emissions impact. Sen et al. (2017) have found fuel downstream (tailpipe) and electricity upstream GHG emissions as dominant emissions factors for conventional and battery-electric trucks, respectively. Correia et al. (2014) suggest an embodied emissions factor of 32.5 $gCO2_{eq}/kWh$ for the battery in heavy-duty BE-trucks over 200,000 km expected lifetime. Sen et al. (2017) have quoted 4.5 and 8.9 $tCO2_{eq}$ battery's embodied GHG emissions (22.4 $gCO2_{eq}/kWh$) for heavy-duty BE-trucks with 200 kWh and 400 kWh battery capacities assuming a 1500-cycle battery lifetime. That study 's LCA results indicate battery embodied emissions of 13% of fuel-use emissions within a regional grid intensity of 344 $gCO2_{eq}/kWh$ [72]. Additionally, the full LCA demonstrates that for the BE-trucks, the electricity grid mix is a primary factor in the contribution of fuel-cycle upstream emissions to total life-cycle GHG emissions [63], [73], [72], [16].

In this study, the use-phase GHG emissions analysis is conducted considering fuel-cycle GHG emissions associated with the fuel production and distribution, as well as those related to the consumption of fuel. The emissions associated with vehicle manufacturing/recycling (vehicle-cycle emissions) and refueling stations' construction/decommissioning are not considered. The fuel-cycle GHG emissions analysis includes the total GHG emissions of the fuel including the emissions from fuel supply systems (Well-to-Pump (WTP) GHG emissions) and the fuel exhaust/tailpipe emissions

(Pump-to-Wheel (PTW) GHG emissions). The total GHG emissions (Well-to-Wheel (WTW) GHG emissions) is defined by summation of the WTP and PTW emissions [62]. In this study, GHGenius is selected to predict the WTW emissions of the reference diesel fuel of the D-RCT. GHGenius is a life-cycle modeling tool developed by Natural Resources Canada which is used to analyze energy use and emissions of the conventional fuel vehicles and alternative technologies considering the fuel pathways [24]. Table 12 shows the mass of CO_2, CH_4, and N_2O (three greenhouse gases which are included in the calculation of grams of CO_2-equivalent emissions) and the total equivalent carbon dioxide ($CO2_{eq}$) per MJ lower heating value of the diesel fuel, extracted from GHGenius, version 5 [24]. In the Canadian context of the modeling tool, the total $CO2_{eq}$ of the greenhouse gases is calculated based on the Global warming potential (GWP) of the greenhouse gasses over a 100-year horizon (GHG-100). The factor is 21 and 310 for CH_4 and N_2O, respectively as presented in the Intergovernmental Panel on Climate Change report (IPCC 2013) [6].

Table 12) GHG emissions (g/MJ(LHV)) of the diesel fuel based on the GHGenius tool [62]

Greenhouse gas	WTP	PTW	WTW
CO_2	22.64	74.16	96.8
CH_4	0.1135	0.0046	0.118
N_2O	0.0009	0.0033	0.004
Total $CO2_{eq}$ (GHG-100 basis)	25.74	75.210	100.95

Within the reference diesel fuel with density of 846 kg/m^3 and the LHV of 43 MJ/kg, the total equivalent CO_2 per liter of the diesel fuel can be calculated as presented in Table 13.

Table 13) GHG emissions ($gCO2_{eq}/L_D$) of the diesel fuel based on the GHGenius tool [62]

GHG emissions factor	$GHG_{f_{WTP},D}$	$GHG_{f_{PTW},D}$	$GHG_{f_{WTW},D}$
Diesel fuel GHG emissions factor	937	2,738	3,675

The data for electricity WTP emissions considers the emissions from the electric power generation facilities and the GHG intensity attributed to the transmission losses, which is presented in Table 14 based on the BC's electric grid mix reported in 2017 [75].

Table 14) Greenhouse Gas Intensity for British Columbia's electricity grid mixture ($gCO2_{eq}$/kWh electricity generated) [75]

Greenhouse gas	WTP
CO_2	9
CH_4	0.003
N_2O	0.0007
Transmission losses	0.4
$GHG_{f_{WTW,elec}}$ (GHG-100 basis)	9.6

Considering fuel consumption, the operational WTW GHG emissions of the D-RCT, $GHG_{WTW,D}$ ($kgCO2_{eq}$/km), is estimated as follows:

$$GHG_{WTW,D} = 10^{-5} \times GHG_{f_{WTW,D}} \times Fuel_{km,D} \quad \text{Equation 21}$$

where $GHG_{f_{WTW,diesel}}$ is the GHG emissions factor of diesel fuel ($gCO2eq/L_D$) and $Fuel_{km,D}$ is fuel consumption (L_D /100km) of the D-RCT over the adopted duty cycle.

The BE-RCT has no tail-pipe emissions, hence the WTW fuel-cycle emissions of the BE-RCT, $GHG_{WTW,BE}$ ($kgCO2_{eq}$/km), is taken based on the upstream GHG emissions of the charging electric power.

$$GHG_{WTW,BE} = 10^{-5} \times GHG_{f_{WTW,elec}} \times \eta_{charge} \times Fuel_{km,EV} \quad \text{Equation 22}$$

where $GHG_{f_{WTW,elec}}$ is the electricity grid GHG intensity ($gCO2_{eq}$ /kWh), η_{charge} is the charging efficiency which is considered to be 10% according to the value suggested in [76] and $Fuel_{km,EV}$ is energy consumption (kWh/100km) of the BE-RCT which is defined through the simulation. The GHG mitigation effectiveness, GHG_{eff} ($kgCO2_{eq}$/km), of the BE-RCT compared to the D-RCT can be defined by the following equation:

$$GHG_{eff} = GHG_{WTW,D} - GHG_{WTW,BE} \quad \text{Equation 23}$$

Ultimately, the fuel-cycle GHG emissions reduction by the deployment of BE-RCT, ΔGHG ($kgCO2_{eq}$), can be determined as:

$$\Delta GHG = n \times GHG_{eff} \times VKT \quad \text{Equation 24}$$

where n is the lifetime of the vehicle (y) and VKT is the annual vehicle kilometer traveled (km/y).

Chapter 4: Results and discussion

4.1 Study setup

Based on the powertrain model described in Section 2.5.1, energy consumption of the modeled D-RCT and BE-RCT have been examined using ADVISOR. The simulation time step is set to 1 sec, according to the speed trace and hydraulic load profiles. In this chapter, the results for the D-RCT and BE-RCT are discussed. First, energy consumption for the D-RCT and BE-RCT is presented over the representative duty cycle for the base-case scenario (as described in Section 2.3.1) and the potential of the BE-RCT for annual fuel cost savings and GHG mitigation is evaluated. Second, a sensitivity analysis is presented to evaluate the impact of key parameters on energy consumption and the corresponding GHG emissions, including the size of the battery (exclusively for the BE-RCT), the route grade, the payload, and accessory loads. Fuel-based GHG emissions analysis is conducted to evaluate the fuel WTW GHG emissions and estimate the potential of the BE-RCT for emissions mitigation. Ultimately, the total cost of ownership (TCO) is determined for both trucks to examine the economic feasibility of the BE-RCT compared to the D-RCT. Based on the results, strategies are suggested to purpose feasible plans deployment of the BE-RCT in the collection fleet.

The D-RCT use diesel fuel, and fuel consumption value is expressed in L_D/100km considering the lower heating value of 36.4 MJ/L_D for the reference diesel fuel (low sulfur diesel from crude oil); for the BE-RCT the electrical energy use is expressed in kWh/100km. For comparing energy use of both type of trucks, energy consumption for BE-RCT is expressed in diesel liters equivalent ($L_{D,eq}$/100km) as well, which is calculated based on an energy conversion factor of 10.1 $L_{D,eq}$/kWh with respect to the diesel fuel lower heating value.

4.2 Energy consumption and GHG emission analysis

In this section, first we analyze the specific energy demand for the base-case duty cycle which is adopted in Section 2.3.1. The D-RCT and BE-RCT are both simulated over the duty cycle and the simulation results for energy use and WTW GHG emissions of trucks are discussed in detail.

4.2.1 Duty cycle specific energy demand

The specific energy demand explains the road load demand based on the duty cycle metrics. The specific energy (the energy per unit distance of the duty cycle) components estimates the energy required at the wheels to overcome the inertia force and the road resistances which can be used as the duty cycle metrics for investigating the road load energy requirement as well as the recoverable energy over the negative tractive events. Of the other duty cycle metrics, the aerodynamic speed and the characteristic acceleration/deceleration are also helpful parameters to estimate the road demanding/braking energy attributed to the duty cycle characteristics. The aerodynamic speed (v_{aero}) is the ratio of the overall average cubic speed to the average speed and measures the impact of aerodynamics on the total duty cycle energy demand [77].

$$v_{aero,j,j+1}^2 = \frac{\tilde{v}_{j,j+1}^3}{\tilde{v}_{j,j+1}} = \frac{v_{j+1}^3 + v_{j+1}^2.v_j + v_{j+1}.v_j^2 + v_{j+1}^3}{2\,(v_j + v_{j+1})} \Rightarrow$$

$$v_{aero}^2 = \frac{\sum_{j=1}^{n-1} \tilde{v}_{j,j+1}^3.\Delta t_{j,j+1}}{D} \qquad \text{Equation 25}$$

where v_j is the duty cycle speed, $\Delta t_{j,j+1}$ is the time step, $\tilde{v}_{j,j+1}$ is the average speed at each time step, $\tilde{v}_{j,j+1}^3$ is the cubic speed at each time step, $v_{aero,j,j+1}$ is the aero speed at each time step and v_{aero} is the duty cycle aerodynamic speed. The aerodynamic speed is calculated within the integration of the $v_{aero,j,j+1}^2$ over the duty cycle.

The characteristic acceleration ($\tilde{a}_{pos}$) is linked to the inertial work to accelerate the vehicle and/or the slope increase, which equals to the positive kinetic and potential energy per unit mass per unit distance through the driving cycle, and the characteristic deceleration ($\tilde{a}_{neg}$) measures the negative part of the kinetic and potential energy per unit mass per unit distance over the duty cycle. It estimates the braking energy which can be potentially regenerated during the vehicle deceleration [77]. The characteristic acceleration/deceleration can be calculated by Equation 26 and Equation 27, respectively [77]:

$$\tilde{a}_{j,j+1} = 0.5\frac{\left(v_{j+1}^2 - v_j^2\right)}{\Delta D_{j,j+1}} + g\frac{(h_{j+1} - h_j)}{\Delta D_{j,j+1}} \Rightarrow$$

$$\tilde{a}_{pos} = \frac{\sum_{j=1}^{n-1} positive(0.5\left(v_{j+1}^2 - v_j^2\right) + g.\Delta h_{j,j+1})}{D} \qquad \text{Equation 26}$$

$$\tilde{a}_{neg} = \frac{\sum_{j=1}^{n-1} negative(0.5\left(v_{j+1}^2 - v_j^2\right) + g.\Delta h_{j,j+1})}{D}$$ Equation 27

where $\Delta D_{j,j+1}$ is the traveled distance at each time step, $\Delta h_{j,j+1}$ is the elevation change at each time step, g is the gravitational acceleration (9.8m/s^2) and D is the total traveled distance. Table 15 presents the duty cycle aerodynamic speed and characteristic acceleration/deceleration expected for the base-case duty cycle. The high values of characteristic acceleration/deceleration reflect the stop-and-go nature of the RTDC along with the rough grade profile of the duty cycle.

Table 15) Duty cycle aerodynamic speed and characteristic acceleration/deceleration

Duty cycle metrics	
v_{aero} (km/h)	50.1
$\tilde{a}_{pos}$ (m/s^2)	0.52
$\tilde{a}_{neg}$ (m/s^2)	-0.53

Considering the tractive power presented before in Equation 2, the energy required or can be potentially gained over a time period is defined as follows [77]:

$$E_{road,j,j+1} = \frac{1}{2}\rho_{air} C_D A_f \tilde{v}_{j,j+1}^3.\Delta t_{j,j+1} + C_{rr} m_{veh.} g.\tilde{v}_{j,j+1} + m_{veh}.g.\Delta h_{j,j+1} + \frac{1}{2} m_{veh}.(v_{j+1}^2 - v_j^2)$$ Equation 28

The specific tractive energy (SE_{trac}) and braking energy (SE_{brake}) at the wheels can be defined by positive and negative terms of the road energy as presented [77]. The E_{brake} is the maximum amount of energy that can be potentially regenerated through a regenerative system. However, depending on the regenerative efficiency it is been partially regenerated and the rest is lost through the frictional braking [78].

$$SE_{trac} = SE_{road,pos} = \frac{\sum_{j=1}^{n-1} positive(E_{road,j,j+1})}{D}$$ Equation 29

$$SE_{brake} = SE_{road,neg} = \frac{\sum_{j=1}^{n-1} negative(E_{road,j,j+1})}{D}$$ Equation 30

Table 16 shows specific energy components in both traction and braking modes for the refuse truck over the base-case duty cycle. The energy breakdown shows that the RTDC is

considerably energy-intensive subject to the road load demand (even regardless of the truck's vocational operation and auxiliary load demand). About 46% and 28% are the kinetic and potential energy components, respectively and the summation of the drag and rolling resistance is attributed to the 25% of the total energy demand. The high value of the negative tractive energy (1.32 kWh/km) reveals that if the energy can be even partially recuperated through a regenerative braking system the fuel efficiency will improve considerably. This supports the potential of deployment of hybrid/all-electric or hybrid hydraulic technologies in this application.

Table 16) Duty cycle specific energy demand

Duty cycle road load components (kWh/km)	
Aerodynamic energy	0.13
Rolling resistance energy	0.33
Kinetic Energy	0.81
Potential energy	0.51
Total road load	1.78
Brake energy	1.32

4.2.2 Energy consumption and GHG emissions of the D-RCT

Based on the D-RCT's powertrain model described in Section 3.2.1, the D-RCT has been tested over the base-case duty cycle. Table 17 presents fuel consumption and corresponding GHG emissions of the D-RCT for the base-case scenario.

Table 17) Fuel consumption value and GHG emissions of the D-RCT for the base-case scenario

D-RCT energy consumption	Simulation results		Municipal collection fleet	Variation
	Total trip	Per unit distance		
Fuel consumption	71.2 L_D	108.7 L_D/100km	126.2 L_D/100km	13.8%
PTW GHG emissions	195 $kgCO2_{eq}$	297.6 $kgCO2_{eq}$/100km	345.4 $kgCO2_{eq}$/100km	13.8%
WTW GHG emissions	261.7 $kgCO2_{eq}$	399.5 $kgCO2_{eq}$/100km	436.6 $kgCO2_{eq}$/100km	13.8%

Total fuel consumption of the truck is 71.2 L_D over the whole duty cycle, which results in 221.8 $kgCO2_{eq}$ tailpipe emissions. The result is comparable to the values presented in [12]

for fuel consumption of SL-RCTs ranging from 80 to 130 L_D/100km (1.8 to 2.9 mpg) which are captured based on the MOVES vehicle simulator. The validity of the developed model is also compared with average in-use fuel consumption of the D-RCT operating in the municipal fleet. The reported data for the annual fuel use and traveled distance is 203,808 L_D/y and 161,557 km/y for ten trucks. Based on the reported data, for fuel efficiency a 13.8% discrepancy between the predicted and in-use values is found, which is reasonable given the difference in assumed duty cycle parameters of the developed model and actual operating trucks within the collection fleet. As described in Section 2.3.1, the adopted duty cycle is developed based on the available data for the truck #18972 whose traveling route is used to construct the grade profile. Lacking 1Hz speed data for the Saanich trucks, the NREL refuse truck duty cycle is used for developing the speed profile. The difference between the actual and the developed driving speed and the vocational operation condition of the refuse trucks can cause the variation in fuel consumption. Moreover, it should be noted that the reported data is the average fuel consumption over one-year operation of the total fleet (with ten operating trucks) over 235 working days. Each truck operates in a specific collection area each day, different to the others, through a periodic nine-day cycle. The variation in the operating condition between the collection trucks (e.g., drivers' behavior, route conditions, number of collection houses and the corresponding mass and hydraulic cycles) can cause noticeable variations within fuel use of the trucks in the collection fleet [79]. The operational data of the D-RCT over the different sub-cycles of the total trip is plotted in Figure 26. As can be noticed, the engine power demand and the corresponding fuel use rate follow the road tractive power, which is closely correlated to the duty cycle's speed, grade, and hydraulic power demand. Over the first part of the trip, presented in Figure 26-a, the empty truck travels from depo to the collection area with a moderate speed of 43 km/h averaged with a fairly flat route gradient. The engine meets the duty cycle's demand and its power output and corresponding fuel rate are changing from 0 to 95.7 kW and 9.7 g/s, with moderate average values of 47.3 kW and 4.8 g/s, respectively. The hydraulic pump idling increases the auxiliary load by 40% with an average power of 6.3 kW.

Over the collection trip, Figure 26-b, the truck is moving with an average driving speed of 19.8 km/h, considering 17 stops/km and 52.2% idling time the average total speed

decreases to 9.4 km/h. As plotted in Figure 27-b, the higher fuel rates can be noticed with respect to the steep gradient and higher truck's mass, occurring over the first part and last part of the sub-cycle. While the truck's mass increases incrementally over the sub-cycle, with moderate driving speed the average traction and engine power, and fuel rate are found as 82.9 kW, 107.1 kW and 10.6 g/s, respectively. Figure 26-c presents the truck's operation during the first five collection events. With respect to the variable hydraulic load through the idling time along with the 4.5 kW required accessory power, the auxiliary energy demand over the collection phase is reached to 22.5 kWh, about 47.8% of the total duty cycle auxiliary load. Consistent with aggressive braking events and characteristics deceleration of -0.72 m/s^2, the available regeneration energy is about 45.7 kWh with an average potential power of -30.2 kW.

Figure 26-d presents the truck's trip from the collection area to the landfill (the starting 22 min of the trip), and after dumping, from the dumping site to the depo. From the collection area to the dumping site, with the full-payload driving and fairly rough gradient (with an average of 3.7%), the average power demand is 168.2 kW reaches to the maximum value of 238 kW. The insufficiency of the engine power compared to the requested power results in the difference between the achieved vehicle speed and the duty cycle's requested speed over 312 s of the duty cycle time (1.8% of the total cycle duration), as inspected in Figure 26-d. The average fuel use rate over the full-payload is found as 14.3 g/s, the highest compared to rest of sub-activities, resulted in 100.5 L_D/100km fuel efficiency. While the required accessory power is 4.5 kW, the average auxiliary power demonstrates an increase of 91% (with an average power of 8.6 kW) due to the hydraulic pump idle losses. From the dumping site to the depo, the truck travels empty similar to the first part of the duty cycle. However, the steep downgrade gradient profile over the trip (-3.8% average) decreases the power demand and fuel use considerably. The average engine power and fuel use rate is found as low as 12.3 kW and 1.8 g/s, respectively.

Table 18 presents a performance summary of the D-RCT over the proposed sub-cycles. As an overview over the total duty cycle, the average fuel use rate changes between 1.8 g/s to 18.9 g/s and 1.6 g/s to 12.7 g/s during the moving and idling modes, respectively. The values are comparable to the fuel use rate presented in [12] categorized based on the average speed and specific tractive power (STP) over the activity cycles, using the MOVES

simulator. In the reference [12] the fuel use rate rises with the increase in average speed and corresponding STP, ranging between 1.2 g/s for the idling mode (w/o considering the compact load) to 20 g/s for the 72 km/h speed and the tractive power of 251 kW. Average fuel use over the first and last no-payload driving trips is the minimum value of 2.8 g/s, which is consistent with its low characteristic acceleration (0.16 m/s^2). The maximum power demand and fuel use rate occurs in full-payload along with an almost steep uphill driving (6.2% route gradient) with 238 kW and 18.9 g/s, respectively followed by 221 kW and 17.8 g/s through the collection phase where the required speed is 38.6 km/h along with a gradient of 7.9% uphill driving. The characteristic acceleration over the collection phase and the full-payload driving are high, with an average of 0.71 m/s^2 and 0.36 m/s^2 due to the high number of stops in the collection phase and rough route profile over the full-payload driving, respectively. However, the average fuel use rate through the full-payload driving (38.6 L_D/h) is higher than the collection phase (13 L_D/h) due to the full-loaded driving over the steep route and no idling time. As the collection phase covers 90% of the duty cycle duration, it is the greatest contributor to fuel consumption and corresponding GHG emissions with 13 L_D/h and 35.6 $kgCO2_{eq}$/h exhaust GHG emissions, respectively 77% of the total of energy use and GHG emissions. The large standard deviation in engine power (73.8 kW) over the total duty cycle represents the wide span of the tractive road load as well as the auxiliary power demand over the refuse truck duty cycle, consistent with variations in characteristics of sub-cycles. The total duty cycle's fuel use rate is found as 14.5 L_D/h, and considering the hydraulic load over the collection and dump events the fuel use rate during the truck idling is 9.2 L_D /h. The values are consistent with those presented in the literature ([23], [80], [38], [24]) ranging between 8 to 23 L_D/h for refuse truck application. Correspondingly, the PTW and WTW GHG emissions rates are estimated as 39.7 $kgCO2_{eq}$/h and 53.3 $kgCO2_{eq}$/h, respectively over the proposed duty cycle.

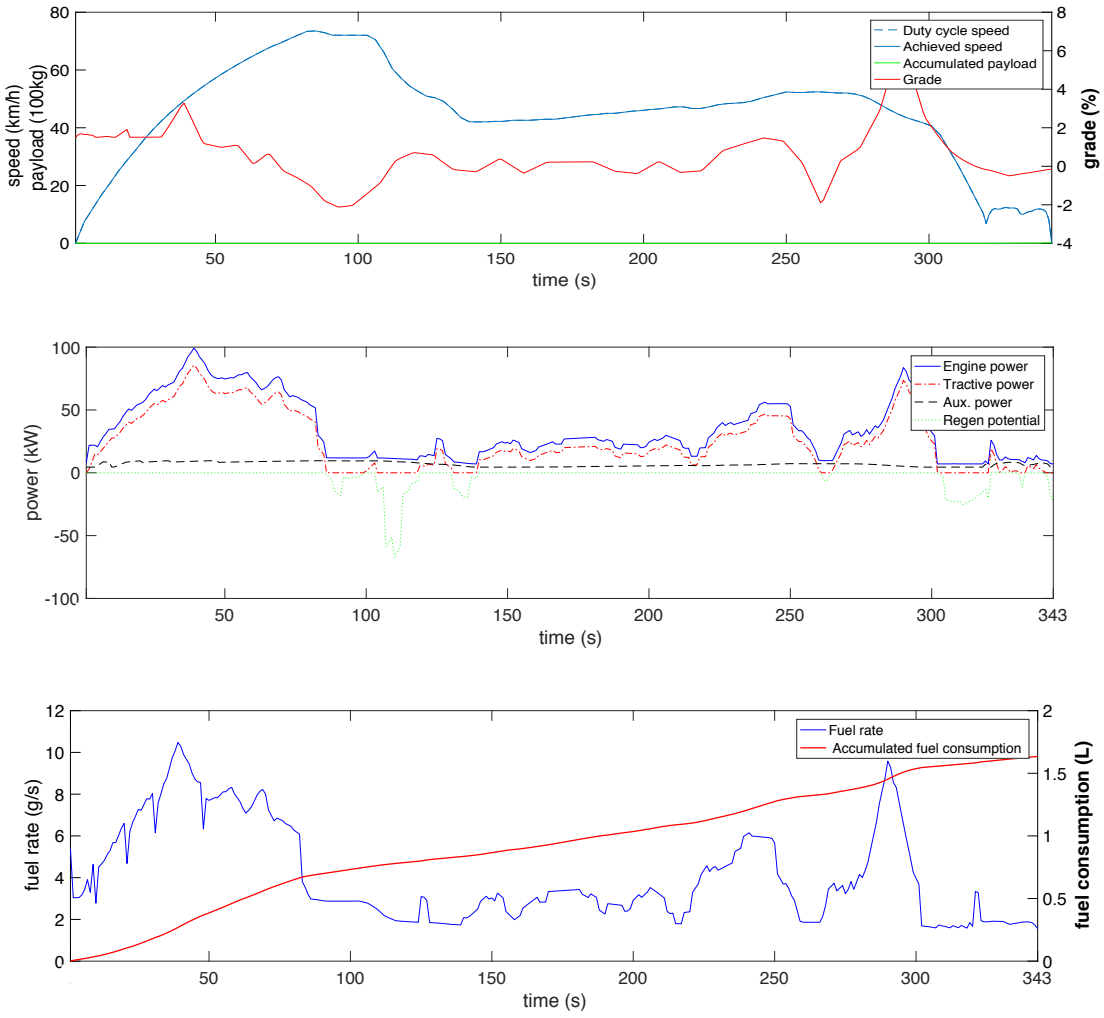
speed (km/h)
payload (100kg)
grade (%)
time (s)
Duty cycle speed
Achieved speed
Accumulated payload
Grade
power (kW)
Engine power
Tractive power
Aux. power
Regen potential
fuel rate (g/s)
fuel consumption (L)
Fuel rate
Accumulated fuel consumption

(a)

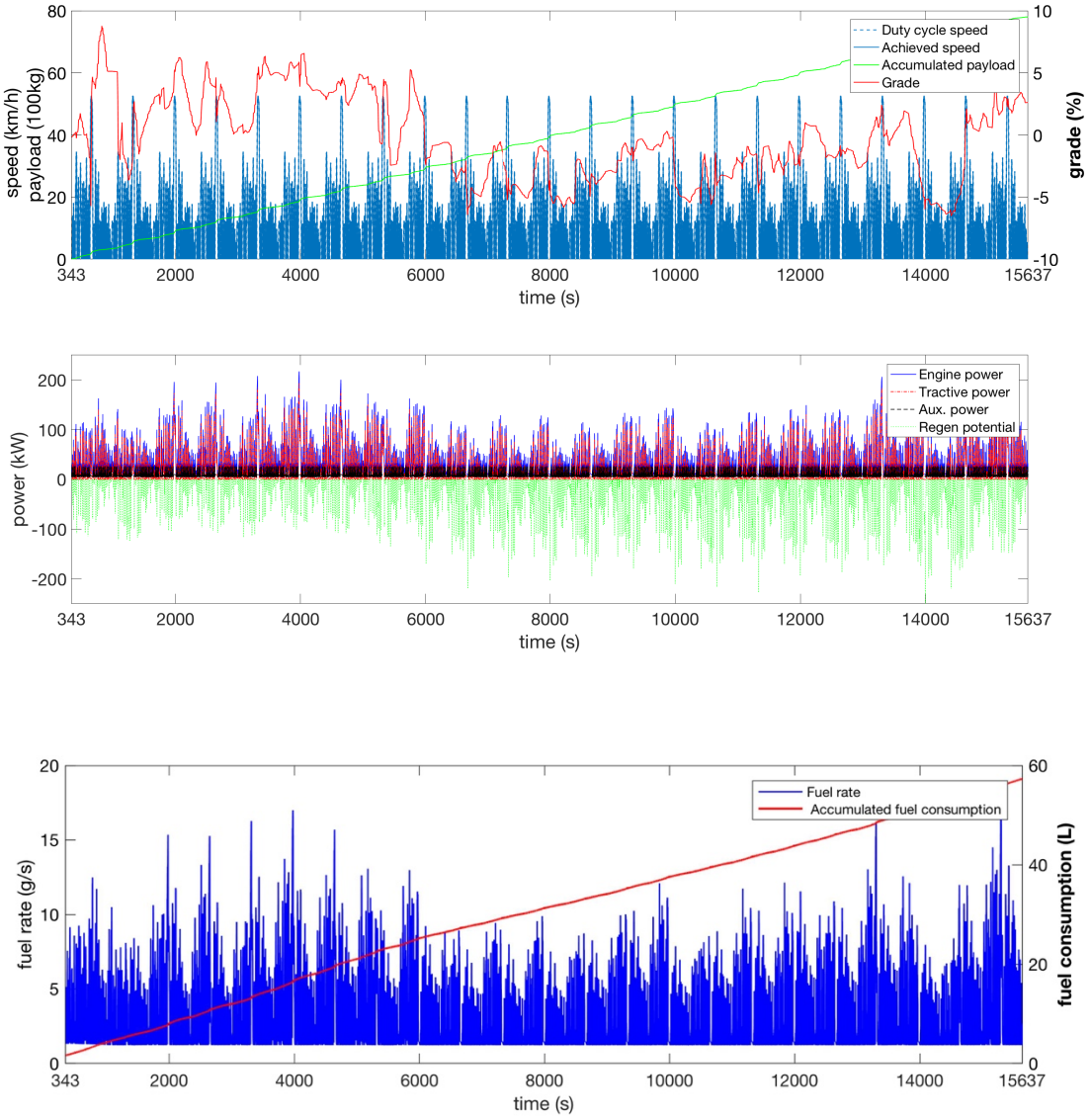
speed (km/h)
payload (100kg)
grade (%)
time (s)
Duty cycle speed
Achieved speed
Accumulated payload
Grade
power (kW)
Engine power
Tractive power
Aux. power
Regen potential
fuel rate (g/s)
fuel consumption (L)
Fuel rate
Accumulated fuel consumption

(b)

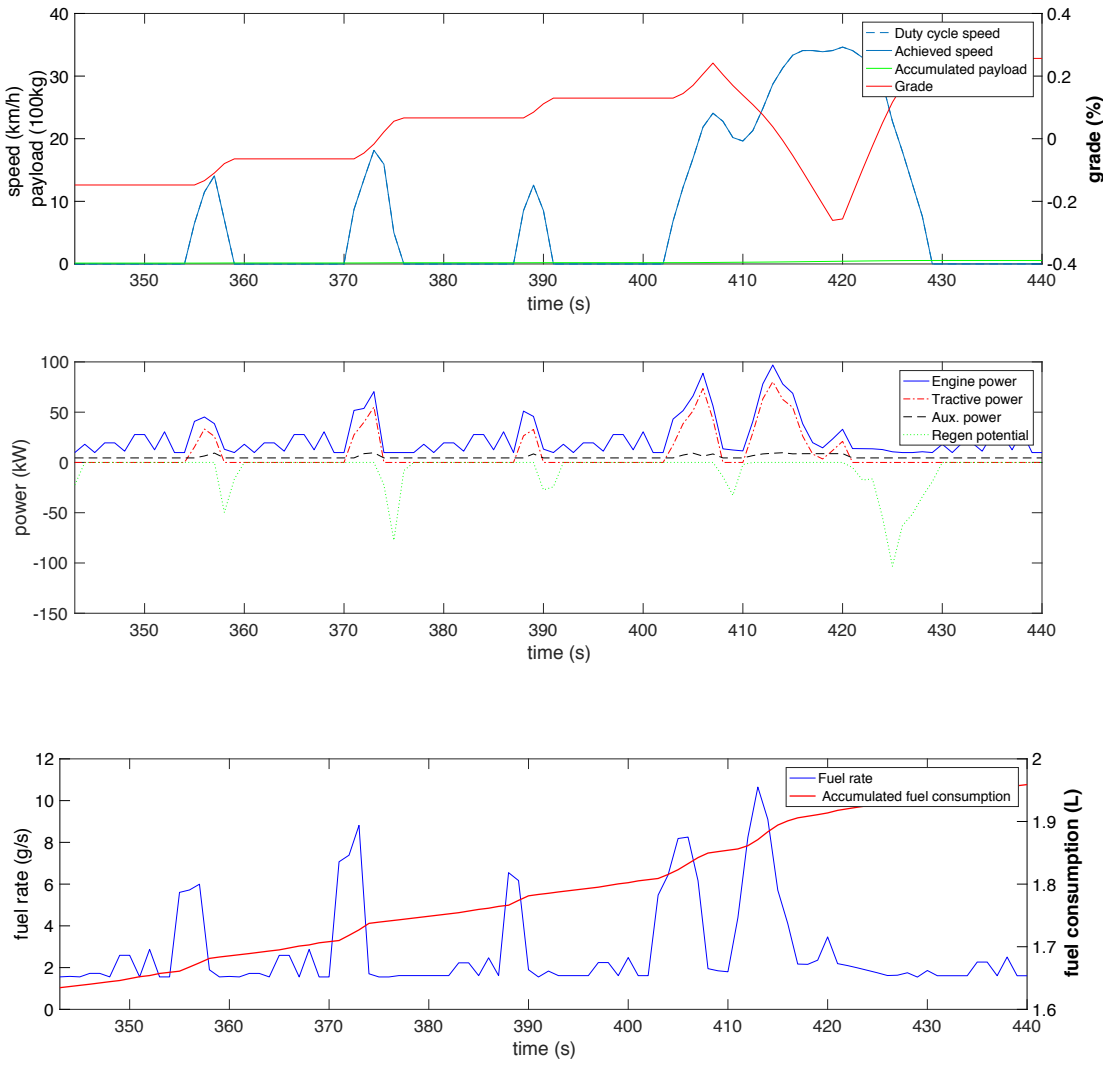
Duty cycle speed
Achieved speed
Accumulated payload
Grade
speed (km/h)
payload (100kg)
grade (%)
time (s)
Engine power
Tractive power
Aux. power
Regen potential
power (kW)
time (s)
Fuel rate
Accumulated fuel consumption
fuel rate (g/s)
fuel consumption (L)
time (s)

(c)

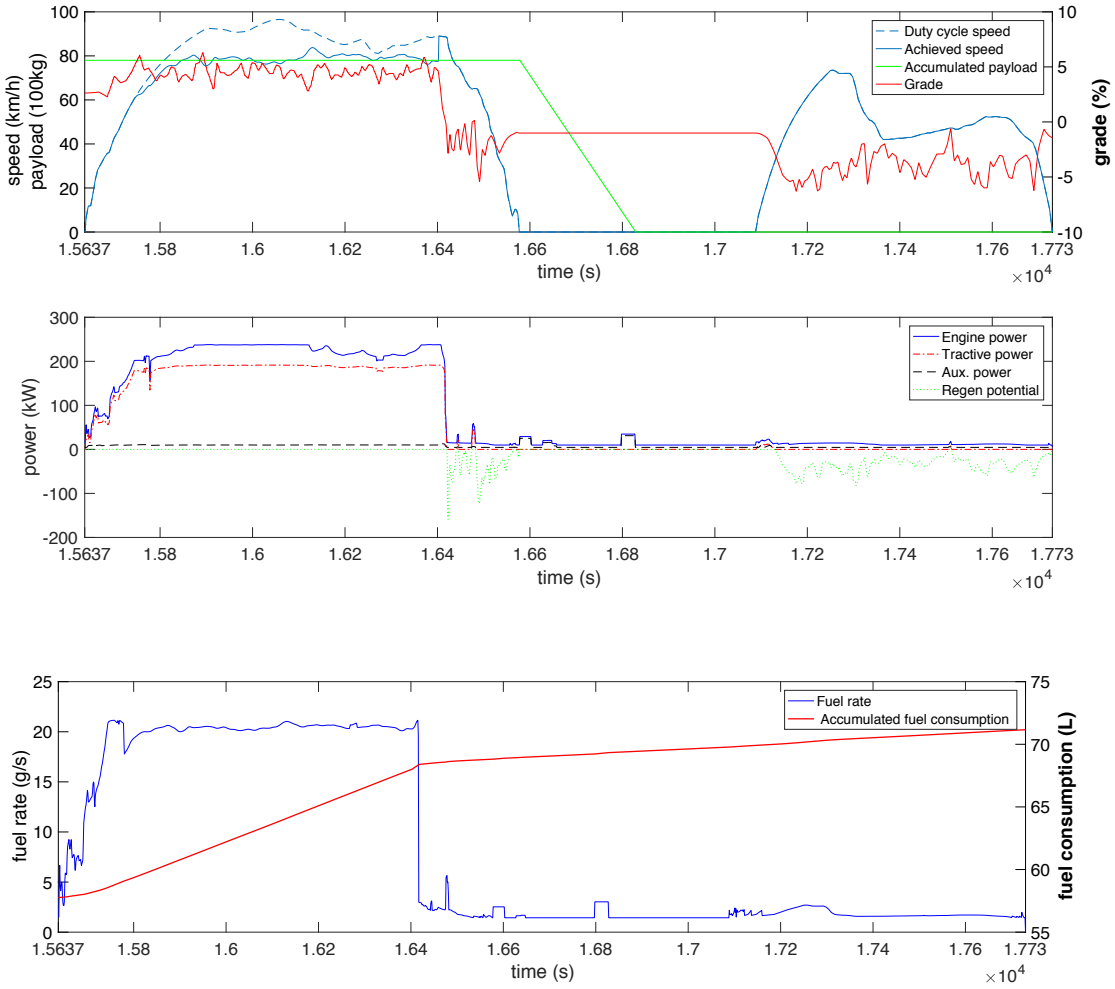

(d)

Figure 26) The simulation results for power demand and fuel consumption of the D-RCT over the activity sub-cycles: a) Depo to collection sub-cycle, b) Five cycles of collection activity, c) Total collection sub-cycle, d) Collection to dump/dump to depo sub-cycle

Table 18) Operational characteristics of the D-RCT through the different activity sub-cycles

Activity characteristics	Unit	No payload driving	Collection phase	Full-payload driving	Total duty cycle (one-day operation)
Time	s	1242	15294	1194	17730
Distance	km	12.6	40.2	12.7	65.5
Ave drv. spd	km/h	45.9	19.8	38.3	24.9
Idle time	s	255	8001	0	8256
	%	20.5%	52.2%	No idle	46.6%
Total fuel use	L_D	3.3	55.1	12.8	71.2
Specific fuel use	L_D /h	9.6	13	38.6	14.5
	L_D /100km	26.2	137.2	100.5	108.7
GHG emission rate (WTW)	$kgCO2_{eq}$ /100km	96.2	504.1	369.3	399.5
% of the total drive cycle energy use/emissions rate	%	4.6%	77.4%	17.9%	100%

4.2.2.1 Energy breakdown of the D-RCT energy use

Energy components of the D-RCT over the examined duty cycle subject to the speed profile, acceleration, route grade, mass, and hydraulic cycles are presented in Table 19. Considering duty cycle metrics and vehicle parameters, the total of 115.9 kWh is required at the wheel to overcome the inertia and road resistances, about 85.8 kWh of which (44.5% of the engine's output energy) is being dissipated through the braking mode which is the potential energy available to be partly recaptured through the regenerative braking system in the BE-RCT. Considering the driveline efficiency, the total energy demand of the duty cycle is 193 kWh, 60.1% and 26% of which is accounted for the tractive road load and auxiliary loads, respectively. The total energy demand and the available regenerative energy of the cycle per unit distance (kWh/km), are estimated about 2.9 kWh/km and 1.3 kWh/km, respectively for the examined RTDC (considering the existence of the vocational hydraulic and accessory loads). The values reflect the energy-intensive of the refuse cycle

along with the high regeneration potential for the energy saving, as consistent with the its characteristics with frequent number of acceleration/deceleration events, rough route gradient, large mass payload and vocational load.

Table 19) The component energy demands of the D-RCT over the refuse truck duty cycle

Duty cycle energy break-down	MJ	kWh	% of the tot energy input
Total road load @ wheels	417.1	115.9	16%
Aux. load	168.9	47.1	6.5%
Engine energy output	694.1	193	26.7%
Fuel energy	2599.7	722.7	100%
Regen potential	308.6	85.8	11.9%

4.2.3 Energy consumption and GHG emissions of the BE-RCT

Similar to the D-RCT, the BE-RCT have been tested in ADVISOR over the base-case duty cycle, resulting in the overall energy consumption and the GHG emissions are presented in Table 20. For in-use fuel economy of the BE-RCTs there was a lack of data available in the literature. The validation of the result is done compared to the manufacturer data, 205 kWh/100km (3.3 kWh/mile) presented in [29], [30]. This value is captured based on the stated performance range, 65 miles with 600 pick-ups, for the proposed BE-RTC specification with the 220 kWh battery capacity. However; any reports on real-world operation energy use or more information about the performance test have not been disclosed by the manufacturer [31].

Table 20) Energy consumption value and GHG emissions of the BE-RCT for the base-case scenario

BE-RCT Energy consumption	Simulation results		Manufacturer data	Variation
	Total trip	Per 100 km distance		
Fuel consumption	161.5 kWh	246.5 kWh/100km	205 kWh/100km [31]	20.2%
	15.9 $L_{D,eq}$	24.3 $L_{D,eq}$/100 km	-	-
WTW GHG emissions	1.55 $kgCO2_{eq}$	2.37 $kgCO2_{eq}$/100km	-	-

Based on the simulation, there is a 20.2% discrepancy between the simulation result and the OEM's fuel economy, which is reasonable as the manufacturers' fuel economy data is based on lab tests which does not cover the real-world operation's conditions and the route topography.

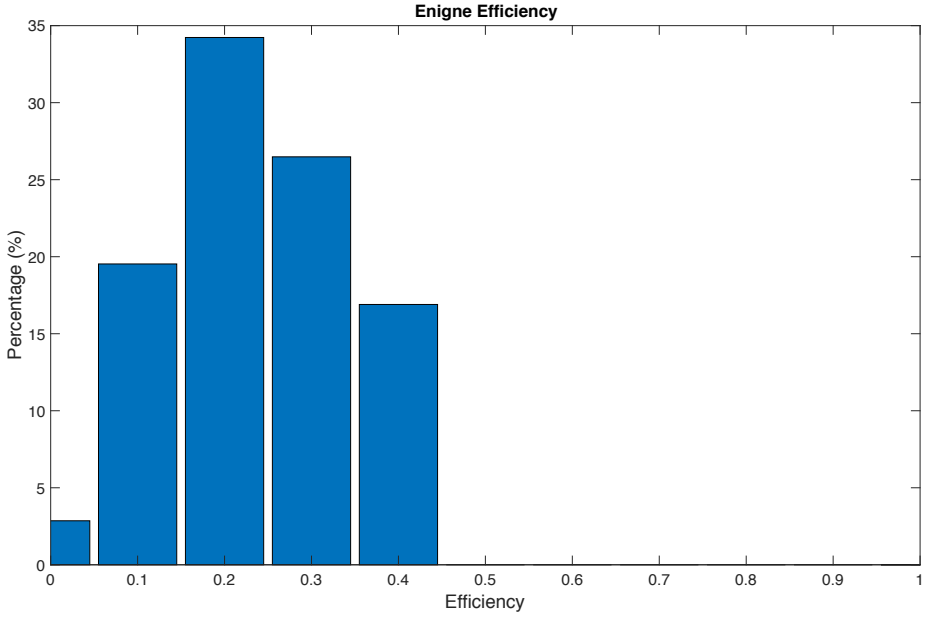

(a)

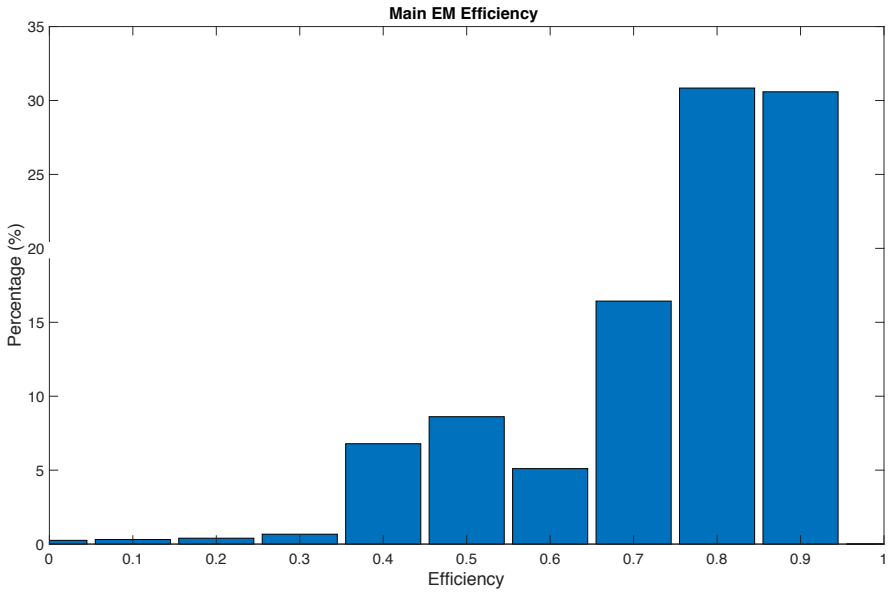

(b)

Figure 27) Fuel converter efficiency histogram: a) D-RCT's engine efficiency distribution, a) BE-RCT's main EM efficiency distribution

The fuel converter energy efficiency of the D-RCT and BE-RCT is presented as a histogram plot in Figure 27. The D-RCT's engine efficiency histogram (Figure 27-a) shows that the diesel engine runs in lower efficiency rather than the peak regions of its map, as the truck operates mostly with low speed, high idling time and frequent stops-and-goes, Distributions for BE-RCT's main EM efficiency (driving mode) reveal that the average efficiency (84.8%) is nearer to the maximum because of the more efficient operation of the EM at low speeds as well as the elimination of power when the truck has stopped. Comparing fuel use of the D-RCT (L_D) and BE-RCT ($L_{D,eq}$) presented in Table 17 and Table 20, respectively the energy use of the D-RCT is about 4.5 times higher than that of the BE-RCT, which is due to operation of the BE-RCT's main EM in higher efficiency ranges (average of 84.8%) compared to the diesel engine (average of 26.7%) over the duty cycle.

For further analysis, the operational data of the BE-RCT over the duty cycle's sub-activities is presented in Figure 28. For each sub-cycle, the plots show the power output of the battery, main/auxiliary EMs, the regenerated power input to the battery, and the battery's rated SOC. The battery power output, considered with the positive sign, covers the total power demand of the main and auxiliary electric motors, as well as the EMs' electric losses and the driveline losses. The battery power input is the fraction of negative traction power which is restored to the battery through the main EM and the regenerative braking system, which is considered as negative power.

The changes in battery power output/input, the main/auxiliary EMs' requested power is traceable with the changes in the duty cycle's speed, grade, and auxiliary power demand. From depo to the collection area, Figure 28-a, with moderate speed, fairly flat route and no payload the tractive power and consequently the battery/main EM's power demand is relatively low. The average battery, main and auxiliary EMs power output is found as 50.3 kW and 40.1 kW, 4.5 kW, respectively. With a relatively flat route and no stop over the sub-cycle, the average battery's regenerative power is found as -1.8 kW. The net energy output of the battery is 4.6 kWh corresponding to 48.5 kWh/h (112 .7 kWh/100km) energy use rate. Figure 28-b and Figure 28-c present the BE-RCT's performance over the total collection phase and five collection events, respectively. The battery and main EM power

output changes with respect to the steep gradient (over the first part and last twenty minutes of the sub-cycle) as well as the incrementally-added payload and over the trip is noticeable. With a moderate speed of 9.4 km/h over the collection trip, the average battery output is found 35.2 kW with an average discharge current of 7.4 amp. High characteristic deceleration (-0.72 m/s^2), correspondent to the frequent braking (17 stops/km) along with average of -2.1% downhill gradient, results in -31.5 kWh energy recuperation to the battery. The net energy use of the battery is 117.7 kWh with the rated SOC of 44.4% at the end of the collection phase. With the variable hydraulic load through each pickup period (as can be noticed in Figure 28-c) the average auxiliary power is found 7.1 kW, resulted in a total of 27.8 kWh auxiliary energy use. The specific energy use based on the sub-cycle's duration and traveled distance is estimated 27.7 kWh/h and 2.93 kWh/km, respectively consistent with the energy-demanding nature of the collection trip.

The truck's trip cycle from the collection area to the dumping site/from dumping to the main depo is plotted in Figure 28-d. Over the full-payload driving with an average speed of 48.3 km/h and 3.7% average upgrade route profile, the average battery and main EM power output increase to 137.2 kW and 124.8 kW, respectively. Subject to the maximum EM's power limit (252 kW), the achieved speed is reduced over 254 s (1.45% of the total duty cycle duration) with an absolute difference of 3.2 km/h between the actual and requested speed. Considering the dumping event, the maximum auxiliary EM's power output reaches to 39.3 kW, with an average of 4.9 kW resulted in 1.7 kWh auxiliary energy use. With average characteristic deceleration of -0.18 m/s^2, the mean regenerative power to the battery reaches -2.5 kW resulted in -0.8 kWh energy restoration. The battery's net energy use over the activity is found 42.5 kWh with 25.1% end-trip's rated SOC. From the dumping site to the depo, the empty truck travels with average driving speed and route gradient of 47.5 km/h and -3.8%, respectively. The mainly downhill driving over this trip resulted in -4.2 kWh energy restoration to the battery, corresponding to -3.3 kWh net energy restoration over the trip, which increases the end-trip's SOC of the battery to 26.5%.

Table 21 presents a summary of the BE-RCT operational data over the introduced sub-cycles. With the total of 161.5 kWh net energy consumption, the rated SOC of the battery at the end of the trip is 26.5% (61.3 kWh energy); however, the usable capacity of the battery will be 15.7 kWh, subject to 80% maximum Depth of Discharge (DOD).

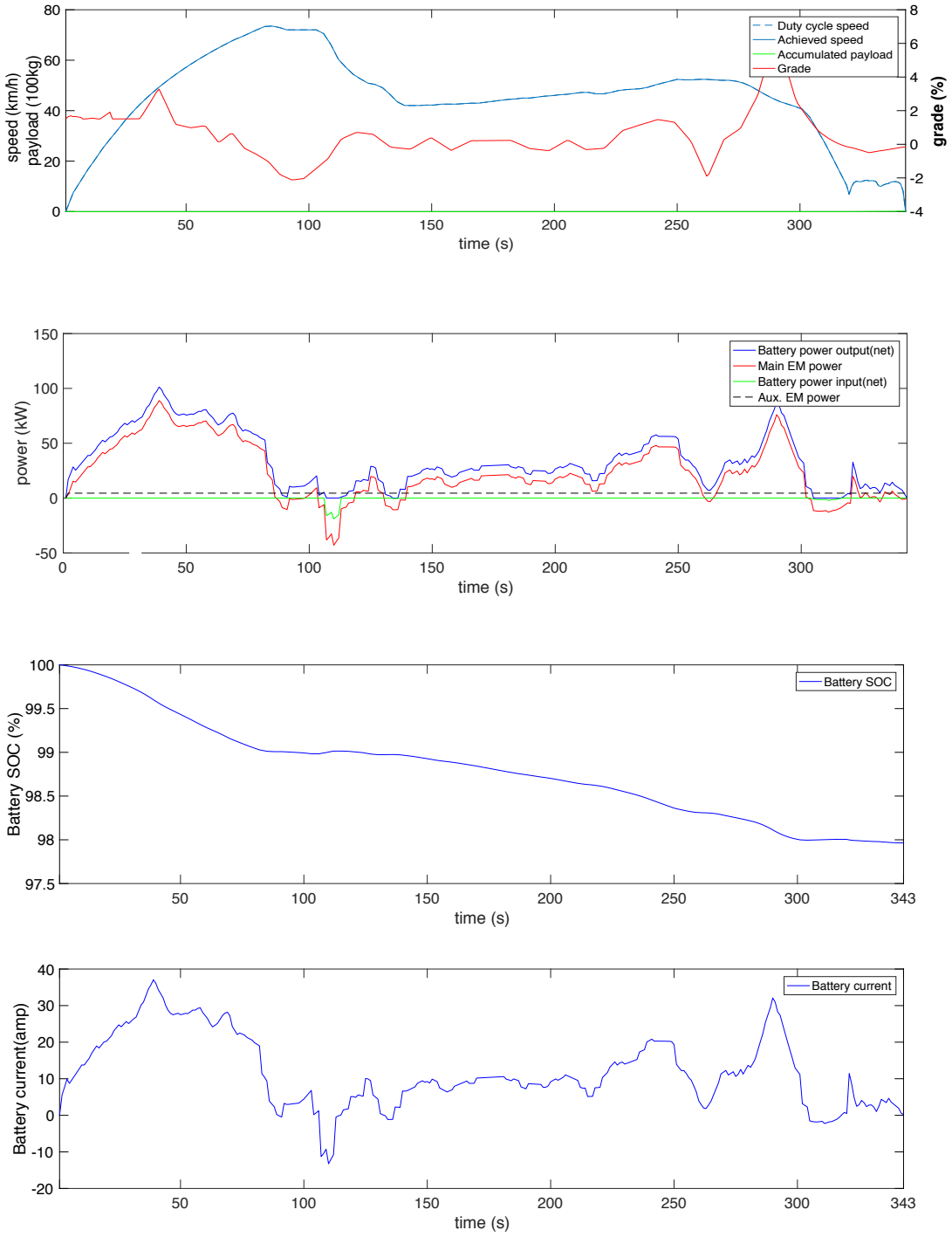
speed (km/h)
payload (100kg)
grade (%)
time (s)
Duty cycle speed
Achieved speed
Accumulated payload
Grade
power (kW)
Battery power output(net)
Main EM power
Battery power input(net)
Aux. EM power
Battery SOC (%)
Battery SOC
Battery current(amp)
Battery current

(a)

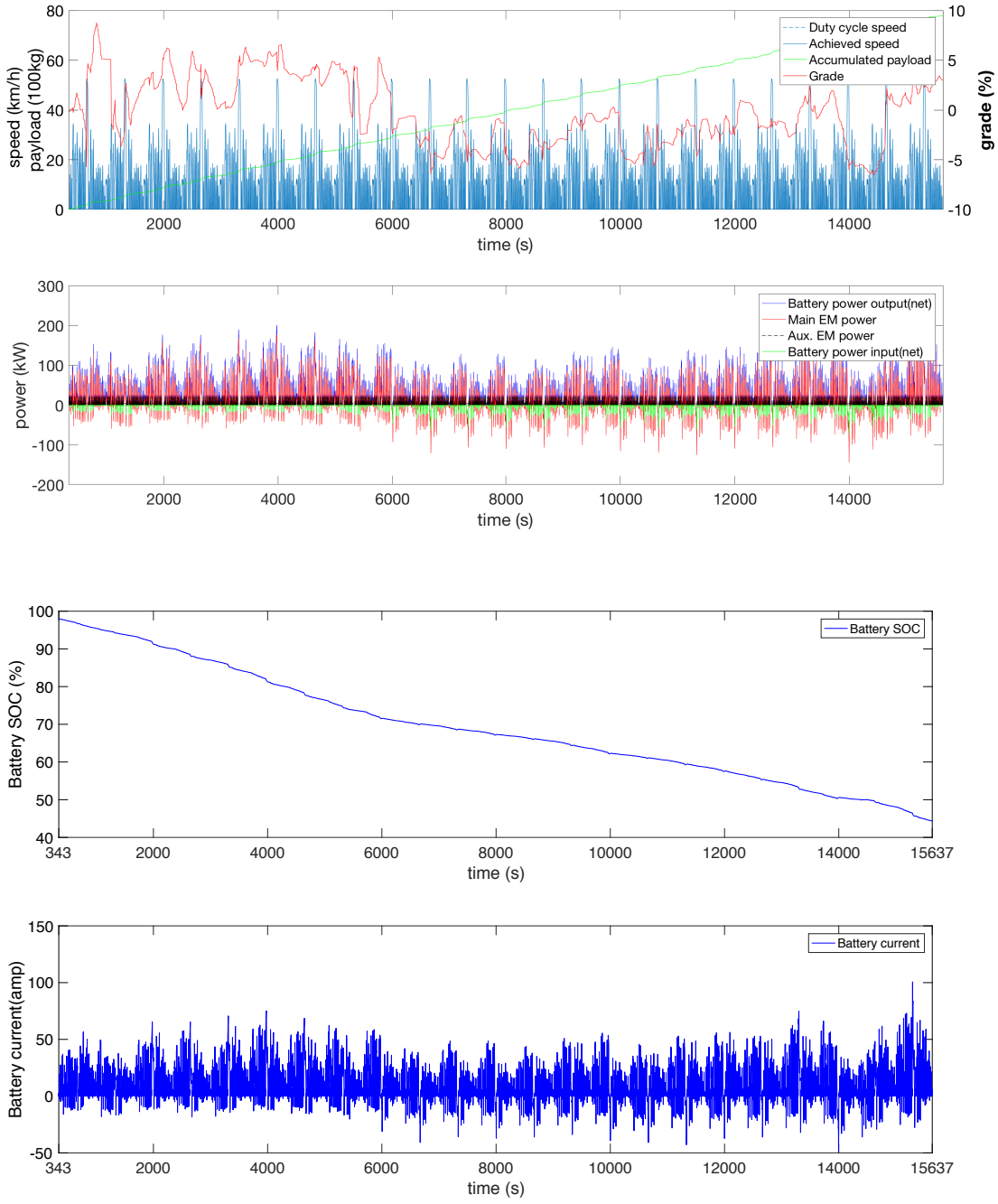
speed (km/h)
payload (100kg)
grade (%)
time (s)
Duty cycle speed
Achieved speed
Accumulated payload
Grade
power (kW)
Battery power output(net)
Main EM power
Aux. EM power
Battery power input(net)
Battery SOC (%)
Battery SOC
Battery current(amp)
Battery current

(b)

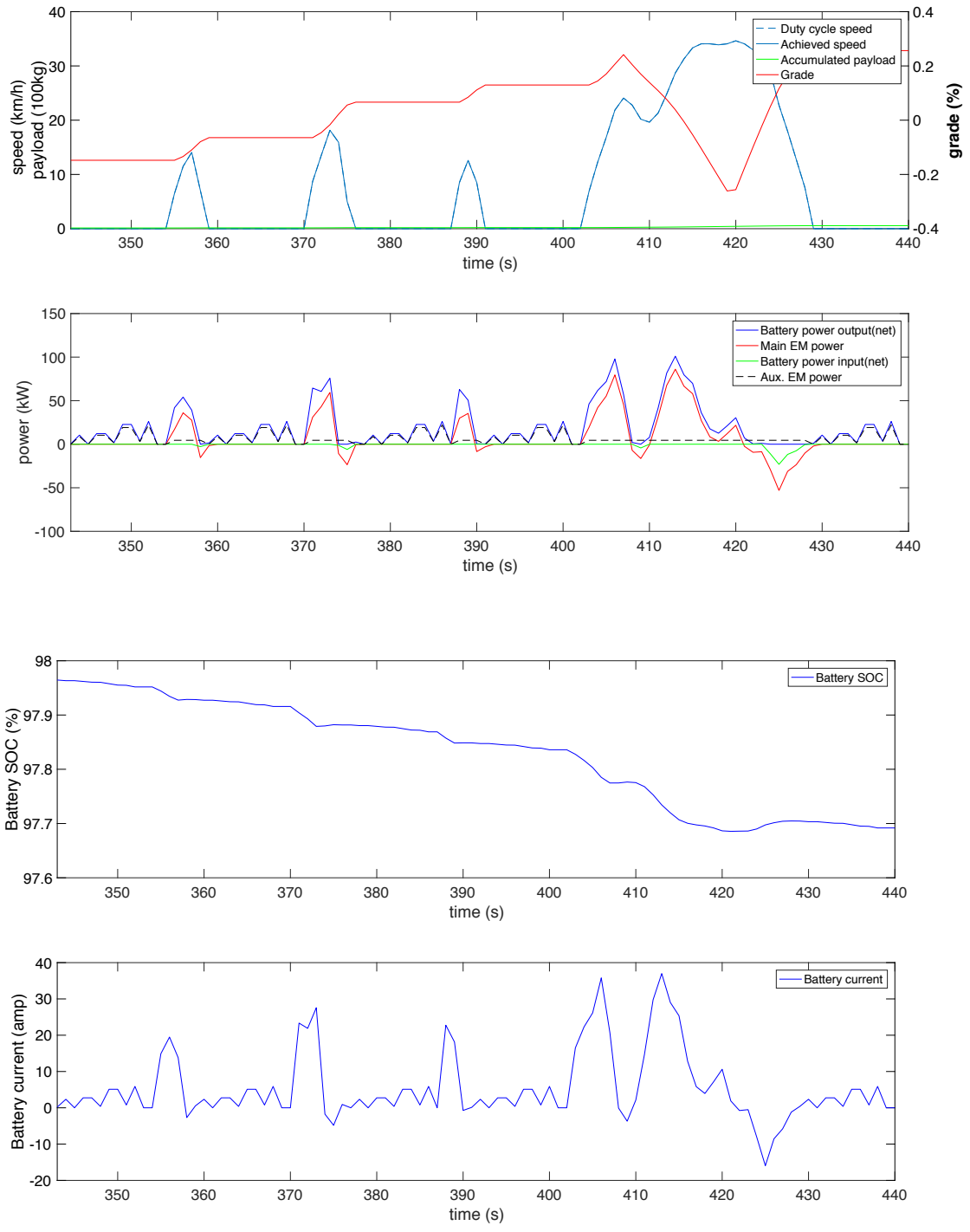
speed (km/h)
payload (100kg)
grade (%)
time (s)
Duty cycle speed
Achieved speed
Accumulated payload
Grade
power (kW)
Battery power output(net)
Main EM power
Battery power input(net)
Aux. EM power
Battery SOC (%)
Battery SOC
Battery current (amp)
Battery current

(c)

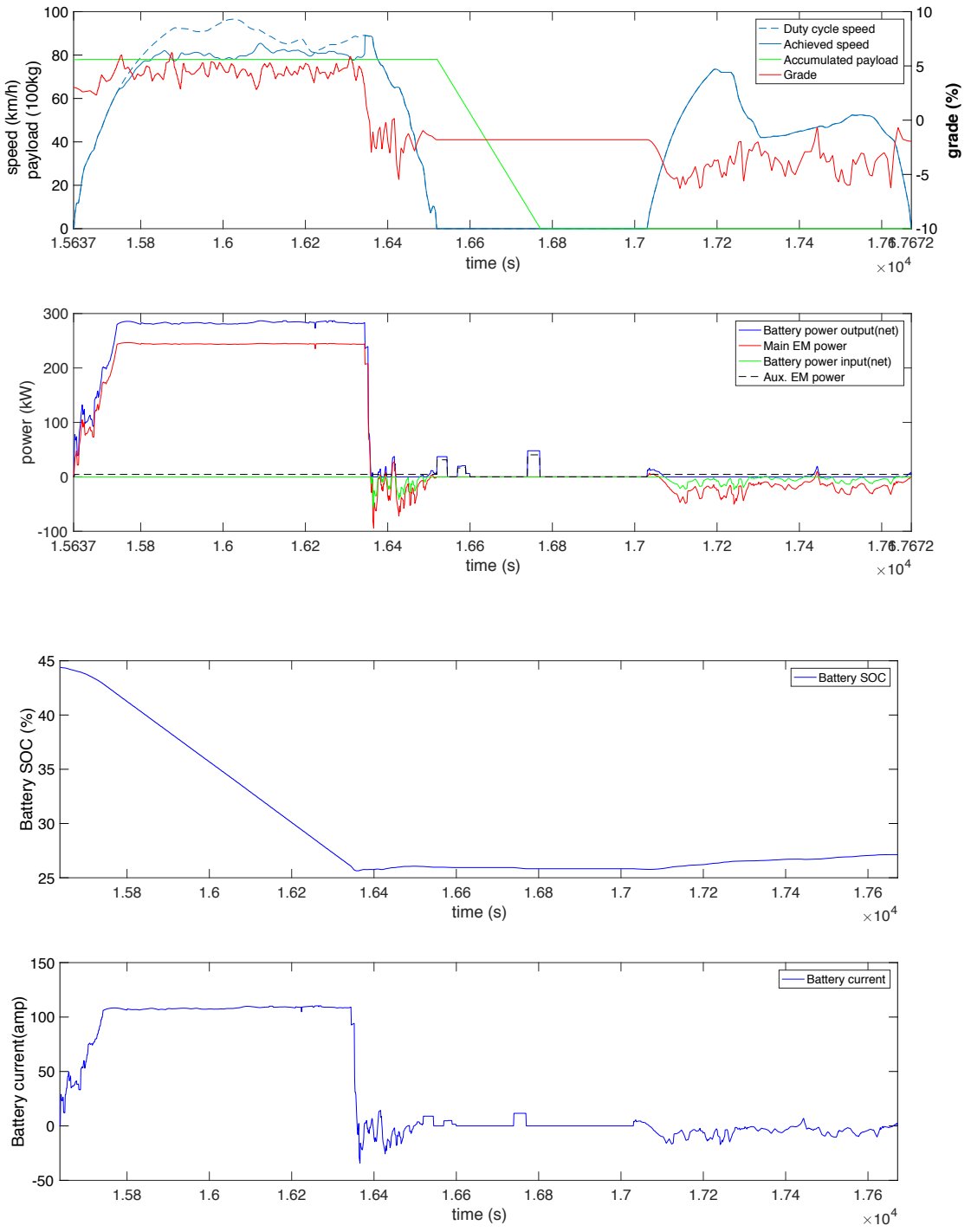

(d)

Figure 28) The simulation results for EMs/Battery demanded/regenerated power, battery SOC, battery current of the BE-RCT over the activity sub-cycles: a) Depo to collection sub-cycle, b) Five cycles of collection activity, c) Total collection sub-cycle, d) Collection to dump/dump to depo sub-cycle

DOD is a key parameter for the reliable and safe operation of the battery. For the deep-cycle lithium-ion batteries, the maximum DOD of 80% is suggested to preserve the battery's efficiency and lifetime [76], [81], [82]. Hence, the battery usable energy is less than its rated capacity which should be considered in selecting the appropriate battery capacity for the BE-RCT. Specifically, in the case of a refuse truck its vocational application within energy use for the on-board hydraulic equipment affects its performance and degradation behaviour, and may accelerate the battery's deterioration along with a shorter life span [16], [82].

Table 21) Operational characteristics of the BE-RCT through the different activity sub-cycles

Activity characteristics	Unit	No-payload driving (from depo)	Collection phase	Full-payload driving	No payload driving (to depo)	Total duty cycle (one-day operation)
Time	s	343	15294	1136	889	17672
Distance	km	4.1	40.2	12.7	8.5	65.5
Ave drv spd	km/h	43	19.8	48.3	47.5	25.1
Idle time	s	0	8001	0	255	8256
	%	No idle	45.9%	No idle	29%	47.4%
Ave bat. output energy	kWh	4.8	149.2	43.3	0.9	198.2
Ave bat. input energy	kWh	-0.2	-31.5	-0.8	-4.2	-36.7
Ave bat. consumed energy	kWh	4.6	117.7	42.5	-3.3	161.5
End-trip battery SOC	%	97.9%	44.4%	25.1%	26.5%	26.5%
Specific fuel use	kWh/h	48.3	27.7	134.7	-13.4	35.2
	kWh/100km	112.2	292.8	334.6	-38.8	246.5
GHG emissions rate (WTW)	$kgCO2_{eq}$ /100km	1.08	2.81	3.21	-	2.53

Based on the simulation results, the examined battery with rated capacity of 220 kWh might be able to meet the duty cycle demand, however, its end-trip SOC is fairly close to the 20% limit. From the battery management perspective, it is suggested to consider a higher capacity for the BE-RCT's battery to assure it operates healthy and reliable within the operational limit. The operational performance of the BE-RCT with higher battery's capacities will be assessed through the sensitivity analysis in Section 3.3.4.1.

4.2.3.1 BE-RCT energy breakdown

The energy components for the BE-RCT are presented in Table 22. Subject to the battery' weight (2000 kg), the tare weight of the BE-RCT is 1060 kg heavier than the D-RCT, resulted in an increase about 3% of the road power components (except the drag resistance which is independent of the vehicle mass). The total road load over the duty cycle is 132.2 kWh and the braking energy, which can be potentially regenerated, is about 97.3 kWh (48.9% of the total energy input).

Table 22) The demanded/regenerated energy components of the BE-RCT over the RTDC

Duty cycle energy break-down	kWh	% of the battery energy output
Road load	132.2	66.5%
Aux. load	32.3	16.2%
Battery energy input (regenerated energy)	37.2	18.7%
Net battery energy use	161.5	81.2%
Braking energy	97.3	48.9%
Regen. efficiency (%)	38.2%	-

Of the 97.3 kWh braking energy, 37.2 kWh (38.2%) is recovered which decrease the total energy use of the BE-RCT by 18.7%. The total energy demand of the cycle is 198.7 kWh. Considering the regenerated energy to the battery, 161.5 kWh of its capacity is depleted which is the net energy use. Within the auxiliary electric-motor efficiency, the auxiliary load is 32.3 kWh, which includes 16.2% of the total energy input. Compared to energy use of the D-RCT (Table 19), total energy use and the auxiliary load of the BE-RCT are decreased by 78.1% and 31.2%. In addition to the higher efficiency of the main EM compared to the diesel engine, the reason is that energy use over the idling time of the

D-RCT's operation (9.2 L_D /h) is eliminated in case of BE-RCT. Besides, for the auxiliary load, the energy losses of the hydraulic pump during its off-load operation is also eliminated when the BE-RCT is in the driving mode. The annual energy consumption and the potential of the BE-RCT in GHG mitigation is estimated based on the fleet's working days and average traveled distance over one year. In daily operation of the BE-RCT, one depletion/recharge cycle is expected to meet the refuse truck duty cycle. In order to examine the potential of the BE-RCT deployment, energy consumption and corresponding WTW GHG emissions for the D-RCT and BE-RCT are evaluated based on the fleet statistics and operational assumptions (Table 23 and Table 24).

Table 23) Fleet statistics and operational assumptions of the refuse trucks

Fleet annual operation statistics	
Fleet annual working days (day/y)	235
Ave. daily traveled distance (km/day)	65.5
Vehicle annual traveled distance (km/y)	15,393
Vehicle lifetime (y)	7
Battery life-cycle (cycles) [8]	1000
Charging efficiency [66]	90%
Charging event	1 charge/day

Table 24) D-RCT's and BE-RCT's simulation-based operational performance for the examined collection fleet

Operational value	D-RCT	BE-RCT
Driving energy consumption	71.2 L_D /day	161.5 kWh/day
Overall energy consumption	71.2 L_D /day	177.6 kWh/day
Annual energy consumption	16,732 L_D /y	41.7 MWh/y
WTW GHG emissions ($kgCO2_{eq}$/y)	61,490	400.7
Lifetime WTW GHG emission ($tCO2_{eq}$)	43	2.8

Table 25) Potential for fuel and emissions savings by adoption of the BE-RCT

Diesel fuel saving (L_D/y)	16,732
WTW GHG emission mitigation ($tCO2_{eq}$/y)	61.1
Lifetime WTW GHG emission savings ($tCO2_{eq}$)	427.7

As can be noticed, the BE-RCT's lifetime WTW GHG emissions are considerably lower (2.8 $tCO2_{eq}$) with the advantage of the clean regional grid. Based on the simulation results shown in Table 25, by adopting a BE-RCT in the examined collection fleet the diesel fuel saving will be 16,732 L_D corresponding to GHG mitigation of 61.1 $tCO2_{eq}$ per year and total of 427.7 $tCO2_{eq}$ over the seven-year proposed lifetime of the trucks. As mentioned in Section 3.3, the electricity grid mix can significantly change the contribution of fuel-cycle upstream emissions to the life-cycle GHG emissions of heavy-duty BE-trucks. That said, within the scope of this study with BC's low grid intensity, the battery's embodied GHG emissions can be compared to the electricity's WTP emissions. Over the assumed seven-year BE-RCT's lifetime, the battery's embodied GHG emissions will be 5.4 tCO2eq, assuming an embodied emissions factor of 22.4 $kgCO2_{eq}$/kWh (Section 3.3) and 220 kWh capacity over 1650 charging/recharging cycles (including one-time replacement w/ 1000 life-cycles). Although the battery's embodied GHG emissions are about 1.9 times higher than fuel upstream emissions, it is only 1.3% of the fuel-cycle emissions difference of the D-RCT and BE-RCT. With respect to the battery's embodied GHG emissions and negligible differences between vehicle-cycle GHG emissions of both type of trucks, ([74], [71]), the potential of the BE-RCT in total GHG emissions mitigation could be as high as 422.3 $tCO2_{eq}$ over the operational lifetime.

4.2.4 Sensitivity analysis

In addition to the base-case simulation, a sensitivity analysis was also conducted to estimate the impact of key simulation parameters on energy use of the D-RCT and BE-RCT. The parameters of interest to evaluate energy use are the battery size of the BE-RCT, the route grade, the payload mass, and the auxiliary load.

4.2.4.1 BE-RCT battery capacity size

We tested the simulated BE-RCT with different battery capacity sizes to examine the effect of the increased capacity and the corresponding added weight on the performance and energy use of the BE-RCT. Through the analysis, the battery specification was considered the same as the base-case with the energy capacity of 1.1 kWh and weight of 10 kg for each module [8], [61]. Based on the newly-introduced BE-RCTs in the market,

two other options for the capacity of the battery were considered in the sensitivity analysis with 250 kWh and 300 kWh nominal energy capacity [17]. The results for energy use, the end-trip SOC of the battery, and the expected range for the BE-RCT (subject the estimated fuel use efficiency and min SOC of 20%) are presented in Table 26.

Table 26) Sensitivity analysis of the battery capacity size impact on BE-RCT energy use and the total expected range

Battery nominal capacity (kWh)	BE-RCT tare weight (kg)	kWh	kWh/100km	End-trip rated SOC	Expected range (km)
220	16,130	161.5	246.5	26.5%	71.4
250	16,431	162.8	248.5	35%	80.5
300	16,880	166.6	254.3	44.4%	94.4

With the higher battery capacity, the usable SOC at the end of the trip is higher; however, energy use (kWh/100km) is increased due to the increase in tare weight of the BE-RCT. Considering max 80% DOD for the batteries [82], usable energy for the proposed batteries will be 200 kWh and 240 kWh, respectively. Based on the battery's usable energy and simulation energy consumption values (kWh/100km), 12.8% to 32.5% increase in the expected range is estimated compared to the base-case duty cycle. Corresponding to 1.9% and 4.7% increase in BE-RCT's tare weight, energy use increases by 0.8% and 3.2%, respectively. Based on the simulation results, the BE-RCT with nominal capacity of 220 kWh might be able to meet the duty cycle demand. However, the vocational application of the refuse truck with energy use for the on-board hydraulic equipment in addition to the fast charging option for the battery may affect the performance and degradation behaviour of the battery and accelerate its deterioration [82]. The maximum charge capacity of an aged battery decreases over the lifetime of the battery [81], hence; it is reasonable to choose the BE-RCT with minimum 250 kWh battery capacity which provides a buffer against the battery's deep discharge to reduce the degradation along with its reliable operation.

4.2.4.2 Grade

To understand the impact of the road grade profile on energy use of the modeled trucks, in addition to the base-case duty cycle the simulation is also tested over an assumed flat

route, as well as through a second route with a different grade profile. The traveled route for the second case duty cycle is mapped in Figure 29.

Figure 29) 2nd Route traveled distance including Collection area #2

In developing the second cycle, the speed profile and the number of collection events (and consequently the mass/hydraulic cycle) are considered the same as the base-case duty cycle but within the different trip route and the corresponding grade profile as presented in Figure 30. Within the same collection sub-cycle, the difference in the total traveled distance and the route topology results in different specific kinetic and potential energy components for the adopted duty cycles and consequently overall energy consumption. Table 27 and Table 28 present fuel consumption and GHG emissions of the D-RCT and BE-RCT, respectively over the developed duty cycles with and w/o considering the route gradient.

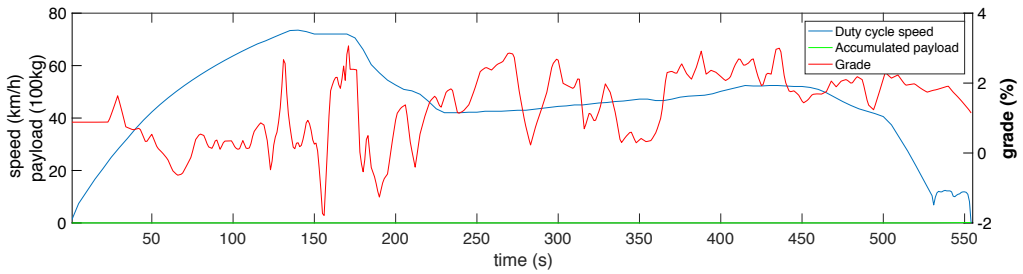

(a)

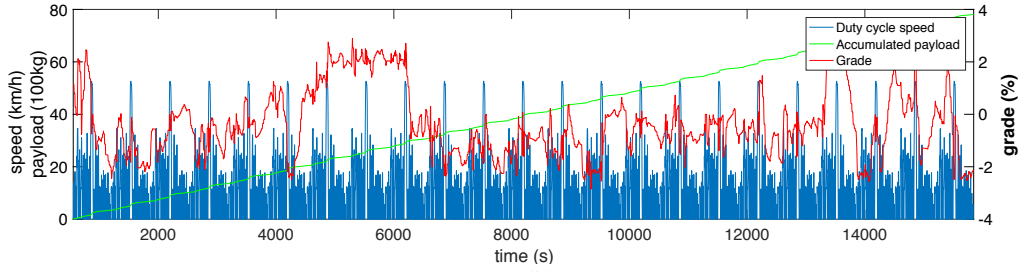

(b)

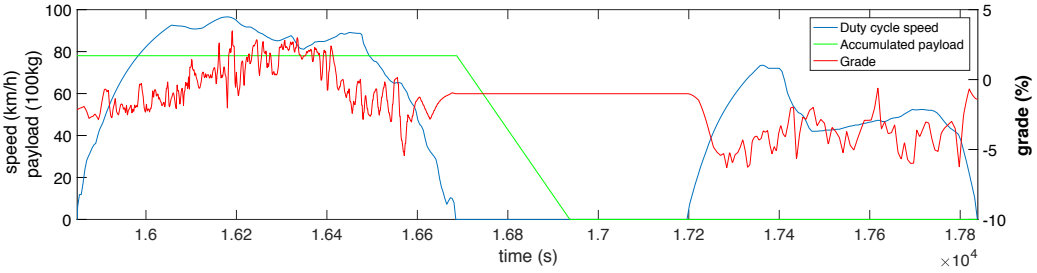

(c)

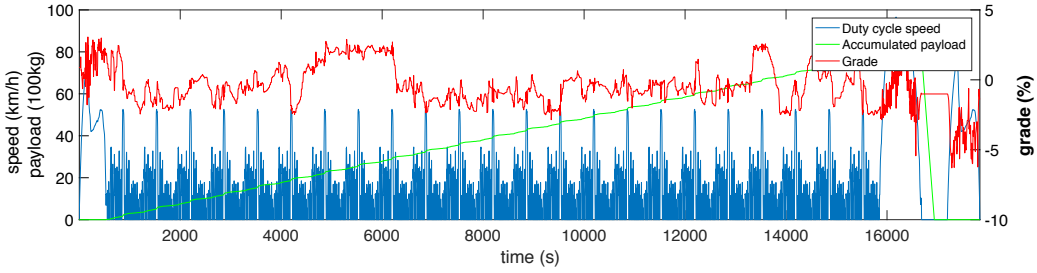

(d)

Figure 30) 2nd Route trip: a) Depo to collection area duty cycle, b) Collection duty cycle, c) Collection to dump/dump to depo duty cycle, d) Total duty cycle

Table 27) Sensitivity analysis of the route grade impact on D-RCT fuel use and GHG emissions

D-RCT energy use/ WTW GHG emissions						
Tested route	Ave route up/down grade (%)	Ave route up/down grade (%)	$L_{D,trip}$	L_D /100km	$kgCO2_{eq}$ /100km	% change compared to the base-case
Base-case Route	w/o grade	0	65.4	99.8	366	-8.9%
	w/ grade	3.2/-3	71.2	108.7	399.5	Baseline
2nd Route	w/o grade	0	67.4	92.7	340.7	-14.7%
	w/ grade	1.7/-2.5	70.5	97.8	359.4	-10.8%

Table 28) Sensitivity analysis of the route grade impact on BE-RCT fuel use and GHG emissions

BE-RCT energy use/ WTW GHG emissions							
Tested route	Ave route up/down grade (%)	Ave route up/down grade (%)	kWh_{trip}	kWh /100km	$L_{D,eq}$ /100km	$kgCO2_{eq}$ /100km	% change compared to the base-case
Base-case Route	w/o grade	0	151.8	231.7	22.9	2.22	6%
	w/ grade	3.2/-3	161.5	246.5	24.3	2.53	Baseline
2nd Route	w/o grade	0	159.7	220	21.7	2.11	-10.8%
	w/ grade	1.7/-2.5	168.7	232.4	22.9	2.23	-5.7%

The characteristic acceleration/deceleration of each cycle is different due to the difference in the grade profile and/or the specific kinetic energy of the cycles. The results indicate the importance of the grade factor and characteristic acceleration in energy consumption of both D-RCT and BE-RCT. It can be noticed that fuel use and corresponding GHG emissions of the D-RCT and BE-RCT are decreased by 8.9% and 6%, respectively without considering the road gradient for the base-case duty cycle. The impact of the route grade for the second duty cycle with a relatively flat terrain is lower compared to the base-case. Over the examined second route, fuel consumption and GHG emissions without considering the grade factor is reduced by 5.8% and 5.3% for the D-RCT and BE-RCT,

respectively. Comparing to the baseline duty cycle, fuel consumption over the second cycle for the D-RCT and BE-RCT is reduced by 18% and 12%, respectively which is consistent with its relatively flat terrain and consequently the lower characteristic acceleration of the second duty cycle compared to the base-case.

The change in energy consumption of both type of trucks is presented in Figure 31 based on the diesel/equivalent diesel fuel use for the developed duty cycles within their grade profiles. The impact of the route grade (compared to the flat terrain) on fuel consumption is lower for the BE-RCT than that of the D-RCT, since the BE-RCT sees the benefit of the regenerative braking over the downhill driving which consequently reduces the overall fuel increase.

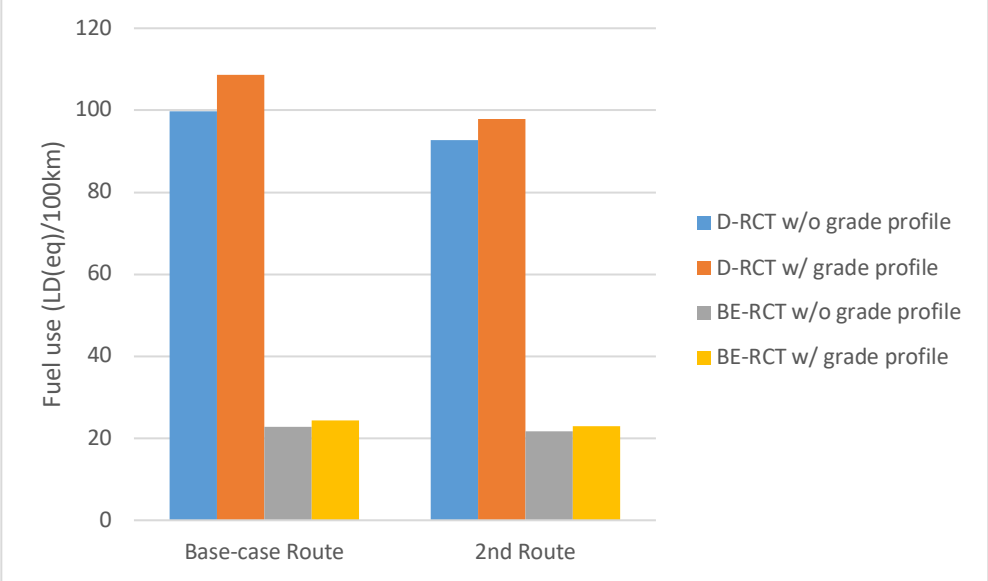

Figure 31) Route grade impact on fuel use of the D-RCT and BE-RCT

4.2.4.3 Payload mass

Another parameter which affects energy use of the collection refuse trucks is the amount of payload added to the vehicle incrementally. Based on the Saanich reported data presented in Section 2.2.2, the average collected waste mass varies between 6600 kg to a maximum of 8600 kg per truck per day. Through the sensitivity analysis, we examined the performance of the refuse collection trucks over the range of 50% and 100% payload capacity (5 to 10 tonnes of waste) to span the minimum, the average and the maximum values expected for the collection fleet

Table 29) Sensitivity analysis of the payload mass on D-RCT's fuel use and GHG emissions

D-RCT fuel use/ WTW GHG emissions				
Payload mass (t)	$L_{D,trip}$	L_D /100km	$kgCO2_{eq}$ /100km	L_D /100km.t
5	65.9	100.6	369.7	20.1
6.6	68.7	104.9	385.5	15.9
7.8	71.2	108.7	399.5	13.9
8.6	73	111.4	409.4	13
10	77.1	117.8	432.9	11.8

Table 30) Sensitivity analysis of the payload mass on BE-RCT fuel use and GHG emissions

BE-RCT fuel use/ WTW GHG emissions					
Payload mass (t)	kWh_{trip}	kWh/100km	$L_{D,eq}$/100km	$kgCO2_{eq}$ /100km	kWh/100km.t
5	145.5	222.1	21.9	2.1	44.4
6.6	153.8	234.7	23.2	2.3	35.6
7.8	161.5	246.5	24.3	2.4	31.6
8.6	168.3	256.9	25.3	2.5	29.9
10	178.5	272.4	26.9	2.6	27.2

The payload mass change is considered due to the change in average mass of each loaded bin; hence the number of stops is assumed to be the same with the base-case duty cycle. It should be noted that within the bin's mass change, same hydraulic pressure/power are considered as set design values for trash pickup/packing/dumping functions. The results of energy use and GHG emissions of the D-RCT and the BE-RCT are presented in Table 29 and Table 30, respectively. According to the results for both D-RCT and BE-RCT, energy use of both trucks increases with the increase in payload mass, as depicted in Figure 32.

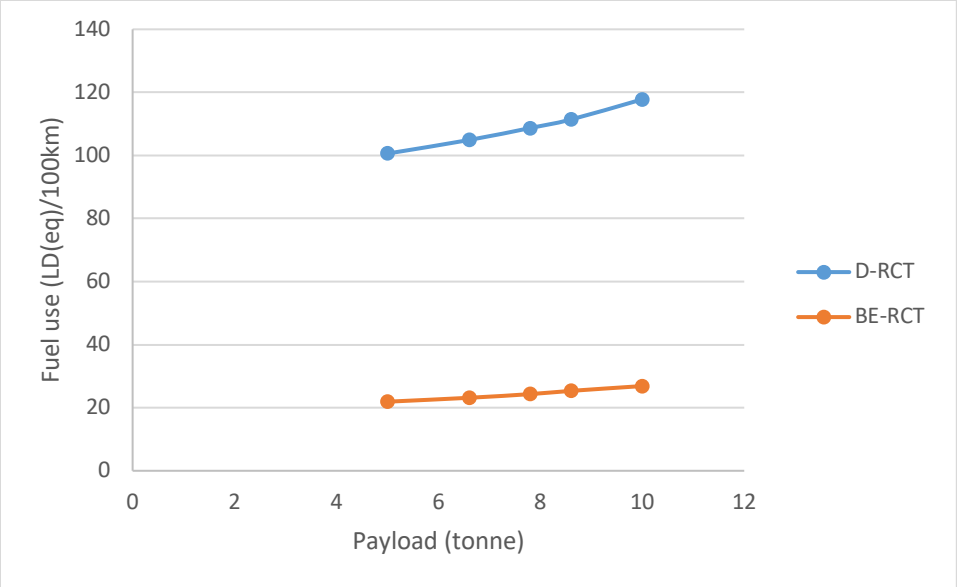

Figure 32) Payload mass impact on fuel use of the D-RCT and BE-RCT

The change in the payload and consequently the total truck's weight affects the rolling resistance, inertia and potential loads proportionally. For the RTDC with the high characteristic acceleration, the inertia and the potential loads are attributed to higher portions of the total energy demand (compared to the aerodynamic energy component), hence vehicle's fuel use is more sensitive to the payload, and consequently the vehicle's mass increase compared to a duty cycle with less kinetic intensities [60]. For the maximum payload capacity of 10 tonnes (28.2% payload increase), fuel consumption will rise by 8.4% and 10.5% compared to the baseline (with 7.8-tonne payload mass) for the D-RCT and BE-RCT, respectively. Similarly, the total energy use of D-RCT and BE-RCT is reduced by 7.5% and 9.9% with 35% reduction in payload mass compared to the base-case scenario. However, the specific energy use per unit of payload (tonne) (L_D/100km.t or kWh/100km.t) decreases while the payload increases. Because within the increase in payload a given percentage weight increase on the empty vehicle becomes a smaller percentage of the total gross weight, therefore the fuel increase per tonne of the payload decreases (considering the fact that the empty truck consumes a certain amount of energy regardless of the payload).

4.2.4.4 Auxiliary loads

As described before in Section 2.3.4, in this simulation the auxiliary load include the accessory loads in addition to the vocational hydraulic load. The hydraulic load is applied as the waste mass is loaded or packed or dumped, but the accessory loads are considered steady loads which are in operation for the whole duty cycle. To evaluate the impact of the accessories load change on energy use of the RCTs, a sensitivity analysis of the accessory power is conducted over a range of 2 kW to 9 kW which is suggested by [60] for heavy duty trucks. Table 31 and Table 32 present energy use and GHG emissions of the D-RCT and BE-RCT, respectively considering the auxiliary load changes. The 100% increase in the accessory power demand (4.5 kW to 9 kW) is founded to increase the energy demand by 15.2% and 14.8% for the D-RCT and BE-RCT, respectively. Reducing the accessory load by 55%, decrease energy consumption by 8.1% and 7.9%, for the D-RCT and BE-RCT, respectively.

Table 31) Sensitivity analysis of the auxiliary load on D-RCT fuel use and GHG emissions

D-RCT fuel use/ WTW GHG emissions			
Acc. Power (kW)	L_D	L_D /100km	$kgCO2_{eq}$ /100km
2	64.5	99.9	367.1
4.5	71.2	108.7	399.5
9	82.1	125.2	460.1

Table 32) Sensitivity analysis of the auxiliary load on BE-RCT fuel use and GHG emissions

BE-RCT fuel use/ WTW GHG emissions				
Acc. Power (kW)	kWh	kWh/100km	$L_{D,eq}$ /100km	$kgCO2_{eq}$ /100km
2	148.7	227	22.4	2.2
4.5	161.5	246.5	24.3	2.4
9	185.5	283.1	27.9	2.7

As presented in Figure 33 fuel use of the diesel truck is more sensitive to the change in the accessory load as the accessory power demand is drawn from the engine (considered as the mechanical accessories) while for the BE-RCT case the power is provided by the battery within the battery discharge efficiency. On the duty cycle for both trucks, energy use

reduction over the collection phase is higher compared to the average value over the whole duty cycle, accounting for 8.7% and 8.4% for the D-RCT and BE-RCT, respectively. The reason is that the average power demand is lower in addition to the high idling time over the collection phase.

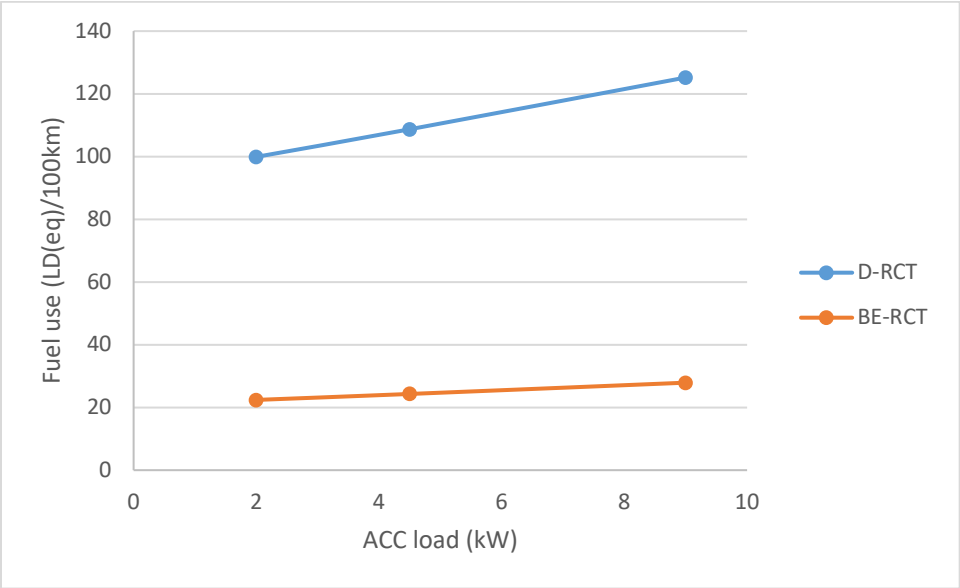

Figure 33) The accessory load impact on fuel use of D-RCT and BE-RCT

4.3 Total cost of ownership (TCO)

Once the trucks' energy use and the GHG mitigation potential of the BE-RCT were defined, to examine the financial competitiveness of the BE-RCT compared to the conventional counterpart the total cost of ownership (TCO) analysis was done for both type of trucks. The TCO presents the full costs of the vehicle over the ownership period, including the purchase cost as well as the operational and future maintenance costs. In order to consider the money value for future costs, the present value formula is applied using two factors: $P_{v,m}$ for future one-time costs occurring in the mth year of operation (i.e., battery replacement cost), and P_v which estimates the integration of future recurring costs over n years of operation (i.e., operational costs).

$$P_{v,m} = \frac{1}{(1+r)^m} \qquad \text{Equation 31}$$

$$P_v = \frac{(1+r)^n - 1}{r \times (1+r)^n} \qquad \text{Equation 32}$$

where r is the discount rate. Considering the present value formulas, TCO can be defined by the following equation [16]:

$$TCO = CAP_c + P_{v,m} \times Bat_{c,rep} + P_v \times VKT \times (O\&M_{c,km} + Fuel_c \times Fuel_{km} + GHG_c \times GHG_{km}) \quad \text{Equation 33}$$

where CAP_c is the purchase cost of the vehicle ($), $O\&M_{c,km}$ is the maintenance cost per km ($/km), $Fuel_c$ is the fuel price ($/$L_D$, $/kWh), $Fuel_{km}$ is the fuel use per km, GHG_c is the emissions tax cost ($/kg$CO2_{eq}$), GHG_{km} is the WTW emissions of the vehicle per km (kg$CO2_{eq}$/km), and $Bat_{c,rep}$ is the battery replacement cost applied for the BE-RCT. The capital cost is the purchase cost of the vehicle, which for the BE-RCT if any governmental/manufacturer's incentive is available, it will be deducted from the initial purchase cost [83]. The end-of-life value is not considered when the trucks are retired. The fuel use of the trucks is applied based on the simulation results, while for the BE-RCT, the charging efficiency of 90% is considered as suggested by [76]. The average daily and annual distance traveled by the BE-RCT and D-RCT trucks are assumed to be the same, considered based on the fleet statistics presented in Section 2.3.1. Based on the simulation results, one charging event is expected for the BE-RCT each day of operation. For a typical Li-ion battery in EV application, the life-span of 2000-4000 cycles is suggested when cycled to min 20% SOC through its operation [76], [84]. However, with a conservative approach, a life span of 1000 cycles is considered for the BE-RCT's battery pack, considering the energy use of the hydraulic equipment. With respect to one discharge/charging cycle a day, one set of battery is required to be replaced during the lifetime of the truck, in the year 5th of operation. The diesel fuel price is considered the average diesel price filling stations in Victoria, BC in 2018, and the electricity cost is applied based on the business rate for the Medium General Service (MGS) defined by the BC Hydro [85], [86]. The input parameters for the financial analysis are presented in Table 33, where the costs are based on the CAD dollar, unless specified. The exchange rate of 1.296 is applied to convert the US dollar to Canadian dollar, based on the official annual exchange rate in 2018 [83]. The operational inputs are defined based on the simulation results for fuel use and Saanich fleet statistics, and the financial input parameters are considered as suggested in the literature and/or manufacturer reports.

Table 33) Operational/financial input assumptions for the TCO analysis

TCO input parameters		
Discount rate [8]	3%	
Vehicle lifetime (y)	7	
Annual working days	235	
km/day traveled	65.5	
Annual km traveled	15,393	
Carbon tax (CAD$/t) [11]	35	
	D-RCT	BE-RCT
Vehicle purchasing cost (1000US$)	160 [87]	500 [8], [88]
Maintenance cost (CAD$/km)	0.65 [24]	0.4 [8], [88]
Energy cost	1.36 CAD$/$L_D$ [86]	0.0968 CAD$/kWh [85]
Battery life-cycle [8]	-	1000 cycles
Battery replacement cost [5]	-	130 (CAD$/kWh)
Charging efficiency [5]		90%

Applying Equation 33, the operational costs and the TCO over the vehicle lifetime can be estimated for both D-RCT and BE-RCT, as presented Figure 34 for the base-case scenario. In addition to the lifetime cost, Table 34 gives the annual operational costs of the trucks and determines the correspondent cost savings through the BE-RCT deployment. Based on the results, by replacing the D-RCT with the BE-RCT, $26,200 operational costs can be saved per year for the examined fleet.

Table 34) The operational costs and TCO over the vehicle lifetime

Financial analysis	D-RCT	BE-RCT	Savings
Capital cost (1000CAD$)	207.8	649.4	-441.6
Amortized capital cost (1000CAD$/y)	33.4	104.2	-70.9
Battery replacement cost (1000CAD$)	-	28.6	-28.6
Amortized Battery replacement cost (1000CAD$/y)	-	3.9	-3.9
Annual maintenance cost (1000CAD$/y)	9.9	6	4
Annual fuel cost (1000CAD$/y)	22.8	2.6	20.1
Annual carbon tax (1000CAD$/y)	2.15	0.01	2.14
Total operational costs (1000CAD$/y)	34.8	8.6	26.2
Total annual cost (1000CAD$/y)	68.2	116.8	-48.6
TCO (1000CAD$)	424.9	727.7	-302.8

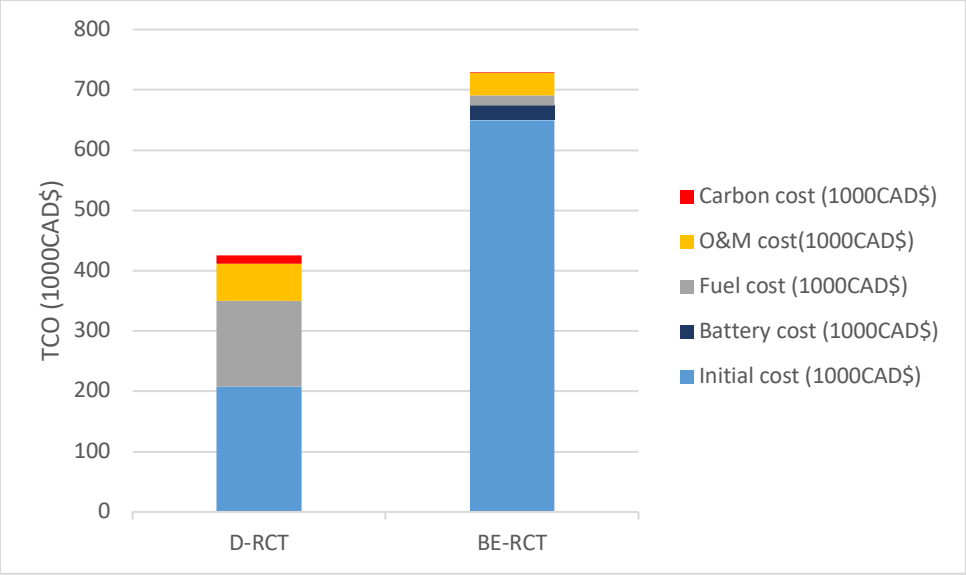

Figure 34) TCO of the D-RCT and BE-RCT for the base-case scenario

As can be noticed, the TCO of the D-RCT and BE-RCT is CAD$424,900 and CAD $727,700, respectively over the 7-year proposed lifetime of the trucks. The BE-RCT demonstrates a higher ownership cost by 171% compared to the D-RCT. Hence, within the expected assumptions, the BE-RCT is not financially profitable compared to the D-RCT. The reason is the high purchase cost of the BE-RCT which strikes the operational cost savings, so in order to bring the BE-RCT deployment as a feasible option, financial strategies are required to be taken. The policies should be taken to compensate for the high upfront cost difference or take advantage of the BE-RCT benefits in lower GHG emissions or the elimination of diesel fuel use. The plan can be an increase in either the diesel fuel price (by increasing the carbon tax), or the incentive to the BE-RCT purchase cost, or a combination of them.

Table 35) Required operational/financial plans for a feasible deployment of the BE-RCT for the base-case scenario

Operational/financial strategy requirements	
Min required utilization (km/y)	43,917
Max initial cost difference (1000CAD$)	139.2
Min carbon tax (CAD$/$tCO2_{eq}$)	790
Min fuel price (CAD$/$L_D$)	2.9

Based on the proposed assumptions and fuel use level of the trucks for the base-case scenario, the minimum threshold for each of the mentioned practices is determined which are presented in Table 35. For instance, if the fuel price increases to 2.9 CAD$/L$_D$ or the purchase cost difference decrease to CAD$139,200 then the BE-RCT can be commercially viable for the examined fleet. Regardless of the financial incentives, if the truck utilization increases to 43,917 km/y (averaged of 187 km/day) the BE-RCT potential in lower operational costs can also compensate the high difference in the purchase cost.

As mentioned earlier in the TCO's assumptions, the lifetime of 1000-cycle is defined for the BE-RCT's battery pack with respect to the vocational application, however, for an EV's Li-ion battery generally 2 to 4 times longer cycle life can be expected if it is being discharged to 80% or higher DOD under normal operation [76], [84]. A second scenario is evaluated considering the same input parameters as presented in Table 33, except for a 2000-cycle life-span assumed for the BE-RCT's battery lifetime. Considering the 2000-cycle battery's life-span, with 235 charge/discharge cycles per year, the battery replacement shifts to the 9th of operation of the BE-RCT. Hence, for the second scenario, there will be no replacement cost over the proposed 7-year operation time, resulted in lower TCO and annual costs of CAD$703,000 and CAD$/y 112.8, respectively. While with no battery replacement cost, the BE-RCT's TCO is reduced by 3.4%, it still costs 1.65 times more compared to the D-RCT over their lifetime (Figure 35).

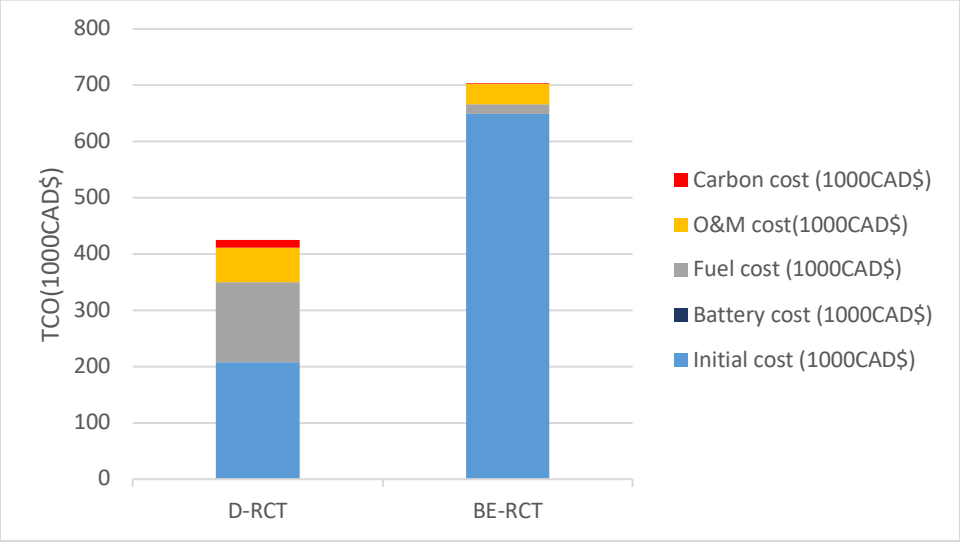

Figure 35) TCO of the D-RCT and BE-RCT for the second scenario (w/o battery replacement)

The financial criteria for the min trucks' purchase difference or diesel fuel price are also reduced in this case compared to the base-case scenario (Table 36). Compared to the base case scenario, without battery replacement cost slighter adjustments to carbon/diesel prices and or the EV's purchase cost are required for a feasible deployment of the BE-RCT in the collection fleet.

Table 36) Required operational/financial plans for a feasible deployment of the BE-RCT for the second scenario (w/o battery replacement cost)

Operational/financial strategy requirements	
Min required utilization (km/y)	41.594
Max initial cost difference (1000CAD$)	163.2
Min carbon tax (CAD$/$tCO2_{eq}$)	730
Min fuel price (CAD $/$L_D$)	2.7

Chapter 5: Conclusion and future work

5.1 Summary

In this work, energy consumption and GHG emissions assessment of a conventional diesel and a battery-electric refuse truck were conducted for a specific collection fleet as a case study using the ADVISOR simulator. The main objective was to predict the potential of the BE-RCT in energy use and GHG emissions reduction if it is deployed in the examined fleet. In so doing, first a refuse truck duty cycle was generated representing the stop-and-go driving nature and vocational operation of the refuse truck including mass and hydraulic cycles. Developing the speed profile of the duty cycle was based on a standard refuse speed profile, NRTC, developed by NREL, and the grade profile was imported considering Google map data of the traveled route. Also, within the duty cycle three phases were introduced with different activity conditions including the no-payload driving sub-cycle, collection phase and the full-payload driving sub-cycle. The second step was developing the vehicle model for both type of trucks in ADVISOR. As a base-case study, the trip route data for a specific truck operating in the collection fleet was considered. The input for the vehicle models was based on the manufacture vehicle data considering the limits assumed in the simulator. Considering the duty cycle and the vehicle model, the operational condition and energy consumption of the trucks over the adopted duty cycle as well as the sub-cycles were estimated which yielded the data to estimate the GHG emissions of the trucks. The GHG emissions analysis was conducted considering a 100-year horizon impact factor for the greenhouse gases. The GHG intensity for diesel fuel was used based on the GHGenius data and for the electricity BC's grid released data. Based on energy consumption values and the WTW GHG intensity of the both fuel types, the WTW GHG emissions of the trucks were determined over the trucks' operational lifetime. A sensitivity analysis over key input parameters, including the battery capacity of the BE-RCT, the loaded trash, and the auxiliary load was also conducted to estimate the influence of each parameter on CO_2 mitigation over the examined duty cycle. A second duty cycle with a different route profile was developed to assess the impact of the route roughness on energy consumption of the trucks. Finally, the lifetime TCO for the both trucks was estimated over a range of financial input parameters from low to high expected values

within three financial scenarios to assess the financial competitiveness of the BE-RCT over the D-RCT.

5.2 Outlook and future work

The energy analysis showed the refuse cycle as a high energy-demanding duty cycle with about 2.9 kWh/km energy use due to the high number of stops along with the vocational operation with the corresponding mass and hydraulic cycles. The stop-and-go nature of the RTDC and the rough grade profile also give the high value of negative tractive energy (1.32 kWh/km) of the refuse cycle and consequently the opportunity of energy savings through the regenerative braking system of the BE-RCT. Along with the regenerated energy, the more efficient driveline of the BE-RCT and no fuel use over the idle periods as well as the elimination of idle hydraulic loads over the moving resulted in 77.7% reduction in total energy use in case of the BE-RCT compared to the diesel counterpart. Within the sub-cycles, the diversity of the sub-cycle metrics (e.g., average total speed, idle time, characteristic acceleration) resulted in large variations in power and energy demand over the sub-cycles compared to one another.

Based on the simulation results for the base duty cycle, a BE-RCT with minimum battery capacity of 220 kWh is required to meet the fleet duty cycle requirements. However, it is recommended to consider a battery pack with a higher capacity of 250 kWh as electric power use of BE-RCT's hydraulic equipment can accelerate the battery's aging process and consequently its usable capacity. By adopting the BE-RCT for the proposed fleet, 16,732 L of diesel fuel can be saved annually resulted in mitigating 61.1t$CO2_{eq}$ /y GHG emissions.

Analyzing higher battery capacities of 250 kWh and 300 kWh for the BE-RCT revealed an increase in energy consumption (kWh/100km) by 0.8% and 3.2%, respectively due to the increase in the truck's tare weight, however, it increased the expected range to 80.5 and 94.4 km, respectively.

Sensitivity analysis of the payload mass revealed that a 28.2% increase in the incremental payload increases energy use of both D-RCT and BE-RCT by 8.4% and 10.5%, respectively. As each tonne of the payload is about 6% of the tare weight of the trucks, and regardless of the loaded mass the empty truck consumes fuel during transportation, the specific energy use per payload tonne is decreased with the payload increase for both

trucks. The change in accessory loads was found to have a considerable impact on energy use for both models due to the significant amount of idling time over the RTDC. As examined, a 50% increase in accessory loads leads to 15.2% and 14.9% increase in energy use of the D-RCT and BE-RCT, respectively. Concerning the route grade, energy use of D-RCT and BE-RCT was analyzed over the base and second duty cycles with and without grade profile. Testing the base duty cycle, energy use is reduced over the flat route by 8.4% and 6.4% for the D-RCT and BE-RCT, respectively. The BE-RCT energy use increase due to the route grade is lower than the diesel counterparts as it takes advantage of the potential to regenerate the negative tractive power. The characteristic acceleration/deceleration of the second cycle was found lower than those of the base cycle resulted in lower energy use compared to it, while for the second cycle energy use without considering the gradient was decreased by 4.6% and 5.6% for the D-RCT and BE-RCT, respectively.

The TCO analysis showed that the BE-RCT cannot financially compete with the D-RCT, as for the base-case scenario the lifetime cost of the BE-RCT is 171% higher than the D-RCT. The high purchase cost of the BE-RCT along with the low cost of the diesel fuel and carbon tax compensate the advantage of the BE-RCT in fuel and emissions costs savings. In order to bring the BE-RCT adoption financially profitable the BE-RCT should be deployed in a fleet with higher annual utilization, or there should be considerable incentive for the purchase cost of the BE-RCT and/or sufficient increase in carbon tax/diesel fuel price which demands effective actions from the government or manufacturers to ease the deployment of the BE-RCT in collection fleets.

The emissions analysis and the financial profitability of the BE-RCT vs. D-RCT are mainly related to the trucks' energy consumption corresponding to the vehicle input data and the operational duty cycle. If any test or on-route data for the trucks' operation, including the drivetrain data and real-world speed profile can be available, it is worth to be applied to the model done in this study. Particularly, with higher accuracy operational data, it can be explored how the diesel and electric drivetrains might be impacted by duty cycle metrics and route grade. Further research could also look at opportunities in other fleets, which can take advantage of the battery-electric vehicles specifically within the fast-pace introduction of the medium-duty and heavy-duty BEVs into the market. That can be looked through fleets which their duty cycles include low/moderate driving speed, high idling

time, high characteristic deceleration (with aggressive and/or a high number of stops-and-goes), e.g., package delivery fleets, port drayage fleets, utility fleets, transit buses, school buses. Also, more exploration can go through the other collection fleets as the duty cycle is specific to each fleet, which impacts the BE-RCT deployment assessment.

The TCO analysis can be extended with respect to technology improvements in the future and/or the near-term changes in financial parameters. The drivetrain efficiency and battery's lifetime improvements can be examined to predict the performance/financial profitability of BE-RCTs compared to their conventional counterparts. Specifically for the BE-RCT, as its initial cost incorporates a considerable part of the total cost, reduced BE-RCT's purchase price can be examined to evaluate the readiness of the market for deployment of this technology in refuse fleets. A degradation model can also be applied to estimate the battery's lifetime and correspondingly the replacement cost significance on the TCO of the BE-RCT. Considering the future energy trends, additional scenarios with predictions for diesel fuel and associated carbon prices can measure the fuel/carbon price impact on the competitiveness of the BE-RCT compared to the conventional counterpart.

Bibliography

[1] EPA, "Sources of Greenhouse Gas Emissions | Greenhouse Gas (GHG) Emissions | US EPA."

[2] European Environment Agency, "Greenhouse gas emissions from transport — European Environment Agency," 2017.

[3] Government of Canada, "Greenhouse Gas Sources and Sinks in Canada Canada'S Submission To the United Nations Framework Convention on Climate Change Executive Summary," 2018.

[4] "Transportation Sector – GHG Emissions | Natural Resources Canada," *Natural Resources Canada*, 2017. [Online]. Available: http://oee.nrcan.gc.ca/corporate/statistics

[5] R. Peel, "Waste Collection Design Standards Manual."

[6] IPCC, "Climate Change 2013," 2013.

[7] Y. Zhao, N. C. Onat, M. Kucukvar, and O. Tatari, "Carbon and energy footprints of electric delivery trucks: A hybrid multi-regional input-output life cycle assessment," *Transp. Res. Part D Transp. Environ.*, vol. 47, pp. 195–207, 2016.

[8] M. K. Jaunich *et al.*, "Characterization of municipal solid waste collection operations," *Resour. Conserv. Recycl.*, vol. 114, pp. 92–102, Nov. 2016.

[9] F. A. Bender, T. Bosse, and O. Sawodny, "An investigation on the fuel savings potential of hybrid hydraulic refuse collection vehicles," *Waste Manag.*, vol. 34, no. 9, pp. 1577–1583, 2014.

[10] G. S. Sandhu, H. C. Frey, S. Bartelt-Hunt, and E. Jones, "In-use activity, fuel use, and emissions of heavy-duty diesel roll-off refuse trucks," *J. Air Waste Manage. Assoc.*, vol. 65, no. 3, pp. 306–323, Mar. 2015.

[11] G. S. Sandhu, H. C. Frey, S. Bartelt-Hunt, and E. Jones, "In-use measurement of the activity, fuel use, and emissions of front-loader refuse trucks," *Atmos. Environ.*, vol. 92, pp. 557–565, Aug. 2014.

[12] G. S. Sandhu, H. C. Frey, S. Bartelt-Hunt, and E. Jones, "Real-world activity, fuel use, and emissions of diesel side-loader refuse trucks," *Atmos. Environ.*, vol. 129, pp. 98–104, Mar. 2016.

[13] “https://www.trashtrucksonline.com” 2017. [Online]. Available: https://www.trashtrucksonline.com/index.php?a=5&c=24&b=182.

[14] “Waste Collection Vehicle,” *Waste Management Resources*, 2009. [Online]. Available: http://www.wrfound.org.uk/articles/waste-collection-vehicle.html.

[15] T. C. Study, “Eaton Power-On-Demand Hydraulic System Helps New McNeilus Side-Loader Refuse Truck Improve Productivity and Fuel,” no. December, pp. 34–36, 2011.

[16] Y. Zhao and O. Tatari, “Carbon and energy footprints of refuse collection trucks: A hybrid life cycle evaluation,” *Sustain. Prod. Consum.*, vol. 12, pp. 180–192, Oct. 2017.

[17] “Volvo unveils new all-electric garbage truck with up to 200 km of range - Electrek.” .

[18] “Scania delivers fuel cell refuse truck | Scania Group.” .

[19] A. Burnham, M. Mintz, M. Rood, and A. Burnham, “Status and Issues for Natural Gas in the United States Alternative Fuel and Advanced Vehicle,” no. February, 2015.

[20] “Hydraulic Hybrid Fleet Vehicle Testing | Transportation Research | NREL.” [Online]. Available: https://www.nrel.gov/transportation/fleettest-hydraulic.html.

[21] C. Nash, “Institute for Transport Studies,” pp. 1–6, 2006.

[22] R. P. Nrel, “NREL Evaluates Performance of Hydraulic Hybrid Refuse Vehicles | NREL,” no. September, p. 80401, 2015.

[23] R. Parish, “Alternative Fuels and Systems for Refuse Trucks,” p. 21, 2005.

[24] L. Rose, M. Hussain, S. Ahmed, K. Malek, R. Costanzo, and E. Kjeang, “A comparative life cycle assessment of diesel and compressed natural gas powered refuse collection vehicles in a Canadian city,” *Energy Policy*, vol. 52, pp. 453–461, 2013.

[25] “First All-Electric Garbage Truck in North America, Developed by Motiv Power Systems, Hits the Road i.” .

[26] “California’s First All-Electric Garbage Truck Headed to Sacramento, Equipped with Motiv All-Electric Powertrain - Motiv Power Systems,” *Motiv Power Systems*. 2017.

[27] “Motiv Names Chicago Partners | ShowTimes Clean Fuel & Vehicle News.” .

[28] J. O’Dell, “Peterbilt Unveils Battery-Electric Garbage Truck | Trucks.com,” *Trucks.com*. 2017.

[29] “Peterbilt Gets Ready To Enter Electric Semi Truck Segment.” .

[30] BYD, “BYD_CLASS 6_ REFUSE TRUCK_Broucher.” BYD.

[31] BYD, “BYD_CLASS 8_LONG RANGE_ REFUSE TRUCK_Broucher.” .

[32] “BYD Will Deliver First Electric Garbage Trucks In Seattle.” .

[33] “BYD Delivers First All-Electric Garbage Truck To Palo Alto.” .

[34] “Volvo unveils new all-electric garbage truck with up to 200 km of range - Electrek.” .

[35] “Volvo Launches First FL Electric Refuse Truck - Video.” .

[36] “Volvo delivers its first electric trucks - Electrek.” .

[37] M. A. Maimoun, D. R. Reinhart, F. T. Gammoh, and P. McCauley Bush, “Emissions from US waste collection vehicles,” *Waste Manag.*, vol. 33, no. 5, pp. 1079–1089, May 2013.

[38] J. M. López, Á. Gómez, F. Aparicio, and F. Javier Sánchez, “Comparison of GHG emissions from diesel, biodiesel and natural gas refuse trucks of the City of Madrid,” *Appl. Energy*, vol. 86, no. 5, pp. 610–615, 2009.

[39] N. R. Council, T. R. Board, D. E. P. Sciences, B. E. E. Systems, and C. A. F. E. T. M. H. D. Vehicles, *Technologies and Approaches to Reducing the Fuel Consumption of Medium- and Heavy-Duty Vehicles*. National Academies Press, 2010.

[40] T. Ercan and O. Tatari, “A hybrid life cycle assessment of public transportation buses with alternative fuel options,” *Int. J. Life Cycle Assess.*, vol. 20, no. 9, pp. 1213–1231, 2015.

[41] Ž. Ivanič, “Data Collection and Development of New York City Refuse Truck Duty Cycle,” 2007.

[42] A. Soliman, K. Kelly, N. Dembski, J. Fravert, and G. Rizzoni, “Development of Refuse Vehicle Driving and Duty Cycles,” *SAE Tech. Pap. Ser.*, vol. 1, no. April, pp. 11–14, 2010.

[43] T. Markel *et al.*, “ADVISOR : a systems analysis tool for advanced vehicle

modeling," vol. 110, pp. 255–266, 2002.

[44] F. Tong, P. Jaramillo, and I. M. L. Azevedo, "Comparison of Life Cycle Greenhouse Gases from Natural Gas Pathways for Medium and Heavy-Duty Vehicles," *Environ. Sci. Technol.*, vol. 49, no. 12, pp. 7123–7133, 2015.

[45] D.-Y. Lee, V. M. Thomas, and M. A. Brown, "Electric Urban Delivery Trucks: Energy Use, Greenhouse Gas Emissions, and Cost-Effectiveness," *Environ. Sci. Technol.*, vol. 47, no. 14, pp. 8022–8030, Jul. 2013.

[46] District of Saanich, "District of Saanich Climate Climate Action Action Plan Plan," p. 42, 2010.

[47] "Leading Fleet Management Software Globally | Fleet Complete." .

[48] Saanich Municipality, "Peterbilt 320 spec, #18-572." .

[49] NREL, "Drive Cycle Analysis Tool — DriveCAT | NREL," 2018. [Online]. Available: https://www.nrel.gov/transportation/drive-cycle-tool//drive-cycle-tool.html.

[50] S. M. Lajevardi, J. Axsen, and C. Crawford, "Examining the role of natural gas and advanced vehicle technologies in mitigating CO2emissions of heavy-duty trucks: Modeling prototypical British Columbia routes with road grades," *Transp. Res. Part D Transp. Environ.*, vol. 62, pp. 186–211, 2018.

[51] E. Wood *et al.*, "Appending high-resolution elevation data to GPS speed traces for vehicle energy modeling and simulation appending high-resolution elevation data to GPS speed traces for vehicle energy modeling and simulation," *Tech. report, NREL/TP-5400-61109*, no. June, 2014.

[52] C. Iron and B. Design, "PGP / PGM300 Series The Parker Hannifin Gear Pump Division Assures : Consistent quality, Technical innovation, Premier customer service."

[53] D. O. F. Philosophy, "Modeling and Real-Time Optimal Energy Management for Hybrid and Plug-in Hybrid Electric Vehicles Supervisory Committee Modeling and Real-Time Optimal Energy Management for Hybrid and Plug-in Hybrid Electric Vehicle," 2017.

[54] Http://adv-vehicle-sim.sourceforge.net/glossary.html [Online]. Available: http://adv-vehicle-sim.sourceforge.net/glossary.html#C.

[55] A. Test and A. V. S. Auto-size, “ADVISOR Glossary.” pp. 1–12, 2018.

[56] C. M. Xi Zhang, *Vehicle Power Management Modeling, Control and Optimization*. 2011.

[57] V. H. Johnson, “Battery performance models in ADVISOR,” *J. Power Sources*, vol. 110, no. 2, pp. 321–329, 2002.

[58] US Department of Energy, “Alternative Fuels Data Center: Maps and Data,” no. September 2011, p. 20740, 2013.

[59] I. The, W. The, and W. Works, “Allison 5th Gen Vocational Model Guide 2015,” 2015.

[60] H. Zhao, A. Burke, and M. Miller, “Analysis of Class 8 truck technologies for their fuel savings and economics,” *Transp. Res. Part D Transp. Environ.*, vol. 23, no. 2013, pp. 55–63, 2013.

[61] “Integrated Lithium-ion Applications | A123 Systems.” [Online]. Available: http://www.a123systems.com/automotive/products/cells/.

[62] I. (S&T)2 Consultants and I. Coordinating Research Council, “Transportation Fuel Life Cycle Assessment: Validation and Uncertainty of Well-to-Wheel GHG Estimates,” p. 293p, 2013.

[63] P. Egede, T. Dettmer, C. Herrmann, and S. Kara, “Life cycle assessment of electric vehicles - A framework to consider influencing factors,” *Procedia CIRP*, vol. 29, pp. 233–238, 2015.

[64] “GHGenius Model.” .

[65] A. N. Laboratory, “Argonne GREET Model,” *Biomass Energy Data Book*, 2011. .

[66] “AFLEET Tool - Argonne National Laboratory.” .

[67] EPA, “MOVES and Other Mobile Source Emissions Models.” 2017.

[68] A. Mayyas, M. Omar, M. Hayajneh, and A. R. Mayyas, “Vehicle’s lightweight design vs. electrification from life cycle assessment perspective,” *J. Clean. Prod.*, vol. 167, pp. 687–701, 2018.

[69] G. N. Correia, T. P. Batista, S. S. Marques, and C. M. Silva, “How car material life-cycle emissions are considered in environmental rating methodologies? Suggestion of expedite models and discussion,” *Renew. Sustain. Energy Rev.*, vol. 38, pp. 20–35, 2014.

[70] H. L. MacLean and L. B. Lave, “Life Cycle Assessment of Automobile/Fuel Options,” *Environ. Sci. Technol.*, vol. 37, no. 23, pp. 5445–5452, 2003.

[71] T. Zhou, M. J. Roorda, H. L. MacLean, and J. Luk, “Life cycle GHG emissions and lifetime costs of medium-duty diesel and battery electric trucks in Toronto, Canada,” *Transp. Res. Part D Transp. Environ.*, vol. 55, pp. 91–98, 2017.

[72] B. Sen, T. Ercan, and O. Tatari, “Does a battery-electric truck make a difference? – Life cycle emissions, costs, and externality analysis of alternative fuel-powered Class 8 heavy-duty trucks in the United States,” *J. Clean. Prod.*, vol. 141, pp. 110–121, 2017.

[73] A. Papathomas *et al.*, “To print this document, select the Print,” *Hist. Work. J.*, vol. 80, no. 3, p. 302, 2016.

[74] H. Ma, F. Balthasar, N. Tait, X. Riera-Palou, and A. Harrison, “A new comparison between the life cycle greenhouse gas emissions of battery electric vehicles and internal combustion vehicles,” *Energy Policy*, vol. 44, pp. 160–173, 2012.

[75] “Canada’s Official Greenhouse Gas Inventory - Open Government Portal.” .

[76] R. Garcia-Valle and J. A. P. Lopes, *Electric vehicle integration into modern power networks*. 2013.

[77] M. P. O’Keefe, A. Simpson, K. J. Kelly, and D. S. Pedersen, “Duty Cycle Characterization and Evaluation Towards Heavy Hybrid Vehicle Applications,” *SAE Tech. Pap. Ser.*, vol. 1, no. April, pp. 16–19, 2010.

[78] L. H. Björnsson and S. Karlsson, “The potential for brake energy regeneration under Swedish conditions,” *Appl. Energy*, vol. 168, pp. 75–84, 2016.

[79] J. Pérez, J. Lumbreras, E. Rodríguez, and M. Vedrenne, “A methodology for estimating the carbon footprint of waste collection vehicles under different scenarios: Application to Madrid,” *Transp. Res. Part D Transp. Environ.*, vol. 52, pp. 156–171, 2017.

[80] M. Farzaneh, J. Zietsman, and D.-W. Lee, “Evaluation of In-Use Emissions from Refuse Trucks,” *Transp. Res. Rec. J. Transp. Res. Board*, vol. 2123, no. 1, pp. 38–45, Jan. 2009.

[81] W. Chen, J. Liang, Z. Yang, and G. Li, “A review of lithium-ion battery for electric vehicle applications and beyond,” *Energy Procedia*, vol. 158, pp. 4363–

4368, 2019.

[82] X. Han *et al.*, “A review on the key issues of the lithium ion battery degradation among the whole life cycle,” *eTransportation*, vol. 1, p. 100005, 2019.

[83] “Annual Exchange Rates - Bank of Canada.” .

[84] Battery-University, “How to Prolong Lithium-based Batteries - Battery University.” 2016.

[85] BC Hydro, “General Service Business Rates,” *BC Hydro Power Smart*. 2016.

[86] Statistics Canada, “Monthly average retail prices for gasoline and fuel oil, by geogrophy.” 2017.

[87] “2014 Peterbilt 320, Heil Python ASL - LOW MILES! : Side Loaders.” .

[88] “Hayward manufacturer turns diesel-burning trucks into all-electric vehicles – East Bay Times.” .

Appendix

Financial calculation:

Amortization, and present value factors:

Amortization factor: $f_{amr} = \frac{r \times (1+r)^n}{(1+r)^n - 1}$

For future one − time costs: $P_{v,y} = \frac{1}{(1+r)^y}$

For future recurring costs : $P_v = \frac{(1+r)^n - 1}{r \times (1+r)^n}$

D-RCT:

$O\&M_{c,tot} = VKT \times (O\&M_{c,km} + Fuel_c \times Fuel_{km} + GHG_c \times GHG_{km})$
$= 65.5 \frac{km}{day} * 235 \frac{day}{yr} * \left(0.65 \frac{CAD\$}{km} + 1.087 \frac{l}{km} * 1.36 \frac{CAD\$}{l} + 0.035 \frac{CAD\$}{kgCO2eq} * 3.675 \frac{kgCO2}{L} * 1.087 \frac{l}{km}\right) = 1000\text{CAD\$} * (9.9 + 22.8 + 2.15) = 34.8\ (1000\text{CAD\$})$

$Tot\ Annual\ Cost_{amortized} = CAP_c * f_{amr} + O\&M_{c,tot}$
$= 207.8 * \frac{0.3 \times (1+0.3)^7}{(1+0.3)^7 - 1} + 34.8 = 33.4 + 34.8 = 68.2\ (\frac{1000CAD\$}{yr})$

$TCO = CAP_c + \sum_{n=1}^{7} {P_{v,y}}^n \times O\&M_{c,tot} = CAP_c + P_v \times O\&M_{c,tot}$
$= 207.8 + \frac{34.8}{(1+0.3)^1} + \frac{34.8}{(1+0.3)^2} + \frac{34.8}{(1+0.3)^3} + \frac{34.8}{(1+0.3)^4} + \frac{34.8}{(1+0.3)^5} + \frac{34.8}{(1+0.3)^6} + \frac{34.8}{(1+0.3)^7}$
$= 207.8 + 34.8 \times \frac{(1+0.3)^7 - 1}{0.3 \times (1+0.3)^7} = 207.8 + 217.9 = 424.9\ (1000\text{CAD\$})$

BE-RCT:

- **Base-case scenario: W/ Battery replacement @ 5th year of operation**:

$O\&M_{c,tot} = VKT \times (O\&M_{c,km} + Fuel_c \times Fuel_{km} + GHG_c \times GHG_{km}$

$= 65.5\frac{km}{day} * 235\ \frac{day}{yr} * (0.39\ \frac{CAD\$}{km} + 1.776\frac{kWh}{km} * 0.0968\frac{CAD\$}{kWh} + 0.035\frac{CAD\$}{kgCO2eq} *$
$0.0096\frac{kgCO2}{kWh} * 0.290\frac{kWh}{km}) = 1000\text{CAD\$} * (6 + 2.6 + 0.01) = 8.6\ (1000\text{CAD\$}\ )$
$Tot\ Annual\ Cost_{amortized} = \left(CAP_c + P_{v,5} \times Bat_{c,rep}\right) *\ f_{amr} + O\&M_{c,tot}$
$= \left(649 + \frac{28.6}{(1+0.3)^5}\right) * \frac{0.3 \times (1+0.3)^7}{(1+0.3)^7 - 1} + 8.6$
$= (649 + 24.7) * 0.16 + 8.6 = 108.2 + 8.6 = 116.8\ (\frac{1000CAD\$}{yr})$

$TCO = CAP_c + \sum_{n=1}^{7} P_{v,y}{}^n \times O\&M_{c,tot} + P_{v,5} \times Bat_{c,rep} = CAP_c + P_v \times O\&M_{c,tot} +$
$P_{v,5} \times Bat_{c,rep} =$
$649.4 + \frac{8.6}{(1+0.3)^1} + \frac{8.6}{(1+.3)^2} + \frac{8.6}{(1+.3)^3} + \frac{8.6}{(1+.3)^4} + \frac{8.6+28.6}{(1+.3)^5} + \frac{8.6}{(1+.3)^6} + \frac{8.6}{(1+.3)^7}$
$= 649.4 + 8.6 \times \frac{(1+0.3)^7 - 1}{0.3 \times (1+.3)^7} + 28.6 \times \frac{1}{(1+0.3)^5}$
$= 649.4 + 52.68 + 24.67 = 727.7\ (1000CAD\$)$

- **2nd scenario: W/O Battery replacement cost:**

$O\&M_{c,tot} = VKT \times (O\&M_{c,km} + Fuel_c \times Fuel_{km} + GHG_c \times GHG_{km}$
$= 65.5\frac{km}{day} * 235\ \frac{day}{yr} * (0.39\ \frac{CAD\$}{km} + 1.776\frac{kWh}{km} * 0.0968\frac{CAD\$}{kWh} + 0.035\frac{CAD\$}{kgCO2eq} *$
$0.0096\frac{kgCO2}{kWh} * 0.290\frac{kWh}{km}) = 1000\text{CAD\$} * (6 + 2.6 + 0.01) = 8.6\ (1000\text{CAD\$}\ )$
$Tot\ Annual\ Cost_{amortized} = \left(CAP_c + P_{v,5} \times Bat_{c,rep}\right) *\ f_{amr} + O\&M_{c,tot}$
$= 649 * \frac{0.3 \times (1+0.3)^7}{(1+0.3)^7 - 1} + 8.6 = 104.2 + 8.6 = 112.8\ (\frac{1000CAD\$}{yr})$

$TCO = CAP_c + \sum_{n=1}^{7} P_{v,y}{}^n \times O\&M_{c,tot} + P_{v,5} \times Bat_{c,rep} = CAP_c + P_v \times O\&M_{c,tot} +$
$P_{v,5} \times Bat_{c,rep} =$
$649.4 + \frac{8.6}{(1+0.3)^1} + \frac{8.6}{(1+.3)^2} + \frac{8.6}{(1+.3)^3} + \frac{8.6}{(1+.3)^4} + \frac{8.6}{(1+.3)^5} + \frac{8.6}{(1+.3)^6} + \frac{8.6}{(1+.3)^7}$
$= 649.4 + 8.6 \times \frac{(1+0.3)^7 - 1}{0.3 \times (1+.3)^7}$
$= 649.4 + 52.68 = 703\ (1000CAD\$)$